Fakultät für Medizin

Cooperation of A20 and ABIN-1 in counteracting CBM complex signaling in activated T cells

Hongli Yin

Vollständiger Abdruck der von der Fakultät für Medizin der Technischen Universität München zur Erlangung des akademischen Grades eines

Doctor of Philosophy (Ph.D.)

genehmigten Dissertation.

Vorsitzende/r: Priv.-Doz. Dr. Christian Sorg

Betreuer/in: Prof. Dr. Marc Schmidt-Supprian

Prüfer der Dissertation:

1. Prof. Dr. Philipp J. Jost
2. Prof. Dr. Daniel Krappmann

Die Dissertation wurde am 29.04.2022 bei der Fakultät für Medizin der Technischen Universität München eingereicht und durch die Fakultät für Medizin am 03.07.2022 angenommen.

With my signature below, I assert that the work in this thesis has been composed by myself independently and no source materials or aids other than those mentioned in the thesis have been used.

Su Zhou, 26.04.2022

TABLE OF CONTENT

LIST OF FIGURES

LIST OF TABLES

1 Summary

Protective adaptive immunity is induced by T cell activation and the CARMA1-BCL10-MALT1 (CBM) complex serves as a scaffold to connect proximal antigen-receptor signaling to downstream signaling pathways, activating canonical nuclear factor-κB (NF-κB) signaling and lymphocytes in the process. Excessive adaptive immune responses, on the other hand, can result in autoinflammatory and autoimmune disorders. To avoid overshooting reactions and preserve immunological homeostasis, compensatory mechanisms are required. The tumor suppressor A20 can block NF-κB signaling pathway in response to diverse stimuli, and the A20 binding inhibitor of NF-κB activation 1 (ABIN-1) gene as an A20-binding protein that is also necessary for autoimmunity prevention. While most study has focused on the negative regulatory impact of A20 and ABIN-1 in inflammatory conditions, their mechanistic contribution to inhibiting T cell receptor (TCR)-induced signaling in an adaptive immune response is less clear. In this study, ABIN-1 was discovered as a CBM complex interactor in activated T cells utilizing quantitative mass spectrometry. In active T cells, both A20 and ABIN-1 are required to the CBM complex, which inhibits the activation of human primary CD4 T cells and Jurkat T cells. In the absence of ABIN-1, A20 overexpression reduces CBM complex-triggered NF-κB activation and MALT1 protease activation, however, ABIN-1 has a negative impact only when A20 is present. Furthermore, when T cells undergo prolonged stimulation, A20 and ABIN-1 are degraded by the proteasome, freeing the CBM complex from the inhibitory effects of A20 and ABIN-1. The K48-polyubiquitin chain-mediated degradation of A20 and ABIN-1 is regulated by ubiquitin binding to A20 ZnF4/7. ABIN-1 inhibits MALT1-mediated cleavage of re-synthesized A20, restraining persistent CBM complex signaling in an A20-dependent manner, modulating the negative regulatory role of A20 in T cells. Taken together, we describe and analyze how the A20/ABIN-1 module balances and tunes T cell signaling, and we demonstrate that interdependent post-translational processes regulate A20/ABIN-1 silencing module expression and activity in T cells. As a result, we uncovered the mechanisms that control the A20 and ABIN-1 counterbalancing activities in TCR-mediated adaptive immune pathways.

1 Zusammenfassung

Die T-Zell-Aktivierung induziert eine schützende adaptive Immunität, und der CARMA1-BCL10-MALT1 (CBM)-Komplex dient als Gerüst, um die proximale Antigen-Rezeptor-Signalübertragung mit nachgeschalteten Signalprozessen zu verbinden, wodurch der kanonische Nuklear Factor-κB (NF-κB) -Signalweg in Lymphozyten aktiviert wird. Eine überschießende Aktivierung der adaptive Immunantworten kann zu Autoimmunerkrankungen und chronischen Entzündungserkrankungen führen. Daher sind die Kompensationsmechanismen wesentlich, um überschießende Immunreaktionen zu reduzieren und die immunologische Homöostase aufrechtzuerhalten. Die NF-κB-Signalübertragung kann durch das Tumorsuppressorprotein A20 (TNFAIP3) stummgeschaltet werden. Das Protein ABIN-1 (A20 binding inhibitor of NF-κB-1) bindet A20 und es wurde vorgeschlagen, dass ABIN-1 was für die Prävention von Autoimmunität erforderlich ist. Während sich die meisten Studien auf die negativen regulatorischen Auswirkungen von A20 und ABIN-1 bei entzündlichen Erkrankungen konzentriert haben, ist ihr mechanistischer Beitrag zur Hemmung der T-Zellrezeptor (TZR)-induzierten Signalübertragung in der adaptiven Immunantwort weitgehend unklar. In dieser Studie wurde ABIN-1 als CBM-Komplex-Interaktor in aktivierten T Zellen unter Verwendung quantitativer Massenspektrometrie entdeckt. Sowohl A20 als auch ABIN-1 werden in aktivierten T-Zellen zum CBM-Komplex rekrutiert und wirken der Aktivierung von humanen primären CD4- und Jurkat-T-Zellen entgegen. Während die A20-Überexpression die durch den CBM-Komplex ausgelöste NF-κB-Signalübertragung und MALT1-Protease-Aktivierung in Abwesenheit von ABIN-1 unterdrückt, hat ABIN-1 nur dann einen negativen Einfluss, wenn A20 vorhanden ist. Darüber hinaus entbindet der proteasomale Abbau von A20 und ABIN-1 den CBM-Komplex von den negativen Wirkungen beider Regulatoren. Die Bindung von A20 ZnF4/7 an Ubiquitinketten fördert die destruktive K48-Polyubiquitinierung von A20 und ABIN-1. Darüber hinaus hemmt ABIN-1 die MALT1-katalysierte Spaltung von neu synthetisiertem A20, und schränkt die anhaltende CBM-Komplex-Signalübertragung in eine A20-abhängige Weise ein. ABIN-1 moduliert somit die negative regulatorische Funktion von A20 in T Zellen. Zusammengenommen beschreiben und

analysieren wir hier wie das A20/ABIN-1-Modul die Balance der Signalübertragung in T Zell-Signalgebung steuert. Wir zeigen, dass voneinander abhängige posttranslationale Prozesse die Expression und Aktivität des A20/ABIN-1-Moduls in T Zellen regulieren und decken die Mechanismen auf, die die Aktivitäten von A20 und ABIN-1 in der TZR-vermittelten adaptiven Immunwegen steuern.

2 Introduction

2.1 The immune system

The immune system is the body's primary immunological response system, and it protects the body against illness by recognizing and excluding antigenic foreign substances, collaborating with other bodily systems to maintain homeostasis and physiological balance. The immune system is a cooperative system composed of two broad cellular defenses: innate immunity and adaptive immunity.

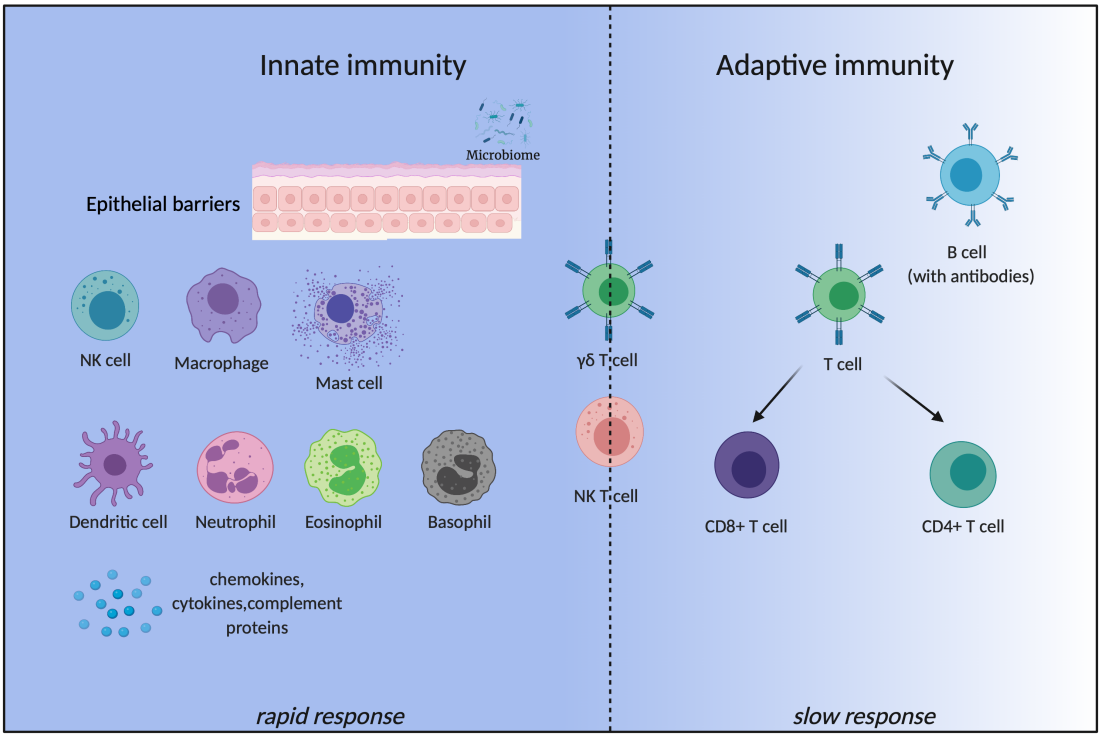

Figure 2-1. Cells of the innate and adaptive immune system.
Innate immune mechanisms provide rapid protection against infection as the first line of defense. While the physical barrier protects against pathogens, non-specific immunity is capable of engulfing and taking up intruders, releasing digestive enzymes to degrade and destroy them within their own cells. It is involved in a variety of functions, is swiftly processed, and participates in immune responses; In contrast, adaptive immunity, also known as specific immunity, is recognizes specific antigens of foreign pathogens; its responses occur later and are antigen specific. A crosstalk is required between these two types of immunity.

2.1.1 Innate immunity

Innate immunity, also known as non-specific immunity, is the immune system's initial line of protection. Because it is found in all species, it is also referred to as genetic or natural immunity.

The process of this system is precise and efficient, capable of responding quickly to harmful pathogens, and is essential for the onset of immunity[1]. As shown in **Figure 2-1**, there are several types of innate immune cells (macrophage, natural killer cells, dendritic cells, etc.) as well as innate immune chemicals (complement, cytokines, enzymes, etc.). The innate immune system's cells perform a variety of activities that are critical for pathogen defense. Due to its non-specific anti-infective immunological characteristics, it can also help the body eliminate damaged, aging, or aberrant cells and participate in adaptive immune responses. Complement, opsonin, lysozyme, and interferon, together with other nonspecific bactericidal chemicals found in normal bodily fluids, can help immune cells to remove invading bacteria[1,2].

The initial uptake and phagocytosis of microorganisms by antigen-presenting cells (APCs) is assisted by receptor-mediated identification of microbial compounds. Pattern recognition receptors (PRRs) are required for proper innate immune activity. They are mostly found on APCs like dendritic cells (DCs) and macrophages, but they are also present on other immune and non-immune cells[1]. These receptors identify conserved molecular structures referred to as pathogen- or damage- associated molecular patterns (PAMPs or DAMPs) present in microorganisms such as bacteria, viruses, parasites, or fungi. Cell surface receptors and complement receptors both contribute to this process. The activation of PRRs is critical for initiating innate immunity, which serves as a first line of defense until more specific adaptive immunity can be triggered[2].

2.1.2 Adaptive immunity

For most species, a physical barrier combined with an innate immune system is sufficient, but an adaptive or specialized immune system is required for vertebrates. Since certain viruses, such as influenza, are immune to the first line of protection, the second line of defense is triggered to fight infections that can enter physiological fluids or even cells, allowing individuals to defend themselves against practically all invading pathogens. Adaptive immunity, also known as specific immunity, is a type of immune response that utilizes antigen-specific receptors to recognize foreign antigens presented by APC. Unlike innate immunity, the adaptive immune response takes longer to form. Lymphocytes, a kind of white blood cell, are responsible for adaptive immune responses. Immune responses can be divided into two categories:

humoral- and cellular-immunity, which are both mediated by two distinct types of lymphocytes called B cells and T cells, respectively[3]. Because the adaptive immune system is capable to generate memory B and T cells, it develops a unique immunological memory that allows for rapid recognition and elimination upon reinfection with the same or similar pathogens. Helper T cells and suppressor T cells are two types of T cells that participate in the adaptive immune response. And natural killer (NK) T cells, as well as gamma-delta (γδ) T cells, are involved in both the innate and adaptive immune responses, whereas B cells only participate in humoral immunity. Both cellular and humoral immunity can be divided into three phases: initiation, activation, and effector[4,5]. All immune systems in the body, whether cellular or humoral, work together to form an exceedingly sensitive, sophisticated, and precise defense system.

2.1.2.1 Humoral immunity

Humoral immunity is an antibody-mediated response that is primarily driven by B cells and occurs when foreign antigens are detected in the body and the antigen binds to membrane immunoglobulin on naïve B cells. During antibody-mediated responses, B cells differentiate into plasma B cells with the support of helper T cells and interleukins for costimulation, and secrete antibodies against a specific antigen[6]. Of note, in most circumstances, an antigen and a costimulatory are both needed to active a naïve B cell and induce B cell proliferation.

Antibodies are produced by plasma B cells and circulated throughout the body, where they bind to foreign antigens circulating inside or outside infected cells. B cells can also develop memory cells, providing further immunity[3,6].

2.1.2.2 Cellular immunity

In cellular immunity, activated T cells swiftly respond to a foreign antigen on the host cell surface. An infected host cell that produces foreign antigens can be killed by T cells, halting viral replication. Additionally, the T cell generates signaling molecules, which activate macrophages and cause them to eliminate the intruders by phagocytosis.

T lymphocytes (termed T cells) arise from hematopoietic stem cells within the bone marrow and move to the thymus for maturation. In addition to targeting infected host cells, they also

activate other immune cells, secrete cytokines, and direct the immune response. The typical mature T cell should respond to a variety of foreign antigens as well as be immune to self-antigens. Thus, during T cell maturation, they first experience T cell receptor (TCR) gene rearrangement, express a diversity of TCRs, and then undergo positive and negative selection to prevent becoming self-reactive and triggering autoimmunity. Positive selection occurs when TCRs bind to MHC complexes in a moderate level, allowing mature $CD8^+$ and $CD4^+$ T cells to recognize MHC complexes to survive. TCRs that bind too tightly to MHC complexes cause cell death, which is known as negative selection. The bulk of TCRs are comprised of two heterodimeric peptide chains, α and β, and a minority of T cells expressing the γ/δ TCR. The immunoglobulin gene locus is composed of multiple gene segments, including variable segments (V), joining segments (J), and diversity segments (D). These four TCR genes are assembled via different mechanisms of V-D-J recombination. The α chain is encoded by the V and J gene segments, and in the β chain, V, D, and J recombination occurs. During the early phases of T cell maturation and differentiation, each locus contains numerous alleles and undergoes gene rearrangement, transcription, and translation into peptide chains. Therefore, the rearrangement of the two chain genes can form tens of thousands TCR molecules with different specificities, allowing the TCR to recognize a wide diversity of antigens to trigger the protective immunity.

Following a successful gene rearrangement at the TCRαβ loci, thymocytes show both CD4 and CD8 co-receptors. They next go through positive selection to find cells with TCRs that have potentially beneficial ligand specificities. CD4/CD8 lineage selection occurs following positive selection of thymocytes to differentiate them into $CD4^+$ or $CD8^+$ T cells.

Adaptive immunity is based on the specific recognition of an antigenic peptide bound to class I or II molecules of the major histocompatibility complex (MHC) on all somatic cells (MHC I) or a APC (MHC II) by an αβTCR. APCs are cells that can internalize and digest antigen, degrade it into peptides, and express them on the cell surface in association with MHC molecules, where they can engage with suitable TCRs. T cells' sensitivity and reactivity to cognate peptide–MHC ligands has been shown to be enhanced by membrane-associated proteins CD4 and CD8, which are displayed on helper T cells and cytotoxic T cells, respectively.

T cells are classified into numerous subtypes based on their function and surface characteristics. $CD8^+$ T cells are termed as cytotoxic T lymphocytes (CTL). They recognize and eliminate tumor cells that exhibit specific antigens and MHC class I molecules. They help prevent some lymphatic cancers and eradicate antigen-modulated tumor cell variations. $CD4^+$ T cells, also termed as T helper (Th) cells, which are the largest T cell subgroup, are categorized into numerous subtypes and perform a variety of activities. $CD4^+$ T cells are classified as Th1, Th2, Th3, Th17, and T regulatory (Treg) cells. They recognize peptides presented on MHC class II molecules rather than MHC class I molecules expressed by APCs. When $CD4^+$ T cells recognize the peptide of an APC, they are activated, rapidly develop into effector or regulatory/suppressive T cells and generate cytokines that activate other immune cells and help B cells to produce antibodies. Cytotoxic, helper or regulatory T cells are all types of effector T cells, which are responsible for the functions of an immune response. While these three types of effector cells account for the majority of immune responses, they are not the only T cell subtypes. Even after a pathogen has been eradicated, some T cells outlast. These long-lived lymphocytes are known as memory T cells, and they are capable of rapidly releasing effector cytokines in response to reintroduced antigens, hence increasing cellular immunity. Of course, there are additional types of T cells, such as natural killer T cells (NKTs), that have pro- and anti-inflammatory functions and act as an immunomodulatory factor in diseases such as cancer, autoimmune, allergies, infections, and graft-versus-host disease. Hence, T cells come in a range of types, which contributes to their diversity and enables them to attack a greater number of viruses and tumor cells.

2.2 NF-κB signaling

2.2.1 The NF-κB transcription factor family

Nuclear factor-kappa B (NF-κB) is a transcription factor that has been widely studied in the immune system since it regulates a large number of genes and biological responses and is implicated in a range of physiological and pathological processes[7]. NF-κB is a multifunctional transcription factor family that includes the proteins p50 (p105), p52 (p100), RelA (p65), RelB, and c-Rel, which can form different homodimers or heterodimers to mediate gene transcription

regulation[7]. The evolutionarily conserved proteins regulate a number of key cellular functions, including inflammation, stress response, cell growth, cell survival, and apoptosis. It affects a variety of immune cells and the development of innate and adaptive immune responses[8]. As illustrated in **Figure 2-2**, the members of the NF-κB family shared an N-terminal Rel homology domain (RHD), which enables them to form homodimers and heterodimers and regulate gene expression by combining promoter and enhancer regions of genes. RHD also contains as a nuclear localization signal (NLS), promoting the dimer complex's entry into the nucleus. Furthermore, RelA, c-Rel, and RelB possess a transcriptional activation domain (TAD) that can induce target gene expression. Due to the absence of the TAD domain in p50 and p52, their homodimers can inhibit transcription until they bind to a protein containing the TAD domain. Multiple dimers, including p50/p65, p50/c-Rel, p65/p65, and p65/c-Rel, exhibit transcriptional regulatory activity. Because p50 and p65 are the primary components of the active form of NF-κB in the majority of cells, the p50/p65 heterodimer is the most abundant and well-studied form of NF-κB[7,8]. Additionally, two types of proteins play critical roles in regulating NF-κB activity: NF-κB inhibitory protein (IκB) and IκB kinase (IKK). NF-κB dimers are kept inactive in the cytoplasm of resting cells through interaction with IκBs. The IκB family proteins bind to homo- and heterodimers of NF-κB/Rel proteins, preventing them from translocating to the nucleus by masking the NLS and, consequently, DNA-binding activity[9]. When various inducers initiate signal transduction cascades that phosphorylate, polyubiquitinate, and degrade IκB proteins via the proteasome pathway, NF-κB dimers are released and migrate to the nucleus. An NF-κB dimer can bind to DNA regulatory regions called κB sites on the promoter/enhancer of its target genes once it reaches the nucleus, activating or inhibiting transcription. The most well-studied κB sites match the consensus κB site pattern, 5′-GGGRNYYYCC-3′ (where R is any purine, Y is any pyrimidine, and N is any nucleotide)[10].

IκBα, IκBβ, IκBε, IκBγ, p100, p105 are all members of the IκB protein family. Their C-terminal sequences all contain an Ankyrin (Ank) repeat sequence, which is a 33-amino acid motif involved in protein–protein interactions **(Figure 2-2)**. 5–7 ANK repeats are present in the IκB proteins, which are needed for interaction with the RHD of NF-kB factors and thus their inhibitory activity[10]. Bcl-3 and IκBζ are two members of the IκB protein family of nuclear IκB

proteins that control NF-κB activity in a different way. IκBζ is nuclear localized, implying that it controls NF-κB activity in the nucleus rather than its translocation from the cytoplasm[11]. Bcl-3 has a transactivation domain. It binds to p50 homodimers and stabilizes this transcriptionally inactive complex, hence inhibiting NF-κB-induced gene expression[12].

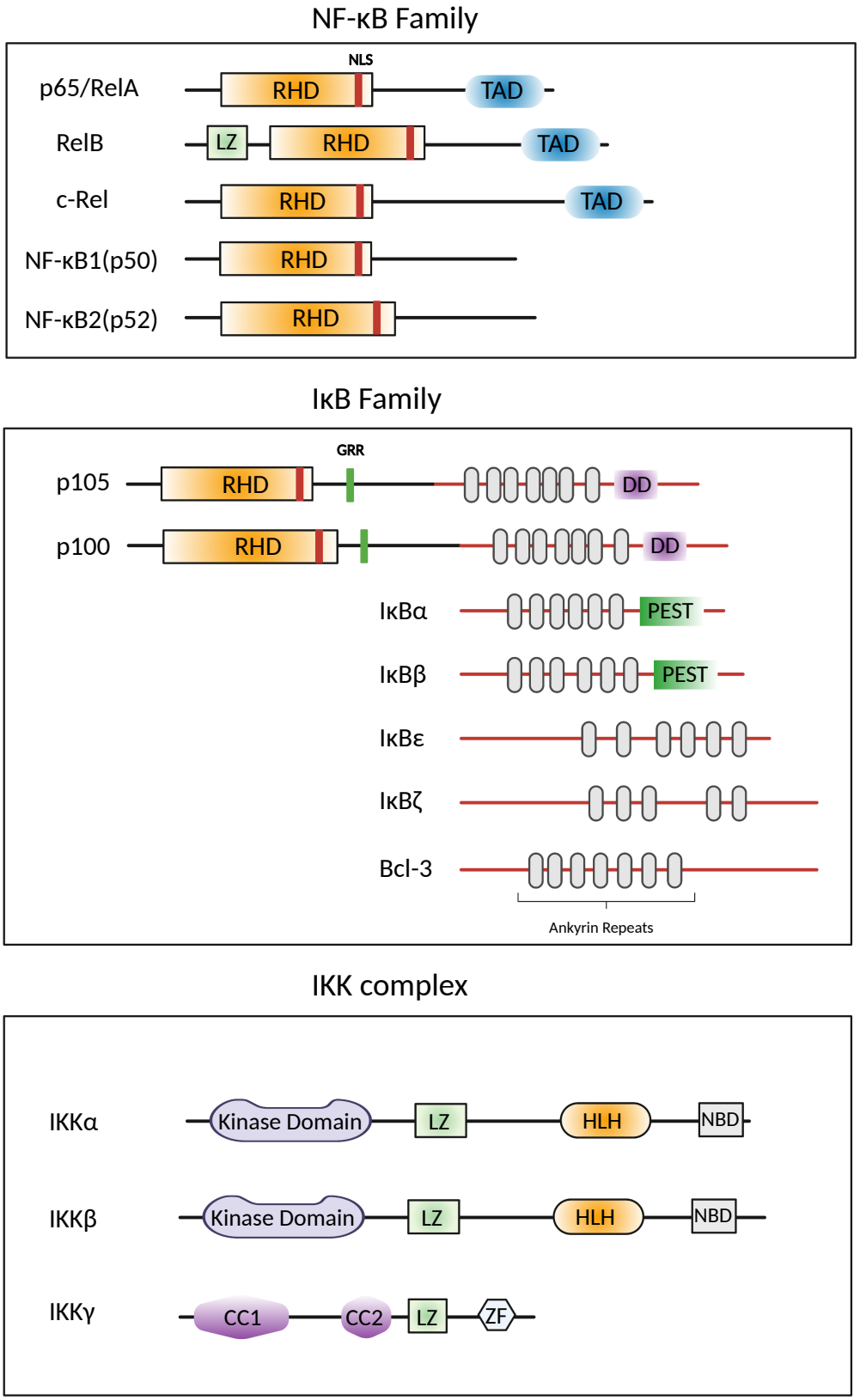

Figure 2-2. Schematic representations of NF-κB, IκB and IKK family members.

RHD: Rel homology domain; NLS: nuclear localization signal; TAD: transcriptional activation domain; LZ: leucine zipper; DD: death domain; CC: coiled-coil; ZF: zinc finger; HLH: helix-loop-helix; NBD: nemo binding domain.

2.2.2 Canonical and non-canonical NF-κB pathway

There are two distinct NF-κB pathways, canonical and non-canonical, each with its own unique activation mechanism[13]. It is widely accepted that a range of external stimuli activate the canonical NF-κB transcription factor, which is involved in inflammation, immunological response, cell proliferation, differentiation, and survival, including TCR ligands, B-cell receptor (BCR) ligands, TNFR ligands, ligands of cytokine receptors as well as pattern-recognition receptors[9,14]. In the so-called "canonical pathway", when cells are stimulated, the inhibitor factor IκB protein is phosphorylated and its lysines 21 and 22 are ubiquitinated, allowing IκB to be degraded by the 26S proteasome[15] **(Figure 2-3)**. To catalyze polyubiquitination of IκBα, E2 ubiquitin-conjugating enzymes of the Ubc4/5 family cooperate with the E3 ubiquitin ligase SCF-βTrCP[16,17].. The βTrCP complex is made up of two proteins, βTrCP1 and βTrCP2, both of which are capable of recognizing phosphorylated IκB. The SCF complex, on the other hand, has the RING domain protein Roc1/Rbx1 and interacts with Ubc4/5, enabling it to polyubiquitinate IκB at the two conserved lysine residues[18]. Finally, NF-κB is released, resulting in nuclear translocation. It translocates to the nucleus and interacts with the corresponding κB site, initiating transcription of the specified target gene. The destruction of the IκB protein is mostly dependent on the IKK, which is a trimeric enzyme complex made of three subunits: the two catalytic subunits, IKKα, IKKβ, and a non-catalytic regulatory subunit NEMO (also termed as IKKγ). As shown in **Figure 2-2**, IKKα and IKKβ have homologous kinase domains and activation loops. IKKα and IKKβ are functionally diverse despite their structural and molecular similarity[19]. Canonical NF-κB activation is temporary because it induces the production of negative regulators such as p105, IκBα and A20, resulting in an inhibitory feedback loop[20,21].

The noncanonical NF-κB pathway, in comparison to the canonical NF-κB pathway, responds selectively to a limited set of stimuli, such as lymphotoxin β, B-cell activating factor (BAFF), and CD40, among others, can activate IKKα via NF-κB-inducing kinase (NIK), which is not dependent on IKKβ and IKKγ. It directly phosphorylates one of the IκB subunits, p100, resulting in p100's ubiquitination and destruction. Given that p100 interacts and inhibits the NF-κB subunit RelB, p100 processing induces translocation of p52-RelB into the nucleus into

the nucleus to initiate transcription of target genes[22] **(Figure 2-3)**. The cytokine BAFF and the chemokines CXCL12, CXCL13, CCL19, and CCL21 are all targets of this pathway. These proteins contribute to lymphoid development, immune cell trafficking, and angiogenesis[23]. The non-canonical NF-κB pathway promotes immune cell multilayer growth. This system is required for thymic epithelial cell maturation and function, as well as T-cell development in the thymus[24].

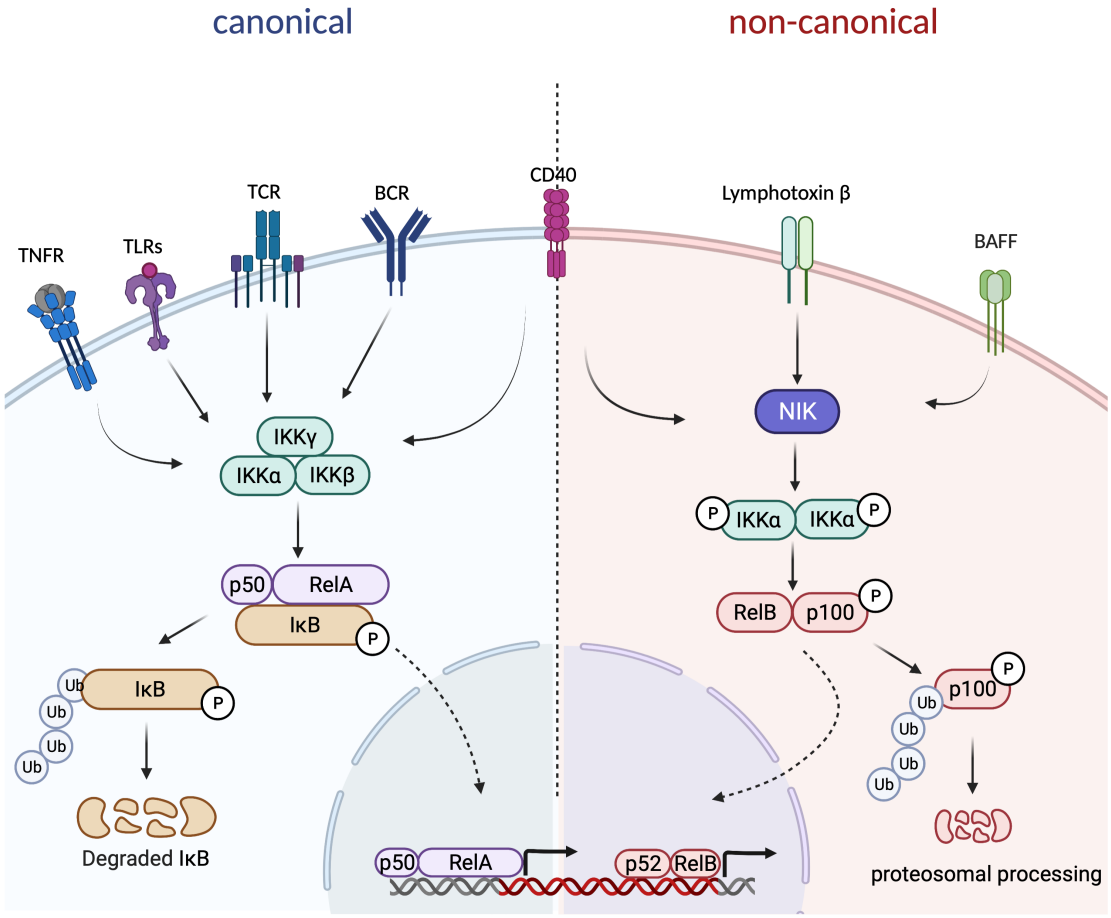

Figure 2-3. Canonical and non-canonical NF-κB signaling pathways.
In the canonical NF-κB signaling pathway, upon antigen receptor ligation, a trimeric IKK complex is formed, leading in the brief nuclear translocation of the classic NF-κB heterodimer RelA/p50 via IKK-mediated phosphorylation and subsequent destruction. The non-canonical NF-κB pathway is based on p100 processing, which requires NIK and IKKα but not the trimeric IKK complex to activate the RelB/p52 complex.

2.3 The ubiquitin system and its role in NF-κB signaling

2.3.1 The overview of the ubiquitin system

Ubiquitin (Ub) is a 76-amino acid protein found in all eukaryotic cells[25,26]. Ubiquitination is a process of post-translational modification that involves a cascade of enzymes covalently bonds one or more ubiquitin proteins to substrate protein molecules, which is an efficient way of protein degradation since intracellular proteins have a dynamic balance of synthesis and degradation[27]. Furthermore, ubiquitination is involved in a variety of physiological processes, such as cell proliferation, apoptosis, autophagy, endocytosis, DNA repair, and immunological responses, due to its complexity and multivalency[26,27].

In general, the ubiquitination process, which is carried out by the coordinated action of three ubiquitination enzymes, consists of three major steps: activation, binding, and ligation, which are carried out by E1 ubiquitin-activating enzymes, E2 ubiquitin-conjugating enzymes, and E3 ubiquitin-ligase enzymes, respectively. In the first phase, Ub is attached to the E1 enzyme in the presence of ATP to give energy for the activation of the Ub molecule before being transferred to an E2 enzyme. The E1 enzyme then transports activated Ub molecules to the E2 enzyme, and the E3 enzyme connects E2-bound Ub to target proteins[25] **(Figure 2-4, A)**. This is a two-way dynamic protein modification regulation mechanism, similar to the phosphorylation and dephosphorylation processes. In vivo, the ubiquitin ligase system ubiquitinates the substrates and the act of removing ubiquitin molecules from substrates is referred to as deubiquitination, which is carried out by deubiquitinases (DUBs). Ubiquitination and deubiquitination are intracellular physiological processes linked to protein degradation and cell signaling pathway regulation[26]. Since ubiquitin can conjugate on ubiquitin moiety to substrate proteins (monoubiquitination) or attach multiple ubiquitin molecules consecutively and form various types of Ub chains (polyubiquitination), different substrate proteins show the different type and lengths of ubiquitination modification. Monoubiquitination happens when a substrate protein binds a single ubiquitin molecule, which can affect various physiological functions such as protein localization and activity, receptor trafficking, and DNA repair[28,29]. When a single ubiquitin molecule tags several lysine residues of a substrate protein simultaneously, this is known as multi-monoubiquitination. Polyubiquitination occurs when a single lysine residue of

a substrate protein bind to several ubiquitin molecules[26] **(Figure 2-4, B)**. The modification of polyubiquitination comprises eight distinct types of connections; the key difference is the approach by which ubiquitin molecules are joined together, that is, which amino group of the former ubiquitin is connected to the C-terminus of the succeeding ubiquitin. Seven of these include the linkage between lysine (K) inside the ubiquitin chain and glycine (G) at the C-terminus of the ubiquitin molecule, including polyubiquitination modification at position K6, K11, K27, K29, K33, K48, and K63[29], producing ubiquitin chains of different lengths and shapes. The polyubiquitination modification of K48 and K63 have received increased attention, with the polyubiquitination modification of K48 mostly involved in degradation and the K63 polyubiquitination modification involved in signal transduction and DNA repair activity. Another approach for attaching ubiquitin chains is linear (M1) ubiquitination modification. The ubiquitin chain is created by joining the amino group of ubiquitin methionine (Met) to glycine (G) at the ubiquitin molecule´s C-terminus. According to existing research, linear ubiquitination is important in a variety of process, including innate immunity and the control of inflammatory responses[26].

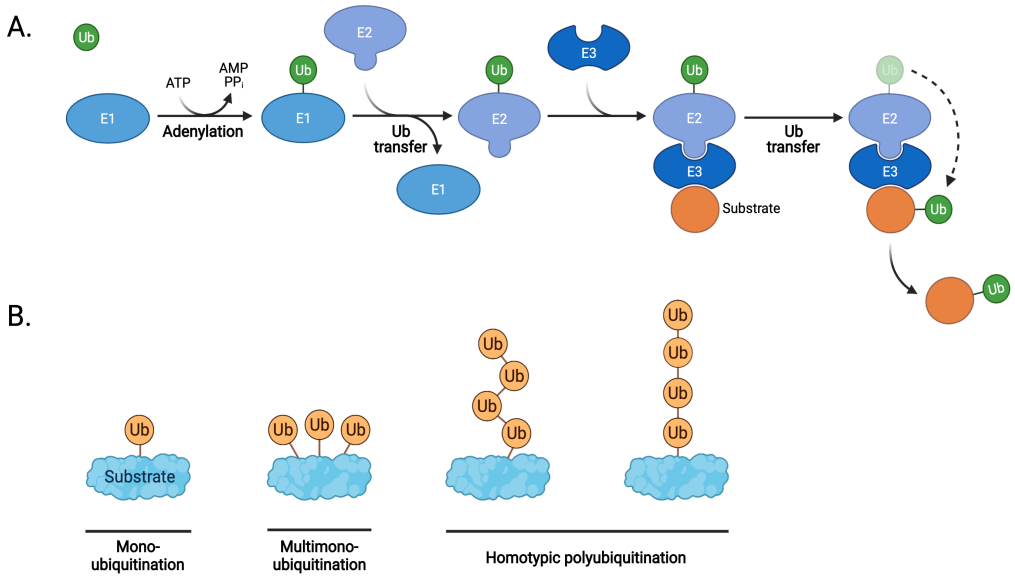

Figure 2-4. The overview of the process and mechanism of ubiquitination.
A, Schematic of the enzymatic cascade that leads to substrate ubiquitination. Ubiquitination is accomplished by a series of processes involving three types of enzymes (E1, E2, and E3). B, Three different forms of ubiquitination: monoubiquitination, multi-monoubiquitination and polyubiquitination. Adapted from "Protein Ubiquitylation Pathway for RING-type E3 Ligases", by BioRender.com (2020). Retrieved from https://app.biorender.com/biorender-templates.

2.3.2 Ubiquitin binding motifs to direct cellular complexes

Following ubiquitination modification of substrate proteins, the mono-ubiquitin or polyubiquitin chains associated with the substrate protein can be identified and non-covalently bound by distinct ubiquitin binding domains (UBDs) of other proteins, regulating different cellular processes by transmitting signals from ubiquitinated proteins to proteins containing one or more UBDs[28]. The avidity of binding, which may be controlled by multivalent connections between ubiquitinated targets and proteins containing UBDs, is hypothesized to influence ubiquitin and UBD physiological interactions[29].

UBAN (UBD in ABIN proteins and NEMO) is a UBD found in NEMO, optineurin, and A20 binding inhibitor of NF-κB activation (ABIN) proteins that is implicated in the modulation of NF-κB signaling pathways[30,31]. The UBAN domains of NEMO, ABIN-1 and ABIN-2 preferentially bind to K63-linked polyubiquitin chains or M1-linked polyubiquitin chains, but only the UBAN domain of ABIN-3 has been found to interact with monoubiquitin[29,31]. Besides, the fourth and seventh zinc finger (ZnF) domains of A20 have been demonstrated to serve as an UBD, with strong affinity for K63- and M1-linked polyubiquitin[32,33]. Furthermore, the ZnF domain of TAXBP1 was also discovered to bind K63-polyubiquitin chain linked TRAF6 and RIP in TNF and Interleukin-1 (IL-1) activated cells[29,34].

2.3.3 The regulatory role of ubiquitin system in NF-κB signaling pathway.

As indicated in the previous chapter, the NF-κB signaling system is engaged in a wide range of physiological processes and its activity is finely controlled by a variety of post-translational events, such as phosphorylation and ubiquitination[35]. It is inactive in most cells since the NF-κB is confined in the cytoplasm by IκB family proteins, inhibiting its activity. The ubiquitin proteasome system (UPS) rapidly degrades IκB family proteins in response to a diverse stimuli, enabling NF-κB to reach the nucleus and initiate the transcription of a variety of genes[16]. The phosphorylation of IκB protein and p100 mediated protein mediated by IKK complex is just a prerequisite for subsequent ubiquitination and proteasome destruction. Furthermore, the IKK complex can undergo ubiquitination modification, which is controlled by its upstream signaling components and plays an important role in IKK complex activation for both positive and negative regulation of NF-κB signaling.

NEMO is required for IKKβ activation since it contains a UBD and as a target for ubiquitination. The capacity of the NEMO protein to active the IKKβ protein is lost when the UBD is mutated by point mutation, as shown in immunodeficient individuals with ectodermal dysplasia[36]. Upon stimulation of various stimuli of cells, multiple sites of NEMO are modified by polyubiquitin, which may be associated to IKKβ activation[35]. TRAF6 protein, for example, is an E3 ligase that, together with the E2-binding enzyme complex formed of UBC13 and UEV1A proteins, promotes the synthesis of K63-linked polyubiquitin chains. The ubiquitinated TRAF6 binds TAK1 and the auxiliary proteins TAB1 and TAB2, activating the IKKβ and, eventually, NF-κB[35]. DUB protein can negatively regulate IKKβ protein, indicating that polyubiquitination modification is critical in the activation of IKKβ protein. These DUB proteins include the tumor suppressor CYLD protein, and the NF-κB inhibitor protein A20[35].

2.4 TCR/CD28 co-engagement triggers T cell activation

2.4.1 T cell activation

T cell activation is essential for mounting an immune response; activation of T cell surface receptors and costimulatory molecules regulate most of their functions[37]. Dual signal stimulation is required for T cells to be activated, to proliferate and differentiate into effector T cells. The first signal which is mediated by APCs, such as macrophages, determines the specificity of T cell activation[37]. APCs ingest a pathogen, digest it, and transfer pathogen pieces (peptides) to the cell surface, where they are transmitted to the TCR through peptide-MHC complexes. Of note, this first signal is not sufficient to elicit a full immune response; another signal is necessary, which is given by a costimulatory interaction between the signaling protein B7 on the surface of APCs and the CD28 receptor on T cells, therefore boosting TCR signals **(Figure 2-5)**. CD28-mediated costimulatory signals have been found to promote T cell differentiation, proliferation, and cytokine production. The first signal determines the specificity of T cell activation, while the second signal is transmitted to T cells by APCs in order to promote clonal proliferation, cytokine secretion, and effector activity[38,39].

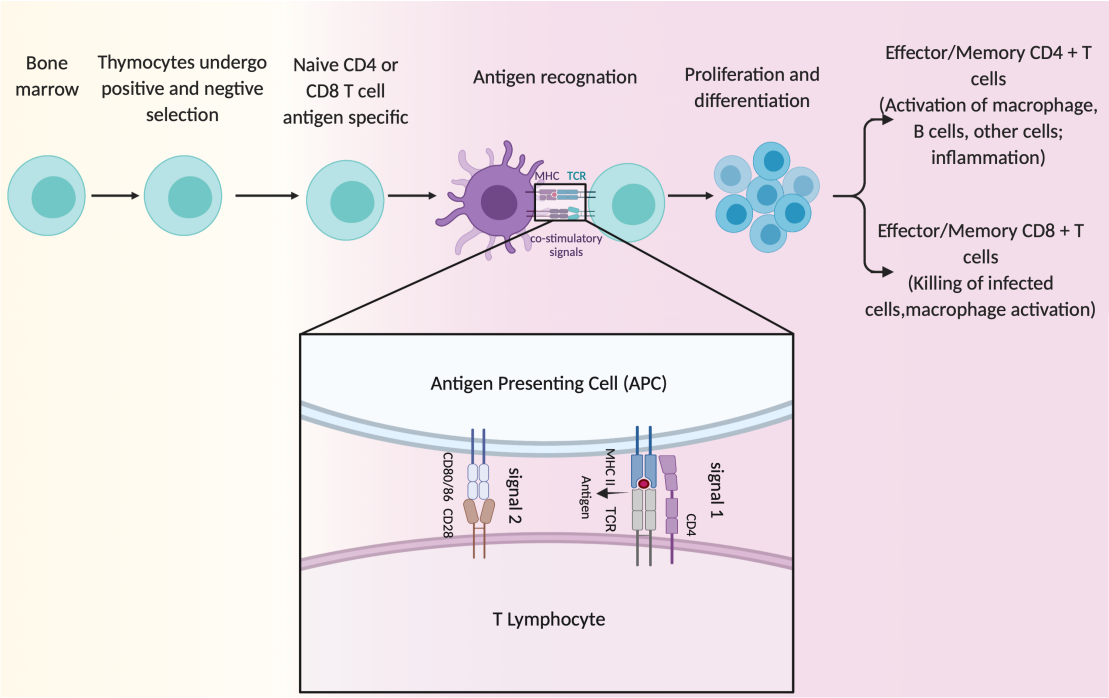

Figure 2-5. Schematic diagram of T cell activation mechanism.
Signal 1 is antigen-specific signaling mediated by the interaction of pathogenic peptides by MHC molecules via TCR. Signal 2 is received in conjunction with a costimulatory signal (e.g., engagement of CD28 by B7-1/2).

2.4.2 TCR signaling pathway

Transduction of the signaling pathway begins following TCR engagement[40]. The engagement of the antigenic peptide loaded MHC to the TCR promotes Src family kinase phosphorylation of downstream immunoreceptor tyrosine-based activation motif (ITAM) sequences of the CD3 chains, which serve as binding sites and cause the recruitment and activation of the intracellular tyrosine kinase ζ-chain–associated protein kinase 70 molecules (ZAP-70)[41,42]. ZAP-70 recruits a variety of signaling effectors, both positive and negative, to the TCR complex. ZAP-70, in addition to acting as a scaffold via self-phosphorylation, phosphorylates the tyrosine site of the adaptor proteins LAT and SLP-76 in response to TCR ligation. Phosphorylated SLP-76 facilitates the assembly of multi-subunit complex comprised of VAV1 and ITK, which activates PLCγ1. Activated PLCγ1 hydrolyzes PIP_2 to form the second messenger's IP_3 and diacylglycerol (DAG). Among these, IP_3 causes calcium release and the activation of Calcineurin, and membrane-bound DAG activates at least a few of key signaling pathways, including RasRP1 and ERK1/2 pathway, and in parallel protein kinase Cθ (PKCθ) -mediated pathways[43].

In response to activation, T cells undergo cytoskeleton remodeling, metabolism, and gene expression alterations. The three major pathways used to modulate transcription via TCR activation are the MAP-kinases (MAPK), NF-κB, and nuclear factor of activated T cells (NF-AT) pathways, which have a significant impact on the expression and nuclear location of different transcription factors that control T cell activation genes[44,45].

ERKs, p38 MAPK, and JNKs are all members of the MAPK family. These signal transduction pathways play a critical role in immune response regulation[46]. The NFAT transcription factor family, which comprises NFAT1-5, with NFAT1, NFAT2 and NFAT4 being well-known for their involvement in T cell activation, differentiation and development[47,48].

For NF-κB signaling pathway, PKCθ has a limited expression pattern throughout the body but is prominent in T cells, which has little effect on T cell maturation, but is engaged in their activation[49]. Furthermore, in response to antigen-specific signals, it can be rapidly recruited to the immunological synapse, thereby linking the proximal TCR signaling mechanisms mentioned above with the distal events that eventually result in NF-κB activation. CD28 acts as a costimulatory factor for T cells and promotes PI3K activity at the immunological synapse regardless of its ability to bind with the p85/p110 heterodimer[50], which is required for a variety of physiological responses, such as cell survival and proliferation. The cytoplasmic tail of CD28 has a PI3K-binding motif named the YMNM motif. It has been demonstrated that PI3K binds to the YMNM phosphotyrosine, resulting in PI3K activation. The activation of PI3K by CD28 is thought to be involved in the recruitment of phosphoinositide-dependent kinase 1 (PDK1) and AKT to the immunological synapse, where they are activated[51,52,53,54]. When PKC□ is activated by TCR/CD28 co-stimulation, CARD-containing MAGUK protein 1 (CARMA1) is phosphorylated, facilitating the recruitment of B-cell lymphoma 10 (BCL10) and Mucosa-associated lymphoid tissue lymphoma translocation protein 1 (MALT1) and the formation of the CBM (CARMA1-BCL10-MALT1) complex [55,56]. The CBM signal transduction complex, which is composed of the scaffold protein CARMA1, the adaptor protein BCL10, and the paracaspase enzyme MALT1, is required for signal transduction from antigen receptors on T and B cells to the NF-κB, JNK pathways and MALT1 protease activation, thereby regulating lymphocyte function and activation.

2.5 The role of CBM signalosome complex in TCR-induced signaling pathway

2.5.1 CARMA1 functions as a seed to induce NF-κB signaling pathway

PKC-dependent phosphorylation of CARMA1 has been demonstrated to trigger the critical signaling scaffold that governs IKK and NF-κB activation, leading to lymphocyte activation and proliferation[56,57,58,59]. CARMA1 (CARD11), CARMA2 (CARD14), and CARMA3 (CARD10) are members of the CARMA protein family, and their structures are extremely homologous and conservative[60,61,62]. CARMA1 contains a caspase recruitment domain (CARD) and a coiled-coil (CC) domain and a membrane-associated GUK (MAGUK) domain at its C-terminus, which is composed of a PDZ domain, an SH3 domain, and a Guanylate Kinase-like (GUK) domain. Additionally, a linker region exists between the CC and MAGUK domains[63] **(Figure 2-6)**. CARMA1 is required for TCR-induced activation of NF-κB and JNK[58,59], but not ERK or p38[64,65,66]. Many studies have revealed that signal-induced phosphorylation of CARMA1 by PKCs or other kinases is required for CARMA1 activation[56,67,68]. The phosphorylation of the CARMA1 linker region may expose the binding site for BCL10, controlling the conformational transition from an inactive to an active state, resulting in the formation of the CBM complex and activation of NF-κB[56,67,69] **(Figure 2-6)**.

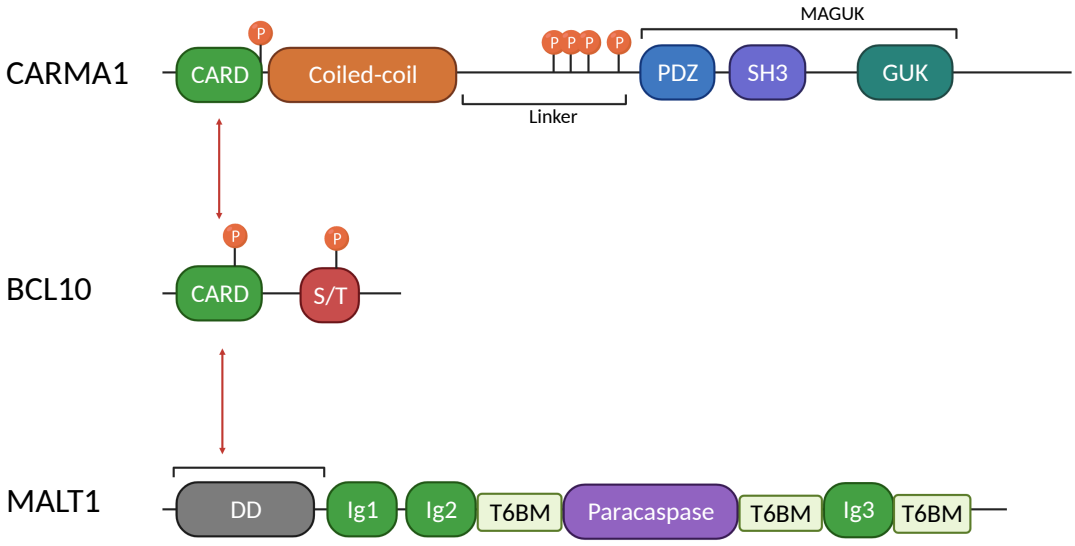

Figure 2-6. Molecular structure diagrams for CARMA1, BCL10 and MALT1.
CARMA1 is composed of an N-terminal CARD, a CC domain and a linker region. CARMA1's C-terminal region comprises a PDZ domain, a SH3 domain, and a GUK motif seen in MAGUK proteins[70]. BCL10 has a CARD domain at its N-terminus and a Ser/Thr(S/T)-rich unknown structure at its C-

terminus. MALT1 is composed of an N-terminal death domain (DD) that is required for BCL10 binding and two Ig-like domains. The C-terminus of MALT1 contains a protease domain, a third Ig domain, and an unknown structural extension[71].

After antigen receptor stimulation, CARMA1 has been shown to be phosphorylated. PKCs, such as PKCθ, may generate this phosphorylation in T cells because PKCθ is the primary isoform of PKCs that translocate into the immunological synapse[72] and facilitate TCR-induced NF-κB activation[73]. S552 and S645 in the linker region were identified as a functional site for PKC-dependent phosphorylation in the first study of CARMA1 mutagenesis. TCR-induced NF-κB activation in T cells is prevented by S552 or S645 mutations, which impede signals from upstream components such as PKCθ[67,74].

2.5.2 The role of BCL10 in the NF-κB signaling pathway

B cell lymphoma 10 (BCL10) is an essential component of the CBM complex that is involved in a number of antigen receptor stimulation signaling pathways, including the TCR signaling pathway[75,76,77]. It is composed of an N-terminal CARD domain and a C-terminal S/T residues-rich domain, and forms CBM complexes with other CARD domain-containing proteins such as CARD11 and MALT1 via heterotypic CARD-CARD interactions[78] **(Figure 2-6)**. Amplification of stimulation-induced signals by BCL10 filaments leads to MALT1 protease activation and canonical NF-κB and JNK signaling[69,79]. Post-translational regulation of BCL10 includes phosphorylation, ubiquitination, degradation and MALT1-catalyzed cleavage. As a result, BCL10 is engaged in both the activation and termination of immune cell signaling, implying that its role goes far beyond that of just a connecting component in CBM complexes. BCL10 loss causes embryonal death in approximately one-third of mice due to the abnormal neural tube closure[80]. T and B cells from BCL10-deficient mice have NF-κB signaling deficiencies similar to those seen in CARMA1 or MALT1-deficient mice, showing that BCL10, in collaboration with these two proteins, manipulates antigen signaling to create an efficient adaptive immune response[81].

BCL10 is modified by multiple forms of ubiquitin chains during antigen receptor activation, triggering downstream signal transduction or self-degradation to end signal transmission. BCL10 degradation via ubiquitination induced by E3 ligases such as cellular inhibitor of apoptosis 2 (cIAP2)[82], Ring Finger Protein 181 (RNF181)[83], Itch and Neuronal precursor cell-expressed developmentally downregulated 4 (NEDD4)[76] is required for proper TCR signal transduction balance[84], and after T cell activation, BCL10 destruction and removal are essential for post-inductive termination of CBM complex signaling, which occurs via autophagy-mediated lysosomal degradation[85,86]. Following TCR activation, the attachment of polyubiquitin chains on BCL10 lysine-17, 31 and 63 (K17, K31, K63) enhances the recruitment of NEMO to the CBM complex and regulates NF-κB activation[87,88,89]. In addition to being modified by the K63 and K48 ubiquitin chains, BCL10 is also linearly ubiquitinated by linear ubiquitin chain assembly complex (LUBAC) during TCR and BCR signaling[89,90], which is also required for BCL10 binding to NEMO and subsequent NF-κB activation.

Of interest, similar to the degradation of IκBα, the degradation of BCL10 also precedes phosphorylation[91,92]. According to multiple studies, phosphorylation of BCL10 is negative regulatory and counteracts CBM complex formation and NF-κB activation. Since researchers demonstrated that IKKβ phosphorylated BCL10 at a serine cluster encompassing S134, S136, S138, S141, and S144, which can reduce NF-κB activation by disrupting the connection between BCL10, MALT1 and NEMO ubiquitination[93].

In addition to phosphorylation and ubiquitination modification, BCL10 is also regulated by the MALT1 paracaspase activity. Upon TCR activation, MALT1 cleaves BCL10 at arginine 228, which is not necessary for NF-κB activation but is essential for integrin-dependent adherence of T cells to fibronectin, and is critical for T cell interaction with antigen-presenting cells[94].

2.5.3 Regulation of NF-κB signaling by MALT1 paracaspase

MALT1, also known as human paracaspase, is a caspase-like protein necessary for cellular activation by surface receptors containing immunoreceptor tyrosine-based activation motifs (ITAMs), such as TCR[95], and is involved in antigen receptor stimulation-induced NF-κB activation[96]. MALT1 was discovered in 1999, when scientists found that the chromosomal

translocation t (11;18) (q21;q21) is frequently identified in patients with MALT lymphomas. This translocation results in the API2-MALT1 fusion protein, which contains the N-terminus of cIAP2 and the C-terminus of MALT1 **(Figure 2-7)**. Findings from studies on MALT1-deficient mice showed defects in T cell activation, proliferation and cytokine production by antigen receptors, and demonstrated that MALT1 is essential for TCR-induced NF-κB and JNK signaling[97,98]. As a paracaspase like protein, MALT1 has both a scaffolding function and proteolytic activity. MALT1 was long assumed to be only a scaffold protein, allowing the recruitment of NF-κB signaling proteins and transmitting signals from T or B cell antigen receptors to NF-κB. This perspective shifted substantially when MALT1 was shown to exhibit proteolytic activity, which modulates immunological responses by cleaving and inactivating substrates involved in the regulation of NF-κB, JNK, mTORC1 and other transcription factors[99,100,101], making it a prospective therapeutic target in autoimmunity and cancer.

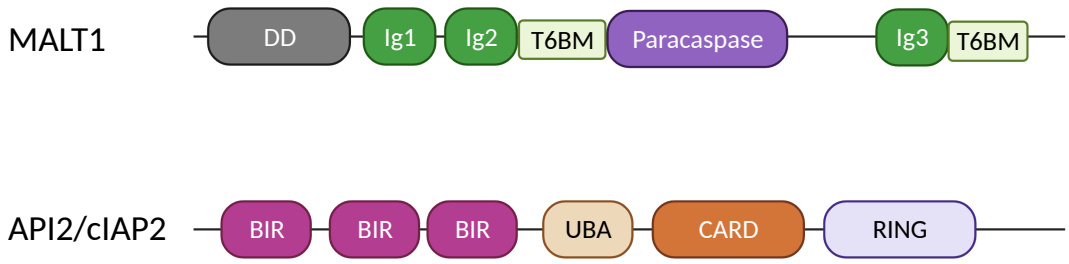

Figure 2-7. Molecular structure of MALT1 and API2 protein.
MALT1 and API2/cIAP2 structural domains. API2 N-terminal domains and MALT1 C-terminal domains are fused to form the API2-MALT1 fusion protein. API2 protein comprises three baculovirus IAP repeats (BIR) domains at the N terminus, followed by a ubiquitin associated domain (UBA), a CARD domain, and a really interesting new gene domain (RING) at the C terminus.

2.5.3.1 Scaffold function of MALT1 in TCR signaling pathways

MALT1 is necessary for activation of the canonical NF-κB pathway after TCR activation. It associates with BCL10 and CARMA1 to form the CBM complex, where MALT1 operates as a key protein scaffold that binds downstream effector proteins to activate NF-κB signaling. MALT1 is composed of a death domain (DD) at the N-terminus, two immunoglobulin (Ig)-like domains, a caspase-like domain, and another Ig-like domain at the C-terminus **(Figure 2-7)**. The scaffolding function of MALT1 is dependent on its multiple protein-protein interaction

domains[71,102,103]. Both in vitro and vivo, MALT1 forms a stable association with BCL10. Cryo-electron microscopy (cryo-EM) of the BCL10-MALT1 complex revealed the precise nature of the BCL10-MALT1 interaction, revealing that MALT1 DD binds the core of BCL10 filament by engaging with the BCL10 CARD motif. This interaction was further confirmed in cells using single point mutations; the BCL10 mutation L104R abolished the attachment of MALT1 to BCL10, and the MALT1 mutation V81R abolished the interaction of BCL10[69].

Aside from its constitutive interaction with BCL10, MALT1 has many lysine residues in its C-terminus that act as acceptor sites for polyubiquitin chain assembly and thus can connect the CBM complex to IKK activation after TCR ligation via the lysine 63 (K63)-linked polyubiquitin chains[104]. MALT1 is polyubiquitinated in activated T cells, where MALT1 recruits and binds to TRAF6, a ubiquitin ligase that synthesizes K63-linked polyubiquitin chains, boosting TRAF6 oligomerization and activating TRAF6 ligase activity to polyubiquitinate MALT1 and NEMO, facilitating IKK recruitment and activation[103,104] **(Figure 2-8)**. Of note, alternate splicing of MALT1 has been demonstrated to influence T cell signaling and activation. Since it has two alternative splice variants (MALT1A and MALT1B), MALT1 B has one functional TRAF6 binding motif (T6BM) at the C-terminal region, while MALT1A has two functional T6BM, one identical to MALT1B and one extra because MALT1A has exon7, which can encodes another T6BM. MALT1 splicing promotes optimal T cell activation by increasing relative MALT1A expression following T cell activation[105]. Furthermore, phosphorylation studies on MALT1 found six phosphorylation sites at C-terminus in activated Jurkat T cells, which influences MALT1 scaffolding function as well as NF-κB and JNK pathway[106].

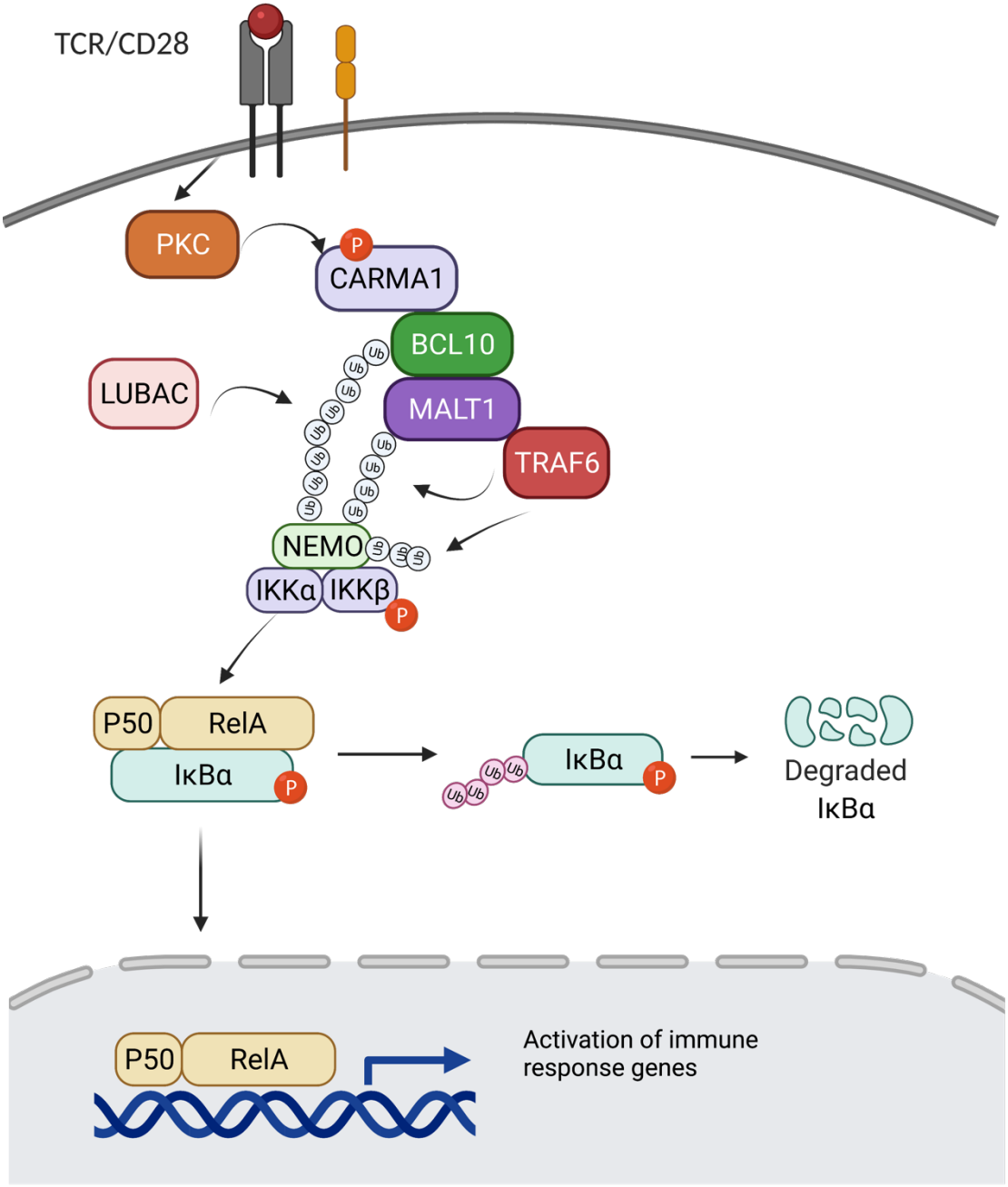

Figure 2-8. MALT1 scaffold function in lymphocytes.

When the TCR is activated, PKC phosphorylates CARMA1, allowing it to bind BCL10/MALT1 and form the CBM complex. Following this, TRAF6 is recruited to the CBM complex and MALT1 and potentially BCL10 are ubiquitinated via TRAF6. NEMO binds to MALT1 ubiquitin chains, is polyubiquitinated by TRAF6, and enhances the recruitment of IKKα and IKKβ. IKK phosphorylates IκBα, causing its proteasomal destruction and allowing NF-κB dimers to enter the nucleus and activate expression of target genes.

2.5.3.2 Protease function of MALT1

The protease activities mediated by MALT1's caspase-like domain is the second key role of MALT1 in CBM signaling. MALT1 is in a resting state in the absence of stimulation, and its protease activity is triggered upon antigenic activation of T cells[77]. MALT1 activation, like other caspases, is dependent on its dimerization, and the single-point mutations at the dimer interface eliminate MALT1 activity in cells, indicating that an intact dimer interface is necessary and MALT1 activation may occur in a direct contact between two MALT1 molecules[107]. MALT1´s protease activity also dependent on its monoubiquitination on lysine 644 (K644) inside the Ig3 domain of MALT1A, and mutations that modify the Ig3-ubiquitin interface affect T cell function[108]. Monoubiquitination of MALT1 is hypothesized to favor or stabilize the active MALT1 dimer because it generates a constitutively active, predominantly dimeric variant of MALT1[108]. Furthermore, at the dimerization interface, MALT1 E549 is necessary for the development of the enzamatically active, monoubiquitinated form of MALT1[109].

MALT1 cleaves various substrates that contain arginine residues around its consensus peptide sequence LVSRG[107]. MALT1 substrate cleavage has been linked to a number of different T cell activities. It was first shown that MALT1 cleaves BCL10[94] and A20[110], and that MALT1's proteolytic activity is critical for NF-κB activation. Later, ubiquitination regulators such as CYLD[111] and HOIL-1[112], the NF-κB subunit RelB[113], and mRNA turnover regulators such as Regnase-1 and Roquin1/2[114] have all been identified as MALT1 proteolytic substrates **(Figure 2-9)**. In the next paragraphs, we will provide a brief overview of various substrates.

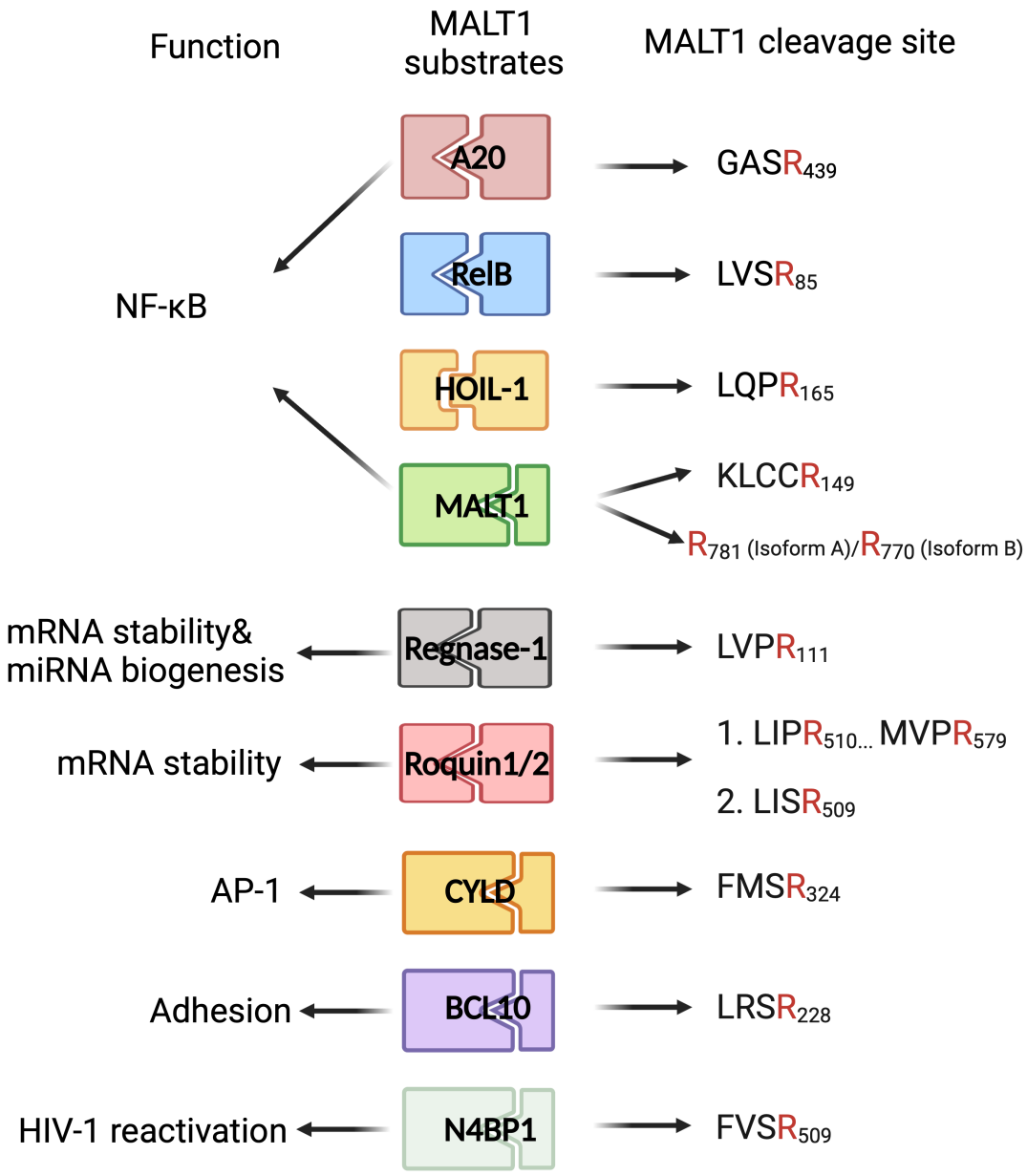

Figure 2-9. Overview of cleavage sites of the major human MALT1 substrates.

CBM components (BCL10 and MALT1)

BCL10 was one of the first discovered MALT1 substrates when researchers discovered a faster moving BCL10 isoform after T cell activation[94]. Notably, they discovered that this faster moving BCL10 isoform was generated by a MALT1-mediated proteolytic cleavage of BCL10 after Arg228, and that it has no effect on TCR-mediated NF-κB activation but is required for T

cell receptor-induced cell adhesion to fibronectin[94]. MALT1 has the ability to cleave proteins via its paracaspase and auto-proteolytic activities. MALT1 self-cleavage was initially identified at Arg149, which had no effect on its proteolytic activity but was required for NF-κB transcriptional activity and regulation of NF-κB target gene expression in activated lymphocytes[115]. Following that, a novel C-terminal auto-cleavage site at Arg781 (in MALT1 isoform A)/Arg770 (in MALT1 isoform B) was identified, and the final 43 amino acids comprising a crucial TRAF6-binding motif were removed via cleavage at this site. This auto-cleavage at the C-terminus has no effect on MALT1 isoform A but is required for MALT1 isoform B. Due to the absence of a critical TRAF6-binding motif in MALT1 isoform B, deleting another TRAF6-binding motif from its C-terminus effectively reduced its proteolytic function and NF-κB activation[116].

Signaling regulators (A20, CYLD, HOIL-1, RelB)

A20 protein was discovered to be a novel MALT1 substrate that was recruited to the CBM complex during T cell activation and acted as a negative regulator of the NF-κB signaling cascade[110]. Following that, the authors observed that A20 immunoprecipitated with MALT1 after TCR stimulation and that less A20 attaches to MALT1 after 20 mins, perhaps due to cleavage of A20 bound to MALT1[110]. Since MALT1 was shown to be an arginine-specific protease that mediates the processing of human A20 after Arg439, it reduces its ability to inhibit NF-κB activation.

The cylindromatosis (CYLD) gene encodes a deubiquitinating enzyme that regulates a variety of cellular functions including immunological responses, inflammation, death, and proliferation[117]. Staal et al. discovered that CYLD can be cleaved at R324 site in response to the activation of TCR or BCR, which requires MALT1 proteolytic activity. TCR-induced JNK activation was significantly reduced in cells expressing the CYLD R324A mutation, although CYLD cleavage had no impact on NF-κB activation, demonstrating that TCR-induced JNK activation is dependent on MALT1-mediated CYLD proteolytic inactivation[118]. However, MALT1 paracaspase mutant mice show normal JNK activation, so the function of CYLD cleavage by MALT1 is not really clear.

HOIL-1 has been discovered as a novel MALT1 substrate by high-confidence terminal amine isotopic labeling of substrates (TAILS), with the cleavage site located at Arg165[112]. HOIL-1 is a part of the linear ubiquitin chain assembly complex (LUBAC), whereas the other components HOIP and SHARPIN cannot be cleaved by MALT1. LUBAC is known to form linear ubiquitin chains on its target proteins. When MALT1 cleaves HOIL-1 in response to TCR stimulation, LUBAC is disassembled, resulting in a decrease in linear ubiquitination of NEMO and RIP1 and a decrease in NF-κB activation[112]. Additionally, it has been demonstrated that cleavage of the C-terminal of HOIL-1 inhibits LUBAC-mediated NF-κB activation[119].

MALT1 was identified to cleave human RelB after Arg85, and RelB cleavage resulted in its proteasomal degradation. This resulted in increased canonical RelA and c-Rel DNA binding in activated T and B cells, as well as ABC-DLBCL cell lines with constant MALT1 activity. RelB overexpression, on the other hand, reduced RelA- and c-Rel-dependent DNA binding, as well as NF-κB target gene expression and TCR-induced NF-κB activation in T cells[113]. These findings suggest that MALT1-mediated RelB cleavage boosts NF-κB dependent gene expression while having no effect on IKK activation, which is consistent with prior findings that MALT1 proteolytic activity has no effect on IKK activation or IκBα phosphorylation[94,100].

Regnase-1, Roquin-1/2 and N4BP1

Regnase-1 (also known as MCPIP-1 or ZC3H12A) and Roquin-1/2 (also known as RC3H1/RC3H2) belong to RNA-binding proteins (RBPs), which are involved in post-transcriptional regulation, degradation of inflammation-related mRNAs and the maintenance of immunological homeostasis[120,121]. Mice with Roquin or Regnase-1 mutations develop severe autoimmune and autoinflammatory disorders[114,120,122,123]. MALT1 cleaves Regnase-1 at Arg111 site, and the cleaved Regnase-1 protein was degraded by a cellular protease response to TCR activation[124]. The authors also confirmed that MALT1 protease activity is required for regulating the stability of a number of mRNAs, implying that MALT1 regulates mRNA stability and prolongs mRNA half-lives by cleaving Regnase-1[124]. Roquin has been shown to impede T helper 17 (TH17) cell differentiation and to repress target mRNA encoding TH17 cell-promoting factors in collaboration with Regnase-1. As with Regnase-1, Roquin-1/2 can be cleaved by MALT1 upon T cell activation, controlling the TH17 differentiation[114]. NEDD4-

binding protein (N4BP1) is an effective HIV-1 restriction factor and the MALT1-mediated cleavage of N4BP1 might assist in the reactivation of latent HIV-1 proviruses[125].

2.5.4 Positive and negative regulators of the CBM complex

To summarize, the CBM complex and NF-κB activation require both positive and negative regulators. TRAF6´s E3 ligase activity is responsible for the K63-linked ubiquitination of MALT1, NEMO and TRAF6, which connects the CBM complex to downstream NF-κB signaling[79]. LUBAC is also required for TCR-induced NF-κB activation, and it promotes the connection of CBM and IKK complexes after TCR stimulation, by catalyzing M1-linked polyubiquitin chains on CBM complex[126] **(Figure 2-8)**. CYLD and A20 are negative regulators. CYLD has been shown to inhibit NF-κB and Mitogen Activated Protein Kinase (MAPK) signaling cascades triggered by TLR or TNF stimuli through deubiquitinating non-K48-linked polyubiquitin chains from signaling transduction-related proteins, including NEMO, TRAF2, and TRAF6[111,127,128]. A20 is also a deubiquitinase that can remove the K63-linked polyubiquitin chains that connect MALT1 and NEMO, whereas the OTU domain has no effect on NF-κB activation[129]. It has been proved that the A20 ZnF4 and ZnF7 domains inhibit IKK activation by binding A20 to NEMO via polyubiquitin chains[130].

2.6 Immunoregulatory function of A20 protein

2.6.1 A20 as a negative regulator and its protein structure

A20 (also known as TNFAIP3) is a powerful anti-inflammatory protein, that works by decreasing NF-κB signaling, inflammatory gene expression, and preventing TNF-induced cytotoxicity[131]. It was discovered in 1990 as a critical response gene in human umbilical vein endothelial cells in response to TNF, which protected the cells from TNF-induced cell death. LPS and IL-1β also triggered A20 expression[132]. TNF significantly increases A20 mRNA expression in all tissues[133]. Stimuli induce A20 expression due to the presence of two κB elements in A20 promoter regions[134]. By studying the full-length A20 cDNA and sequencing, researchers revealed an open reading frame coding for A20 with 790 amino acid residues. A20 belongs to a member of a distinct class of Cys2/Cys2 zinc finger proteins[132,135]. A20 was

discovered as a dual inhibitor of NF-κB activation due to the inclusion of an N-terminal ovarian tumor (OTU) domain and seven C-terminal zinc finger (ZnF) motifs, since TNF stimulation increased A20 expression, which produces a negative feedback loop to stop and balance the response[136]. Originally, overexpression experiments revealed that A20 prevents both TNF-mediated cell death and NF-κB activation[137]. Investigations on A20-deficient mice, which have acute multi-organ inflammation and are very vulnerable to sub-lethal dosages of TNF, supported the crucial physiological role of A20[138].

Ubiquitination is a dynamic system, it is counterbalanced by deubiquitinases, which cut polyubiquitin chains and interrupt downstream signaling cascades[139]. A20 has been suggested to act as a ubiquitin-editing enzyme that modulates the ubiquitination status of particular NF-κB signaling proteins through its deubiquitination and ubiquitination activities, resulting in a negative feedback control of NF-κB activation[140]. It has an N-terminal OTU domain that possesses DUB activity and is responsible for deubiquitinating the ubiquitinated proteins' K63-linked polyubiquitin chains and also K48- and K11-linked polyubiquitin chains[141]. The C-terminal ZnF domains of A20 has E3 ligase activity within ZnF4, resulting in the formation of K48-linked polyubiquitin chains, whereas the linear ubiquitin binding function is dependent on ZnF7[32,140]. A20, in addition to acting as a DUB, can indirectly impact the ubiquitination of signaling mediators by interfering with the interaction of E2 and E3 enzymes, restricting polyubiquitin synthesis[142] **(Figure 2-10)**.

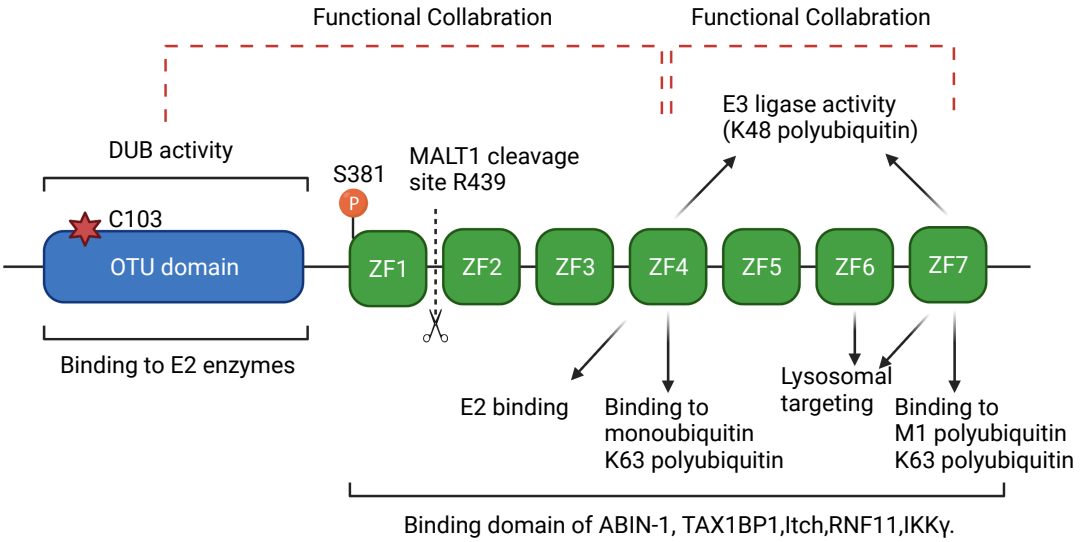

Figure 2-10. Domain structure of A20 and its biological characteristics.

Domain structure of the A20 protein. A20's N-terminus has an OTU domain that functions as a DUB due to the catalytic residue Cys103. The C-terminal region of A20 contains seven ZnF domains. The ZnF4 and ZnF7 domains function as E3 ubiquitin ligases and have a strong affinity for K63-linked polyubiquitin, whereas the ZnF7 domain has a high affinity for linear (M1) Ub chains and the ZnF4 domain has a high affinity for monoubiquitin. The OTU and ZnF4 domains have been reported to interact with the E2 enzymes Ubc13 and UbcH5c, respectively. ZnF6 and ZnF7 have been found to mediate TRAF2 degradation in the lysosome. A20 is phosphorylated at Ser381 by IKKβ in humans, MALT1 cleaves A20 at position R439. OTU: Ovarian tumor; DUB: deubiquitination; ZnF: Zinc finger; TAX1BP1: TAX1 binding protein 1; IKKγ: IκB kinase γ; ABIN1: A20-binding inhibitor of NF-κB; RNF11: RING-finger protein 11.

2.6.2 The role of A20 in the regulation of NF-κB signaling

To elucidate how A20 inhibits NF-κB signaling, *Heyninck et al.* showed that A20 suppresses TNF-induced NF-κB dependent gene expression by interfering with the TNF-induced and receptor interacting protein (RIP-) or TNF receptor associated factor 2 (TRAF2-) mediated signaling pathways involved in NF-κB transactivation[143]. Mice lacking A20 demonstrate severe inflammation and cachexia, as well as increased sensitivity to LPS and TNF, owing to the failure to repress TNF-induced NF-κB signaling[138]. The transcriptional activity of NF-κB triggered by TNF is not decreased in cells from A20-deficient mice. As a result, A20 is critical for chronic inflammation and cell death regulation, as it inhibits TNF-induced NF-κB activation *in vivo*[138]. TNF binding to TNFR1 induces trimerization of the receptor and recruitment of the signaling protein TNF-R1-associated death domain (TRADD) to the receptor´s death domain. TRADD acts as a scaffold for the E3 ligases TRAF2, cIAP1/2, and LUBAC to bind to the

adaptor molecule RIP1[144], which causing K63 or M1-linked polyubiquitin modification of RIP1 for recruitment of proteins with ubiquitin-binding domain[145,146]. TAB2/TAB3 and NEMO ubiquitin-binding adaptors binds to polyubiquitinated RIP1, recruiting the kinases TAK1 and IKK complex, respectively to allow TAK1 to phosphorylate and therefore activate IKKβ[30,147]. According to *Wertz et al.*, mutation of A20 ubiquitin ligase domain ZnF4 significantly decreases the ubiquitin ligase activity. ZnF4 is required for K48-linked polyubiquitination, indicating that A20 promotes substrate degradation[140]. Additionally, the authors established RIP as an A20 substrate by demonstrating that A20 directly ubiquitinates and degrades RIP. In comparision to the A20 wild type, the A20 ZnF4 mutant has no effect on the activation of NF-κB caused by TNF. As a result, they suggest that A20 inhibits TNF-induced NF-κB activation by accelerating the K48-mediated poly-ubiquitination and degradation of RIP. Interestingly, wild-type A20 exhibited a considerable reduction in the ubiquitination of RIP, whereas the A20 OTU mutant did not. Thus, they proposed that RIP was ubiquitinated via K63-linked ubiquitin chains and the A20 OTU domain deubiquitinated these K63-linked ubiquitin chains. TRAF2 was subsequently identified as the mediator of RIP K63-ubiquitination[140]. A20 OTU mutants were less effective at suppressing TNF-induced NF-κB activation than wild type A20. A20 deubiquitinates RIP, which is required for the degradation produced by A20. These findings demonstrate that A20 catalyzes two antagonistic mechanisms involved in the downregulation of NF-κB activation, both of which act synergistically to limit NF-κB activation. The N-terminal OTU domain destroys active RIP by removing its K63-linked ubiquitin chains, allowing the C-terminal ZnF4 domain to degrade it via K48-linked polyubiquitination.

Furthermore, A20 has been shown to be important in blocking interleukin-1 receptor (IL-1R)/Toll-like receptor (TLR)-induced NF-κB signaling by eliminating ubiquitin chains from TRAF6, which is necessary for TLR-induced NF-κB signaling[148]. A20 has also been demonstrated to block TRAF6, TRAF2, and cIAP1 E3 ligase activities in the TLR-induced signaling pathway by competing with the E2 enzymes Ubc13 and UbcH5c. TRAF6 polyubiquitination and activation need its intact RING domain interacting with the E2 enzyme Ubc13[149], and another E2 enzyme UbcH5c interacts with TRAF6 to produce unanchored polyubiquitin chains that activate IKK[150]. This is because the A20 ZnF4 domain is necessary

for the binding of TAXBP1, which regulates the steady-state level of E2 by blocking its proteasomal degradation. As a result, it is required for the degradation of the E2 ubiquitin conjugating enzymes Ubc13 and UbcH5c, allowing for the disassembly of ubiquitination complexes during the TLR signaling pathway[142]. As a result, it appears that A20 employs distinct strategies to block NF-κB activation in various pathways.

Additionally, A20 has also been shown to inhibit T cell activation by regulating the strength and duration of the IKK/NF-κB response[110,129]. A20 functions as a negative regulator of inducible IKK activity in TCR-mediated signaling by boosting the cleavage of K63-linked polyubiquitin chains from MALT1, inhibiting connection between ubiquitinated MALT1 and the downstream IKK complex. Because of proteasomal degradation and the paracaspase activity of MALT1, which has been hypothesized to cleave A20, A20 is rapidly eliminated following T cell activation[129]. A20 deficiency in mouse CD8 T cells resulted in increased pro-inflammatory cytokines such as IL-2 and IFNγ level as well as improved antitumor activity in vivo, suggesting that A20 might be a suitable target gene in adoptively transplanted CD8 T cells to promote tumor rejection[151]. Furthermore, A20-deficient $CD4^+$ and $CD8^+$ mouse T cell compartments have been shown to have improved effector function but lower ability to survive following allogeneic hematopoietic stem cell transplantation, suggesting the severity and mortality of graft-versus-host-disease may be modified because of the negative feedback control of NF-κB[152]. *Onizawa et al.* demonstrated that excessive formation of RIPK1-RIPK3 complexes driven by polyubiquitin chain K5 was detected in A20-deficient mice T cells for the mechanism of A20 protection against inflammatory disease. By exploiting its deubiquitinating activity, A20 prevented RIPK3 ubiquitination and the formation of necroptotic RIPK1-RIPK3 complexes[148].

2.6.3 The mechanistical function of A20

To gain a deeper understanding of the A20 ZnF4 motif's ubiquitin interaction, *Bosanac et al.* discovered that A20 ZnF4 can directly bind mono-ubiquitin and K63-linked polyubiquitin chains **(Figure 2-10)**. A mutation in the ZnF4 domain of A20 impairs ubiquitin binding and

NF-κB signaling[33]. Later research established that A20 ZnF7 is involved in polyubiquitin binding and has E3 ligase activity, playing a critical function in NF-κB signaling[130]. ZnF7 mutations affect polyubiquitin binding, impairing the capacity of A20 to inhibit IKK activation and the expression of NF-κB target genes[130]. Since the attachment of K63 linked polyubiquitin chains on TAK1 and IKK mediates upstream signaling transduction and protein activation upon stimulation. On the other hand, A20 ZnF4 and ZnF7 domains inhibit IKK activation by binding A20 to NEMO. IKK receive both positive and negative regulation as a result of K63 polyubiquitin chain binding, and they collaborate and tightly control NF-κB activation[130]. Additionally, it was discovered that the A20 ZnF7 motif interacts with M1 chains and is needed for TNF-RSC recruitment, implying that it is involved in LUBAC-mediated pathways[32].

A20 also has the unanticipated ability to direct an associated signaling molecule such as TRAF2 to the lysosomes for destruction. ZnF6 and ZnF7 are required for this procedure[153]. Ser381 of A20 has been identified as a potential IKKβ phosphorylation site, as depicted in **Figure 2-10**. IKKβ is a critical activator of NF-κB and has been shown to phosphorylate IκBα, allowing for its degradation by ubiquitin. This phosphorylation step improves A20's inhibitory activity against the NF-κB signaling pathway[154]. Additionally, it was established in vitro that phosphorylated A20 rapidly cleaves K63-linked ubiquitin chains[155].

2.6.4 The binding partners of A20 protein

A20 interacts and requires several partners to carry out its regulatory functions. It can form bigger ubiquitin-editing complexes with other ubiquitin-binding or -modifying proteins such as ABIN1, which has been demonstrated to link A20 to polyubiquitinated NEMO and facilitate DUB activity of A20[143]; TAX1-binding protein1 (TAX1BP1) suppresses TRAF6 ubiquitination and NF-κB activation in an A20-dependent manner[156], and IKKγ, which has been shown to interact with A20 by C-terminal domain and ubiquitin chains, limiting NF-κB activation[130,157]. Furthermore, A20 interacts with several proteins that function as E3 enzymes either directly or indirectly, including TRAF2[153], TRAF6, cIAP1/2[142], itchy E3 ubiquitin protein ligase (ITCH)[158],

and RING-finger protein 11 (RNF11)[158]. These proteins collaborate with A20 to give high levels of specificity and modulation of ubiquitin-dependent signaling.

2.7 Regulation of NF-κB signaling by ABIN-1

2.7.1 ABIN-1/TNIP1 protein structure and expression

Heyninck et al. used a yeast two-hybrid screen of the mouse fibroblast L929r2 cDNA library utilizing A20 as bait to demonstrate for the first time that A20 interacts with a new protein, ABIN-1[143]. The authors demonstrated that when ABIN-1 is overexpressed in TNF, IL-1, and LPS-driven signaling cascades, it mimics A20's NF-κB inhibitory function, showing that A20's function is mediated by its association with ABIN-1[143].

ABIN-1, ABIN-2, and ABIN-3 are members of the ABINs protein family. They share ABIN homology domains (AHD), AHD2, and AHD4, whereas ABIN-2 lacks AHD3. Furthermore, AHD2 is lacking in murine ABIN-3. All three ABINs have a UBD known as the UBAN domain, which includes AHD2[159]. ABIN-1, also known as TNFAIP3-interacting protein 1 (TNIP1), affects NF-κB signaling and immune homeostasis. It is a polyubiquitin-binding protein that inhibits the NF-κB/ JNK/ERK-related signaling pathways[160,161]. TNIP1 and TNFAIP3 genetic variations are highly linked to susceptibility to autoimmune chronic inflammatory diseases[162,163]. The TNIP1 gene comprises 18 exons and is found on human chromosome 5q32-33.1. Exons 2-18 encode the gene, but exon 1 is untranslated. These two 72-kDa TNIP1 isoforms (ABIN-1α and β) arise from different splicing acceptor sites in exon 18[164]. ABIN-1 mRNA is detected in all human tissues, with particularly high levels in peripheral blood cells, the spleen, and skeletal muscle. ABIN-1 mRNA is also found in certain human hematopoietic immune cell lines, including Jurkat T cells, Molt-4, and HL-60[165,166]. As a result, ABIN-1 is highly expressed in immune system cells and organs, indicating its significance. Currently, it is known that ABIN-1 contains three functional domains: AHD1, AHD2, and NBD. It also has AHD3 and AHD4 domains at the N-terminus, but their functions are unknown (as shown in **Figure 2-11**). Each of these three functional domains has been associated to ABIN-1's NF-κB inhibitory activity.

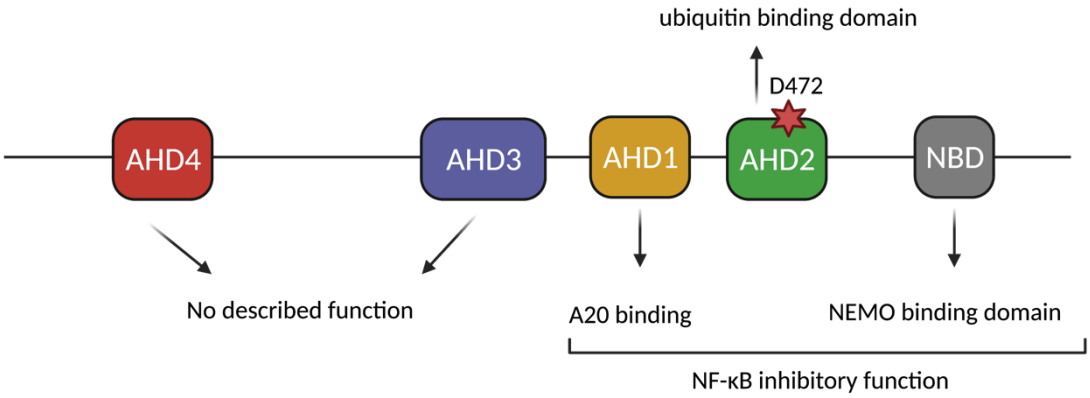

Figure 2-11. Domain structure of ABIN-1 and its biological characteristics.
Functional domains of ABIN-1. AHD: ABIN homology domain, NBD: NEMO binding domain; AHD1 is essential for A20 binding; AHD2 interacts to polyubiquitin and polyubiquitinated proteins, and the site of mutation that affects ABIN-1's interaction with polyubiquitinated proteins; ABIN-1 has a C-terminal NBD domain; the roles of AHD3 and AHD4 are unknown. The AHD1, AHD2, and NBD domain have all been proven to participate in ABIN-1's activity in NF-κB inhibition.

2.7.2 Role of ABIN-1 in NF-κB signaling

As previously stated, ABIN-1 binds to the ubiquitin-editing protein A20, which is recognized for its anti-NF-κB and anti-apoptotic properties. ABIN-1, unlike A20, does not exhibit a ubiquitin-editing activity; yet, like A20, ABIN-1 overexpression in HEK293T cells inhibits NF-κB activation triggered by various stimuli[143,159]. Of note, only TRADD, RIP1 and TRAF2 induced NF-κB activation can be suppressed by A20 or ABIN-1, whereas IKKβ or p65 induced NF-κB activation cannot, implying that the inhibitory function of A20 or ABIN-1 acts upstream of IKKβ but downstream of RIP1 or TRAF2[143,159]. There are two commonly recognized hypotheses about the mechanism by which ABIN-1 inhibits NF-κB activation. One pathway is A20-dependent, whereas another is A20-independent or competitive. Following that, we shall discuss these two mechanisms independently.

2.7.2.1 A20-dependent mechanism

ABIN-1 was assumed to function as an adaptor protein by connecting A20 to downstream NF-κB mediators such as NEMO, hence facilitating A20´s E3 ligase activity or DUB activity[163]. As a result, the regulation of ABIN-1's NF-κB activation is controlled either by disrupting critical upstream interactions, which is accomplished by enhancing the A20 function to remove K63-linked polyubiquitin chains, or by increasing the proteasome degradation of upstream regulators,

which is accomplished by promoting the A20 function to add K48-polyubiquitin chains to target proteins[161]. ABIN-1 promotes NEMO's de-ubiquitination of A20, and A20 downregulation reduces ABIN-1's ability to regulate NF-κB activation. A20 has a significant effect on the ubiquitination of NEMO only in the presence of ABIN-1. ABIN-1 recognizes NEMO in two steps: its UBAN domain binds with the polyubiquitinated chains on NEMO, and its NBD domain directly interacts with NEMO. Furthermore, ABIN-1, A20, and NEMO form a complex, the ABIN-1 ΔNBD mutant binds to NEMO only in the presence of A20, and ABIN-1 increases A20-NEMO association, implying that ABIN-1 may collaborate with A20 and NEMO to change NEMO's ubiquitination state[167]. Furthermore, RNA interference of A20 affects the NF-κB inhibitory impact of ABIN-1 overexpression[167]. Another intriguing observation is that A20 and ABIN-1 can also cooperate to modulate the NF-κB signaling pathway in amphioxus branchiostoma belcheri tsingtauense (bbt)[168]. bbt A20, like human A20, requires bbtABIN-1 to function as a scaffold protein in order to effect bbtNEMO ubiquitination. Nonetheless, unlike human A20, the bbtA20 protein was unable to bind to bbtNEMO. Furthermore, bbtA20 did not promote bbtNEMO deubiquitination via the OTU domain but can cleave K63-linked polyubiquitin chains from bbtRIP1. When co-expressed with bbtABIN-1 and gradient bbtA20, bbtNEMO and bbtRIP1degradation was dosage dependent. This degradation in bbtA20 is ZnF4-dependent and occurs via a protease-dependent pathway[168]. They hypothesized that the role of bbtA20 and bbtABIN-1 in regulating NF-κB signaling is a negative feedback system, because bbtA20 is induced after NF-κB activation and collaborates with bbtABIN-1 in modifying ubiquitinated proteins, resulting in NF-κB activation failing to attenuate excessive inflammation[168].

2.7.2.2 A20-independent mechanism

Another mechanism through which ABIN-1 regulates NF-κB is the A20-independent route. Like bbtABIN-2, which has been shown to compete the K63-linked polyubiquitin binding with bbtTRAF6 upon overexpression to inhibit NF-κB activation[168]. ABIN-1 has been demonstrated to suppress NF-κB activation in cells expressing ABIN-1 ΔAHD1, which cannot bind to A20 protein; consequently, A20 binding is not needed for ABIN-1 to inhibit NF-κB activation[169].

ABIN-1 and A20 appear to work together for some activities but not others. Notably, stimulation of A20-deficient cells with TNF prolongs NF-κB activation, whereas stimulation of ABIN-1-deficient cells results in basically normal NF-κB activation or the production of NF-κB-dependent genes. This could be because other members of the ABIN family, such as ABIN-2 or ABIN-3, are compensating for the loss of ABIN-1[170].

2.7.3 Other biological activities of ABIN-1

ABIN-1's inhibitory functions on Interleukin 17A (IL-17)-induced NF-κB signaling were independent of A20. Following IL-17 signaling, the ABIN-1 protein was destroyed by the proteasome, removing a cellular brake on NF-κB activation[171]. ABIN-1 inhibits the poly (I:C)-mediated innate immune response in both a RIPK1 kinase-dependent and -independent way. Furthermore, after prolonged poly (I:C) stimulation, ABIN-1 degradation was detected in an A20-dependent manner[162]. ABIN-1 has also been found to be recruited to the TNFR1 signaling complex by LUBAC, controlling the recruitment of A20 to regulate RIPK1 K63 deubiquitylation[172].

2.7.4 Physiological functions of ABIN-1

ABIN-1 has been hypothesized to affect NF-κB signaling and regulate immunological homeostasis in a cellular study. Thus, it is vital to conduct gene-targeting investigations in mice in order to gain a better understanding of ABIN-1's function in vivo and the physiological effects of ABIN-1 dysregulation on disease onset and progression[166]. Cells lacking either ABIN-1 or A20 are very sensitive to RIPK1 activation, which promotes necroptosis. ABIN-1 -/- mice die around embryonic day 18.5 due to fetal liver cell death, anemia, and hypoplasia, which may be prevented and rescued by TNF deficiency[170], or the RIPK1 D138N kinase-dead mutation, or RIPK3 deficiency[172,173]. One of ABIN-1's primary activities is to inhibit cell death during embryonic development by regulating TNFR1 signaling. By limiting caspase 8 binding to Fas-associated protein with DD (FADD) in TNF-induced signaling complexes, ABIN-1 prevents caspase 8 cleavage and programmed cell death. Additionally, ABIN-1 directly interacts with polyubiquitin chains, which is required for its anti-apoptotic activity . Mice with a ubiquitin-

binding-defective ABIN-1 mutation (D485N) suffer a lupus-like autoimmune disease characterized by spontaneous germinal center formation, isotype switching, and autoreactive antibody production. Concurrent MyD88 deletion rescued these mice, demonstrating that ABIN-1 plays a key role in regulating TLR signaling to suppress autoimmunity. Of note, the removal of either A20 or ABIN1 from intestinal epithelial cells (IECs) results in negligible disease, but the loss of both A20 and ABIN-1 results in fast IEC mortality and mice fatality[174].

2.7.5 Pathological functions of ABIN-1

TNIP1 participates in a range of physiological and pathological processes in humans. For example, TNIP1 gene variations and the loss of ABIN-1 have been shown to contribute to the development of systemic lupus erythematosus (SLE) and Lupus nephritis (LN) via increased NF-κB activation via the TLR/MYD88/IRAK signals, promoting NF-κB mediated cytokine and chemokine secretion in target cells, and accelerated production and activation of myeloid and B cells in the LN[160,175]. The TNIP1 variations may help identify individuals who are at a higher risk of developing LN, revealing new therapeutic targets and paving the way for individual therapy for people with TNIP1 mutations[175]. Aside from SLE, TNIP1 has been related to psoriasis susceptibility, as researchers discovered that the TNIP1 gene shows highly significant changes in expression between involved and uninvolved skin[176]. Furthermore, TNIP1 has been demonstrated to regulate human keratinocyte proliferation, which is characterized in psoriasis patients by hyperproliferation and abnormal terminal differentiation[177]. Thus, targeting TNIP1 might be an appealing therapeutic target for psoriasis.

3 Aims of the study

The TCR-initiated signal transduction which lead to NF-κB activation is critical in the adaptive immune response. The formation of CBM complex is a crucial step in this process, linking proximal signaling of TCR to MALT1 protease activation and the canonical IKK/NF-κB signaling pathway. Since abnormal NF-κB activation underpins a variety of disease, fine-tuning of CBM complex driven NF-κB activation is critical for regulating immunological responses.

Although A20 is well established for its involvement in suppressing NF-κB signaling and cell death pathways, its mechanistic contribution to counteracting TCR-induced signaling in an adaptive immune response is unclear. ABIN-1 is an A20-binding protein that controls NF-κB signaling and is implicated in immunological homeostasis. A20's negative regulatory influence on pro-inflammatory or innate immune signaling has been proven, but its involvement in T cell signaling is uncertain. In this work, we aim to investigate how A20 and ABIN-1 assist to balance and fine-tune T cell signaling.

The main purpose of this study was to use mass spectrometry to discover novel CBM complex components and investigate their roles in the regulation of MALT1 protease and NF-κB activation. To gain an insight into the roles of A20 and ABIN-1 in MALT1 protease activity and NF-κB signaling pathway, ABIN-1 or A20-deficient human primary CD4 T cells and Jurkat T cells were generated, and rescue experiments with A20 and ABIN-1 were performed to investigate their interdependence. Furthermore, by overexpressing several ABIN-1 mutants in Jurkat T cells or reconstituting several A20 mutants in A20 deficient Jurkat T cells, we discovered the functional domain of these proteins for NF-κB activation regulation. Additionally, multiple studies have shown that ABIN-1 protein is removed following different stimuli; consequently, we further intended to investigate in this work the mechanism of decreased A20 and ABIN-1 upon TCR activation as well as the effect of ABIN-1 on A20 expression and MALT1-mediated cleavage.

4 Results

4.1 Identification of CBM signalosome co-factors by LC-MS/MS

In activated T cells, the casein kinase 1α (CK1α) activity is required for the formation of the CBM complex[106]. CK1α-deficient Jurkat T cells lost the ability to induce CBM complex assembly, which was restored by transduction with CK1α wild-type (WT) but not with the kinase-dead D136N mutant. To investigate whether CK1α activity is required for co-factors recruitment to the CBM complex, mass spectrometry studies utilizing BCL10 immunoprecipitation (IP) were performed. By either treating Jurkat T cells expressing CK1α WT or CK1α D136N mutant with PMA/Ionomycin (P/I) for 20 min or not, we were able to enrich the inducible CBM signaling complex effectively. Because PMA stimulates protein kinase C (PKC) and Ionomycin is a calcium ionophore, these chemicals stimulate T cells without activating the T cell membrane receptor complex and mimics the effect of TCR-induced phospholipase C activation[178] **(Table 1)**. The constitutively bound state of MALT1 and BCL10 was seen in untreated Jurkat T cells, but the CARD11 interaction and the consequently formation of the CBM complex relied on P/I stimulation **(Figure 4-1 A)**. The association of CARD11 and BCL10 was completely dependent on CK1α kinase activity, supporting CK1α's crucial function in CBM signalosome assembly **(Figure 4-1 B)**. We discovered numerous recognized CBM complex interactors, including HOIL-1 (RBCK1), SHARPIN, CK1α (CSNK1A1), and AIP, all of which we found in activated T cells. CK1α kinase activity was required for the binding of all co-factors except AIP **(Figure 4-1 B)**. Additionally, we discovered ABIN-1 (TNIP1), TRAF2 and IKKε (IKBKE) as possible components of CBM complex in activated T cells, although their precise functions in CBM complex-mediated T cell signaling have yet to be established. In this study, we wanted to focus on the new CBM complex interactors ABIN-1 and TRAF2, which are both involved in the regulation of cellular ubiquitination[163,179]. We could confirm binding of ABIN-1 and TRAF2 to the CBM complex **(Figure 4-2 and data not shown)**[180]. However, deletion of TRAF2 in Jurkat T cells by CRISPR/Cas9 technology increased constitutive p100 processing and non-canonical NF-κB activation, but this process did not rely on the CBM complex (unpublished data). Since the

functional role of TRAF2 association to the CBM complex has so far remained elusive, we concentrated on ABIN-1, which was highly enriched after BCL10 IP **(Figure 4-1)** upon T cell stimulation.

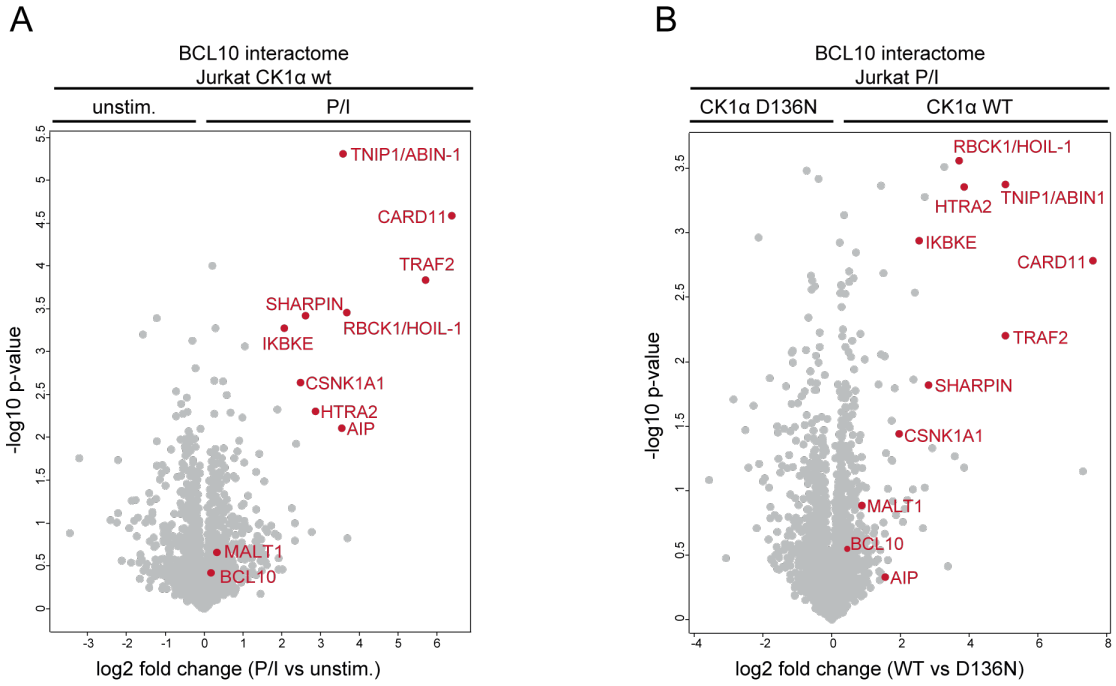

Figure 4-1: Identification of novel CBM complex components by LC-MS/MS.
A, Protein enrichment following BCL10 IP as determined by comparing Jurkat T cells expressing CK1α WT in untreated or 20 min P/I treated conditions. The volcano plot depicts the specific enrichment of BCL10 bound proteins cells treated with P/I compared to unstimulated cells. **B,** Protein enrichment following BCL10 IP as determined by comparing Jurkat T cells expressing CK1α WT or CK1α D136N mutant after 20 min P/I stimulation. The volcano plot depicts the specific enrichment of BCL10 bound proteins in CK1α WT versus D136N (MS was performed in collaboration with Karayel Özge of Matthias Mann laboratory). Panel A, B have been published in Yin et al, Cell Mol Life Sci, 2022, 79:112

4.2 ABIN-1 is recruited to the CBM signalosome upon T cell activation

T cell activation requires two signals, one of which is delivered via the TCR by CD3. Co-stimulation via CD28 is another signal. As a result, we utilized monoclonal anti-CD3 and anti-CD28 antibodies to mimic antigen-induced T cell activation in this study. As illustrated in **Figure 4-2 A and B**, after 20 min of P/I or CD3/CD28 stimulation, we were able to observe the formation of a CBM complex by BCL10 IP and to validate the interaction between ABIN-1 and

BCL10 in Jurkat T cells, showing the recruitment of ABIN-1 to the CBM complex upon stimulation. Additionally, as demonstrated before, A20 acts as a substrate for MALT1 cleavage and suppresses NF-κB activation in T cells via the CBM complex. However, in either unstimulated or stimulated Jurkat T cells, we were unable to discover A20 as a co-factor of the BCL10 interactome using this mass spectrometry approach[110,129] **(Figure 4-1).** To elaborate, we conducted ABIN-1 IP and found that CARD11 and A20 interacted with ABIN-1 upon 20 min P/I stimulation in Jurkat T cells, indicating that the recruitment of ABIN-1 and A20 to the CBM complex occurred concurrently **(Figure 4-2 C)**.

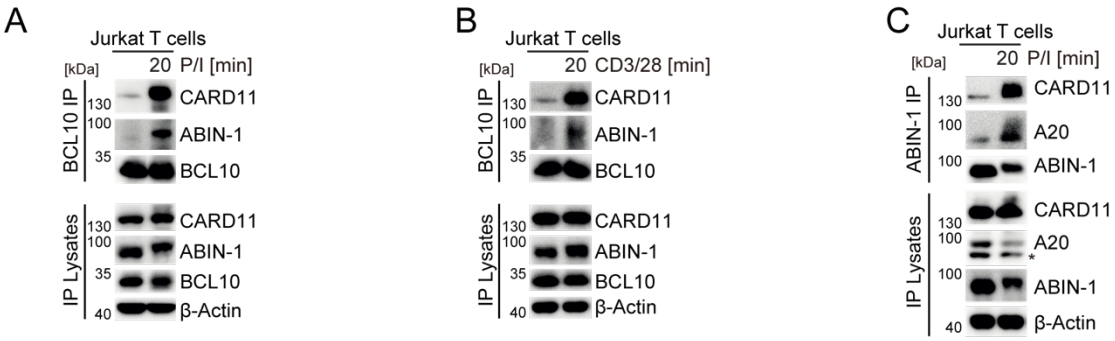

Figure 4-2: ABIN-1 binds to the CBM complex in activated T cells.
A, B BCL10 IP was conducted in Jurkat T cells that were either left untreated or stimulate for 20 min with P/I or CD3/CD28. The interaction of CARD11 and ABIN-1 to BCL10 was then determined by Western blot. **C,** ABIN-1 IP was conducted in Jurkat T cells that were either left untreated or stimulate for 20 min with P/I and the interaction of CARD11 and A20 to ABIN-1 was then determined by Western blot. Asterisk indicates non-specific bands of A20. Panel A, B, C have been published in Yin et al, Cell Mol Life Sci, 2022, 79:112

4.3 A20 and ABIN-1 are essential for NF-κB activation in Jurkat T cells

A20- and ABIN-1-deficient Jurkat T cell lines were generated in order to provide a system for investigating the roles of A20 and ABIN-1 in TCR-mediated NF-κB signaling pathway. By using CRISPR-Cas9 gene editing technology, single guide (sg) RNAs targeting ABIN-1 exon 3 and A20 exon 3 were designed and introduced into Jurkat T cells. Targeting this region results in double-stranded breaks (DSB) that are repaired by nonhomologous end joining (NHEJ), leading in frame shift by insertions or deletions (indels) and the generation of A20 or ABIN-1

KO Jurkat T cell lines. Western blot analysis was used to confirm and identify A20 or ABIN-1-deficient Jurkat T cell clones **(Figure 4-3 A and B)**.

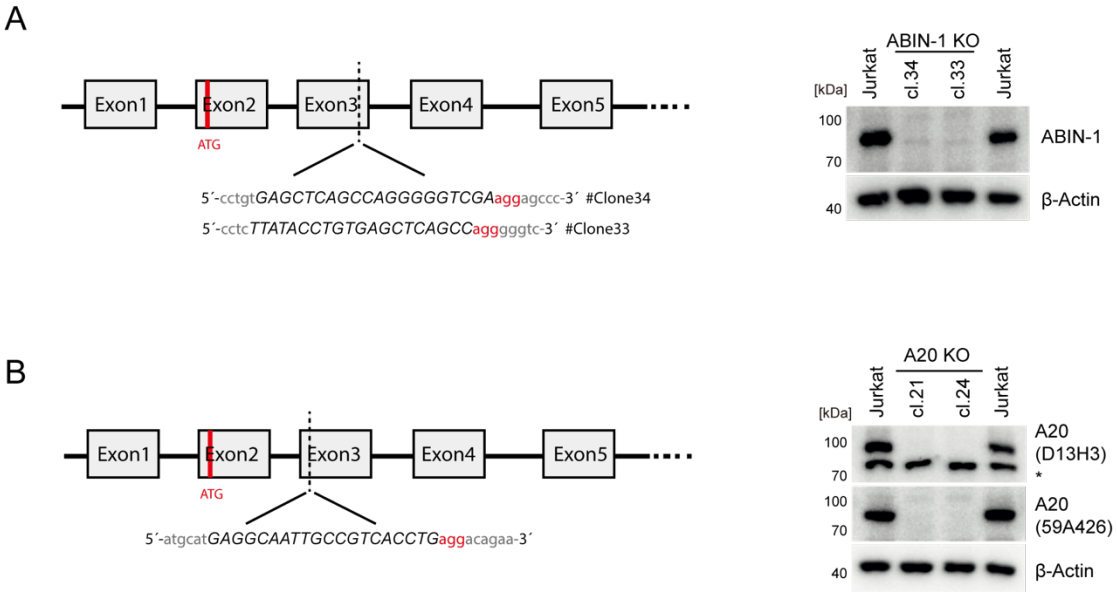

Figure 4-3: Generation of A20 or ABIN-1 knockout Jurkat T cell line.
A, B Simplified schematic of ABIN-1 (A) or A20 (B) knockout targeting strategy, and the efficient knockout of ABIN-1 or A20 was verified by Western blot. Panel A, B have been published in Yin et al, Cell Mol Life Sci, 2022, 79:112

As illustrated in **Figure 4-4 A and B**, A20-deficient Jurkat T cells exhibited a significant increase in NF-κB signaling pathway, as demonstrated by increased IκBα phosphorylation in response to CD3/CD28 stimulation and prolonged IκBα degradation upon P/I stimulation. The same experiments were carried out in ABIN-1-deficient Jurkat T cells, as illustrated in **Figure 4-4 C and D**, and we discovered increased NF-κB signaling pathway in ABIN-1 KO Jurkat T cells upon stimulation. As previously demonstrated following A20 knock-down, TCR/CD28 stimulation boosted NF-κB DNA binding activity in ABIN-1 deficient Jurkat T cells[129] **(Figure 4-4 C)**.

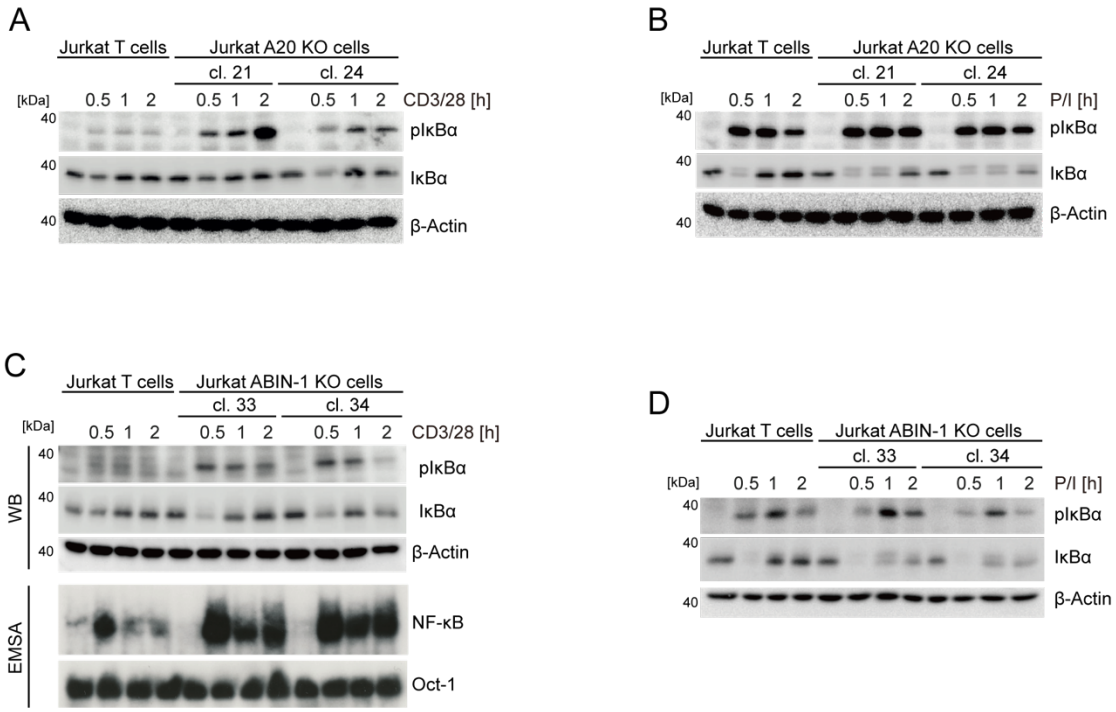

Figure 4-4: ABIN-1 or A20 deficiency enhances NF-κB signaling.
A, B Western blot analysis of NF-κB activation in parental and A20 deficient Jurkat T cells in response to CD3/CD28 and P/I stimulation. **C, D** Western blot and EMSA analysis of NF-κB activation in parental and A20 deficient Jurkat T cells in response to CD3/CD28 and P/I stimulation. Panel A, B, C, D have been published in Yin et al, Cell Mol Life Sci, 2022, 79:112

To examine the transcriptional response of NF-κB and determine the contribution of A20 or ABIN-1 deficiency for NF-κB activation, we infected parental and A20 (clone 21) and ABIN-1 (clone 34) deficient Jurkat T cells using a viral NF-κB-EGFP reporter plasmid. The NF-κB-EGFP reporter plasmid contains six copies of the NF-κB sites and the conalbumin (cona) minimal promoter, followed by a hygromycin-EGFP-fusion gene (HygEGFP)[181] (details in materials and methods), resulting in EGFP expression regulated by NF-κB **(Figure 4-5 A)**. The activation of NF-κB transcription was determined by identifying EGFP-positive Jurkat T cells utilizing flow cytometry. After 4 h of CD3/28 stimulation, the median fluorescence intensity (MFI) and the percentage of EGFP-positive cells were considerably raised in A20 defective Jurkat T cells, indicating significantly enhanced NF-κB activation **(Figure 4-5 B)**. The activation of NF-κB reporter following P/I stimulation was boosted in A20 KO Jurkat T cells, although the effect was less pronounced due to the considerably greater reporter gene induction after P/I treatment **(Figure 4-5 C)**. MALT1 poly-ubiquitination has been linked to NF-κB activation, since it promotes IKK complex recruitment to the CBM complex in activated T

cells[104,182]. We aimed to determine whether depletion of A20 protein has an effect on MALT1 poly-ubiquitination. Indeed, lack of A20 resulted in a more robust poly-ubiquitination of MALT1 upon P/I stimulation **(Figure 4-5 D)**.

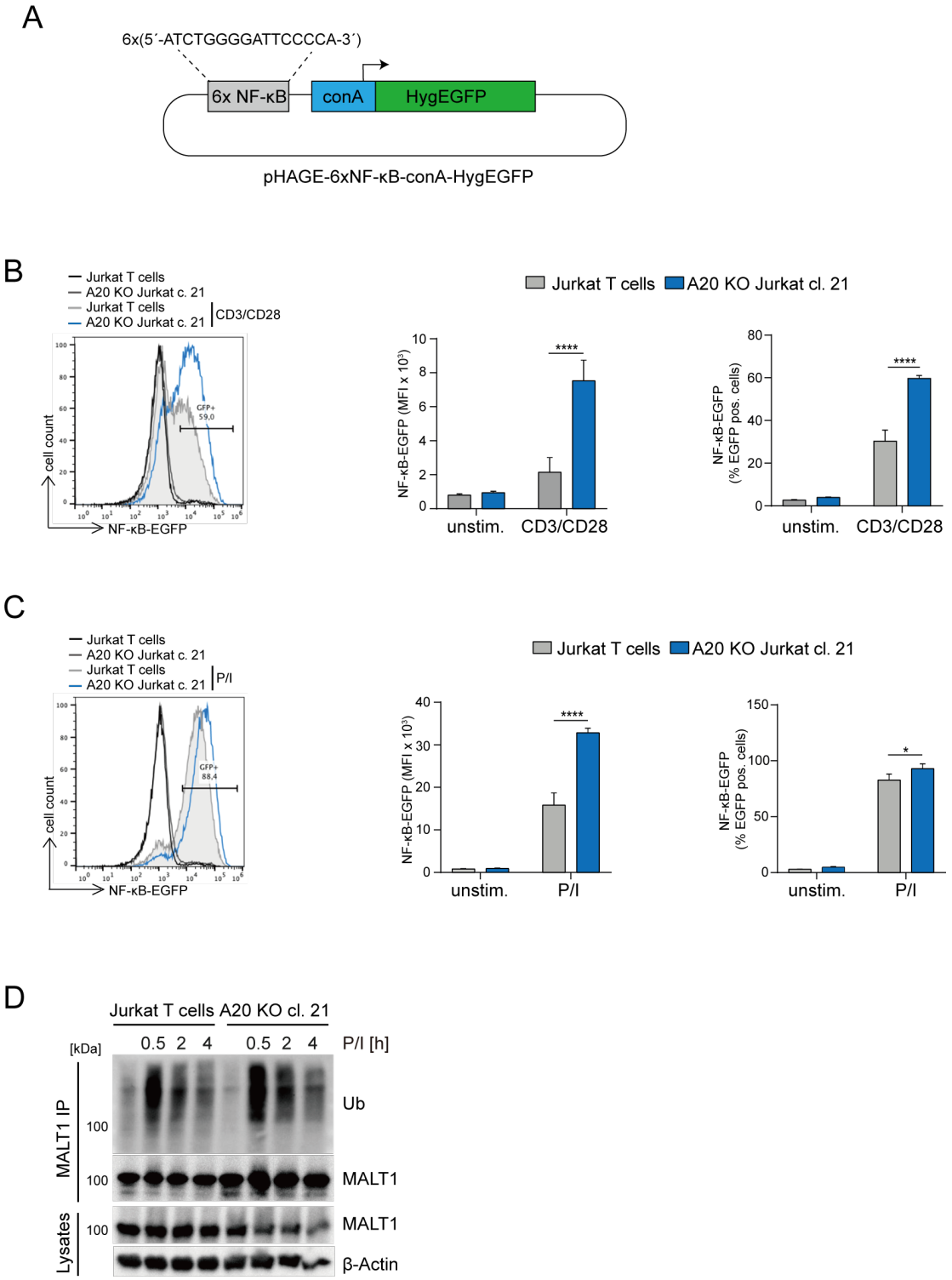

Figure 4-5: A20 deficiency enhanced NF-κB activation.

A, Simplified schematic of NF-κB-EGFP reporter plasmid. The lentiviral NF-κB-EGFP reporter was created by adding six copies of the NF-κB/Rel-binding site of the immunoglobulin κ (Igκ) light chain enhancer and the conalbumin (cona) minimal promoter with a hygromycin-EGFP-fusion gene, resulting in NF-κB-dependent expression of EGFP. **B, C** Flow cytometry analysis of activation of the NF-κB-EGFP reporter in Jurkat T cells and A20 deficient Jurkat T cells upon CD3/CD28 (B) or P/I (C) stimulation (4 h). The MFI and EGFP positive cells were calculated for quantification. The data are shown as means ± SEM (n=3) and quantification was performed using a two-way ANOVA with Tukey's multiple comparisons test, as indicated above. *$p < 0.05$, ****$p < 0.0001$. **D,** MALT1 polyubiquitination was determined in parental Jurkat T cells and A20 defective Jurkat T cells upon P/I stimulation using MALT1 IP. Panel B, C, D have been published in Yin et al, Cell Mol Life Sci, 2022, 79:112

To investigate the effect of ABIN-1 deficiency in Jurkat T cells, we used a similar approach and transduced the viral NF-κB-EGFP reporter into parental and ABIN-1 (clone 34) KO Jurkat T cells. Here, we found that, similar to A20-deficient cells, ABIN-1 deficiency augmented NF-κB activation after P/I or CD3/CD28 stimulation **(Figure 4-6 A and B)**. And lack of ABIN-1 also resulted in a robust poly-ubiquitination of MALT1 upon P/I stimulation **(Figure 4-6 C)**.

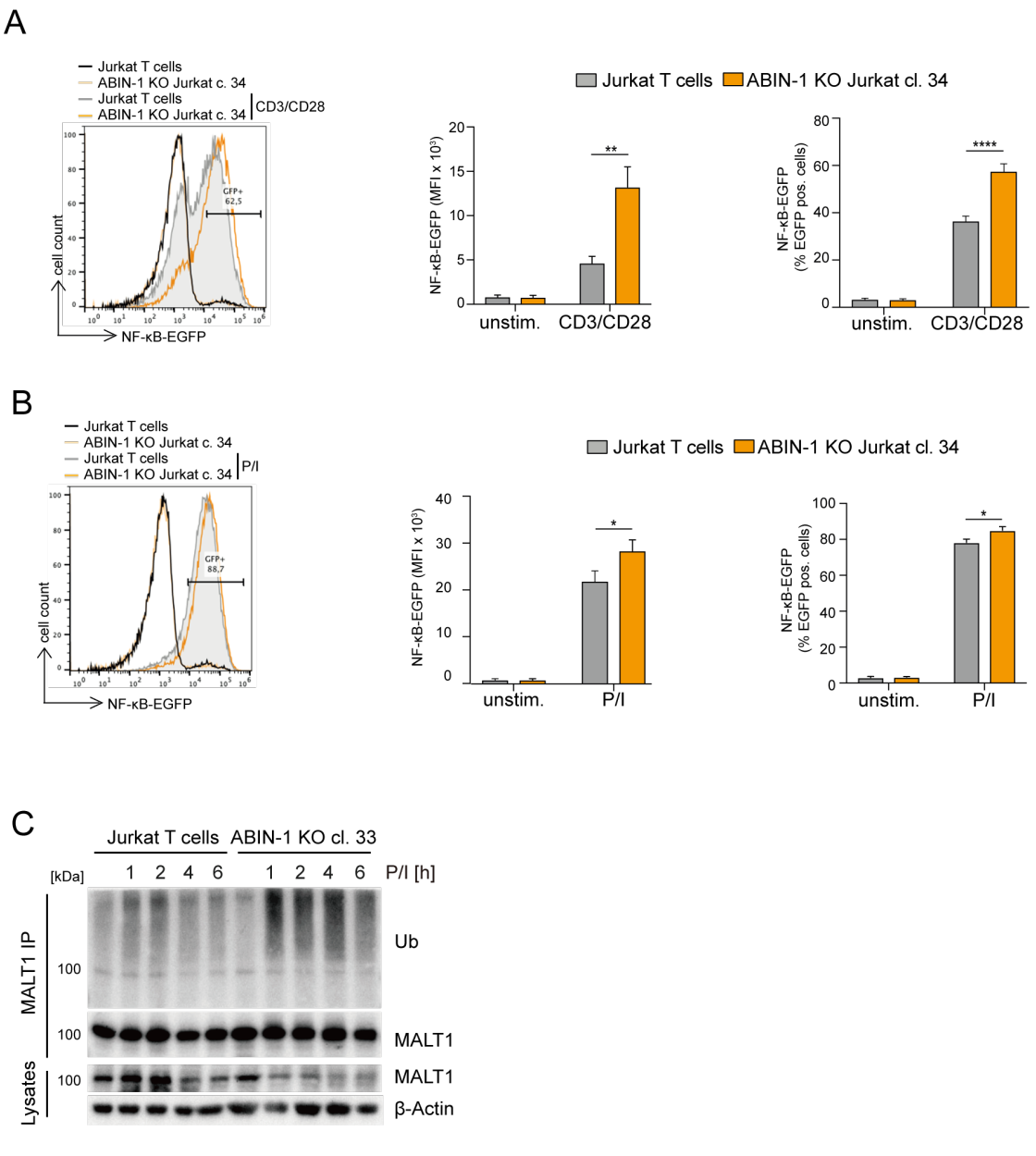

Figure 4-6: ABIN-1 deficiency enahnces NF-κB activation.

A, B Flow cytometry analysis of activation of the NF-κB-EGFP reporter activation in Jurkat T cells and ABIN-1 deficient Jurkat T cells upon CD3/CD28 (A) or P/I (B) stimulation (4 h). The MFI and EGFP positive cells were calculated for quantification. The data are presented as means ± SEM (n=3) (A) or (n=5) (B) and quantification was performed using a two-way ANOVA with Tukey's multiple comparisons test, as indicated above. *p < 0.05, **p < 0.01, ****p < 0.0001. **C,** MALT1 polyubiquitination was determined in parental and ABIN-1 KO Jurkat T cells upon P/I stimulation using MALT1 IP. Panel A, B, C have been published in Yin et al, Cell Mol Life Sci, 2022, 79:112

To study the effect of of A20 or ABIN-1 deficiency on NF-κB signaling upon TNFα stimulation, we treated parental as well as A20 or ABIN-1 KO Jurkat T cells with TNFα for 4 h and monitored the EGFP-positive cells as well as MFI by FACS. As demonstrated in **Figure 4-7 A**,

following 4 h of TNFα treatment, the MFI and EGFP-positive cells were significantly enhanced in A20 KO Jurkat T cells, indicating substantially increased NF-κB activation. Additionally, we detected no difference in NF-κB activation in ABIN-1-deficient Jurkat T cells versus parental Jurkat T cells in response to TNFα stimulation **(Figure 4-7 B)**. However, A20 KO Jurkat T cells showed increased p-IκBα to IκBα ratios compared to parental cells, arguing for an increased IκBα turnover upon prolonged TNFα stimulation and ABIN-1 has no effect for the NF-κB activation after TNFα stimulation **(Figure 4-7 C)**. Thus, while the data confirm that A20 suppresses TNFα-induced NF-κB activation, whereas ABIN-1 deficiency does not significantly elevate NF-κB signaling and gene expression, which is in line with previous results obtained for TNFα signaling in A20$^{-/-}$ ABIN-1$^{-/-}$ murine embryonal fibroblasts[170].

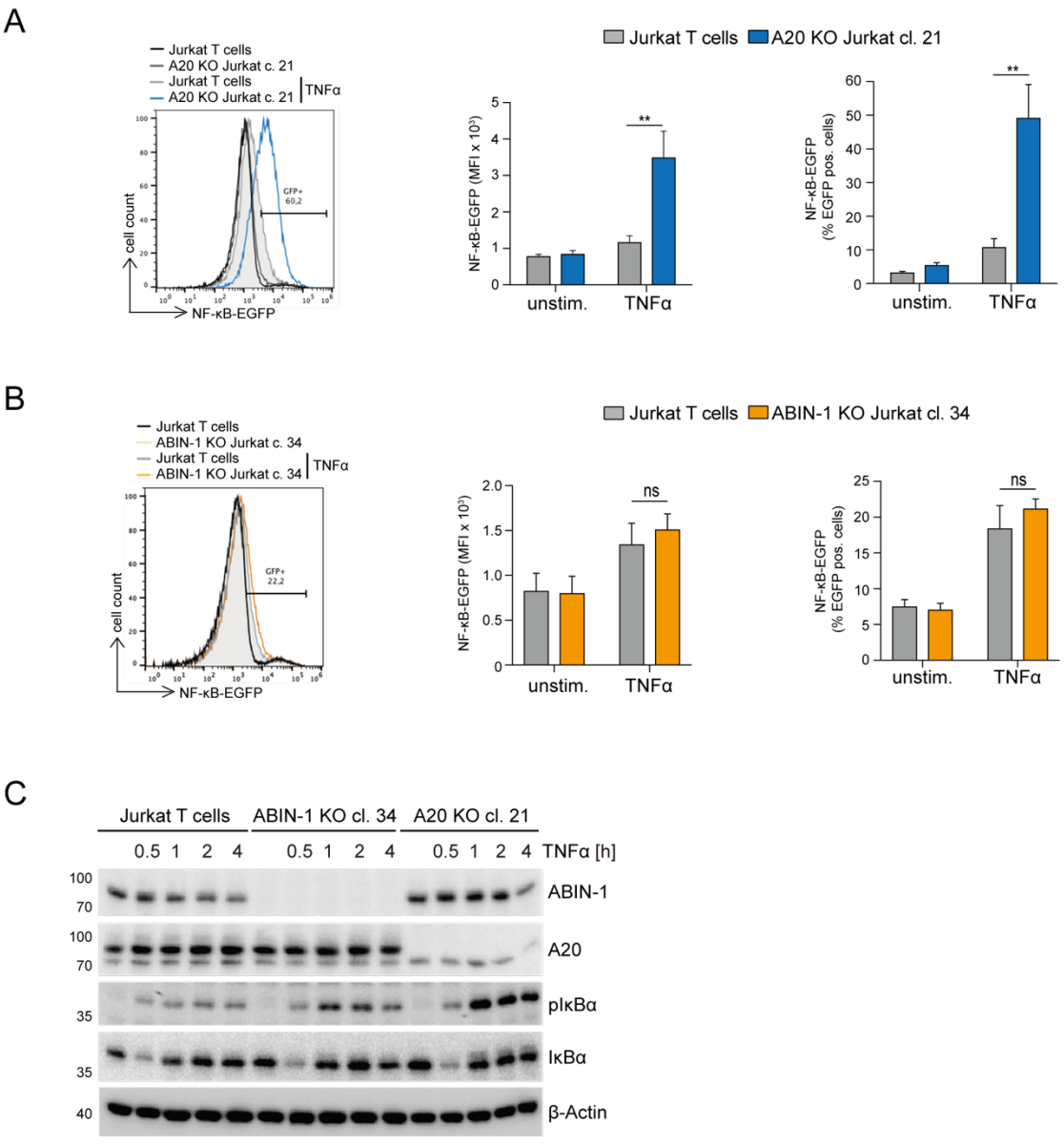

Figure 4-7: ABIN-1 and A20 deficiency enhances NF-κB activation upon TNFα stimulation.
A, B Flow cytometry analysis of NF-κB-EGFP reporter activation in parental and A20 (A) or ABIN-1 (B) deficient Jurkat T cells following TNFα treatment (4 h). The MFI and the EGFP positive cells were calculated for quantification. The data are shown as means ± SEM (n=3) (A) or (n=4) (B), respectively, and quantification was performed using a two-way ANOVA with Tukey's multiple comparisons test, as indicated above comparisions. ns=non-significant, **p < 0.01. **C,** Western blot analysis of NF-κB activation in Jurkat T cells and A20 or ABIN-1-deficient Jurkat T cells upon TNFα stimulation.

4.4 Inhibition of human primary T cell activation by ABIN-1 and A20

To elucidate the function of ABIN-1 and A20 in the control of T cell activation, we established KO primary T cells using the same targeting strategy used in Jurkat T cells. Transfection of ABIN-1 and A20 sgRNAs efficiently eliminated the ABIN-1 and A20 proteins from pools of primary human CD4 T cells, respectively **(Figure 4-8 A)**. The production of cytokines following co-stimulation of T cells was examined. On single cell level, the number of IL-2 and TNFα generating CD4 T cells was increased in either ABIN-1 or A20 KO conditions. Thus, an increase in IL-2 extracellular secretion was seen following TCR/CD28 stimulation, suggesting that both proteins operate as antagonists in primary human CD4 T cells, limiting effector responses **(Figure 4-8 B-D)**.

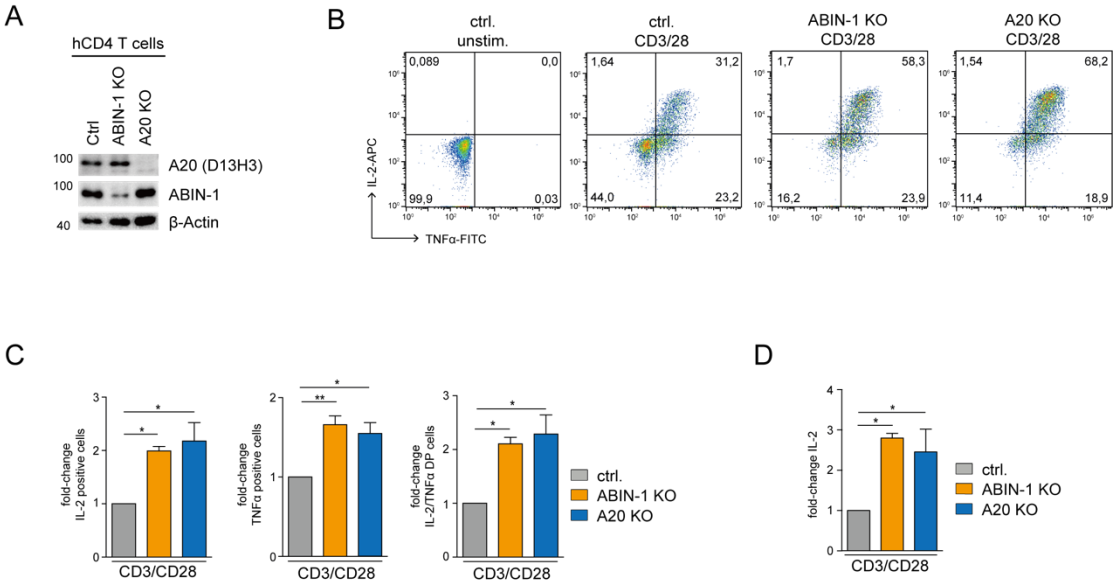

Figure 4-8: ABIN-1 and A20 depletion boosts effector responses in primary human CD4 T cells.

A, Western blot analysis of ABIN-1 and A20 expression in primary human CD4 T cells following CRISPR/Cas9 technology-mediated deletion. **B,** Flow cytometry was used to assess intracellular labeling of IL-2 and TNFα generation in ABIN-1 or A20 deficient primary human CD4 T cells following 4 h of CD3/CD28 stimulation. **C,** The fold change in IL-2, TNFα and IL-2/TNFα positive cells was quantified from three seperate experiments as shown in **B**. **D,** The fold change in IL-2 secretion was quantified by ELISA in the supernatant of ABIN- 1 and A20-deficient primary human CD4 T cells primed with CD3/CD28 for 18 h in three seperate experiments. The data are presented as means ± SEM (n=3) and quantification was performed using one-way ANOVA with Dunnett's multiple comparisons test, as shown above comparisons. *$p < 0.05$, **$p < 0.01$. CRISPR/Cas9 KO in primary human CD4 T cells was performed by Ying-Yin Chao of Christina Zielinski laboratory. Panel A, B, C, D have been published in Yin et al, Cell Mol Life Sci, 2022, 79:112

4.5 TCR-induced MALT1 protease activation is inhibited by ABIN-1 and A20

Since MALT1 protease is required for the maintenance of CBM signaling, we checked the effects of ABIN-1 or A20 KO on MALT1 protease activity in Jurkat T cells by pull-down (PD) assays. Therefore we used a biotin-coupled activity-based-probe (ABP) that covalently modifies and binds MALT1's active center upon MALT1 activation[183]. PD assays demonstrated that TCR/CD28 or P/I stimulation boosted and prolonged MALT1 protease activity in ABIN-1 and A20 KO Jurkat T cells **(Figure 4-9 A-D)**. Because Pelzer et al.[108] demonstrated that the paracaspase MALT1's protease activity is controlled by monoubiquitination, we pre-treated Jurkat T cells, A20 KO Jurkat T cells, and ABIN-1 KO Jurkat T cells with the highly selective allosteric MALT1 paracaspase inhibitor MLT-985[184] to see if this increased MALT1 protease activity is mediated by MALT1 monoubiquitination. In line, MALT1 mono-ubiquitination, which functions as an essential signal for MALT1 protease activation[108], was increased in ABIN-1 and A20 deficient Jurkat T cells upon CD3/CD28 stimulation **(Figure 4-9 E and F)**. The data reveal that ABIN-1 and A20 have a substantially comparable inhibitory effect on CBM-induced NF-κB activation in T cells, indicating a cooperative mechanism of action.

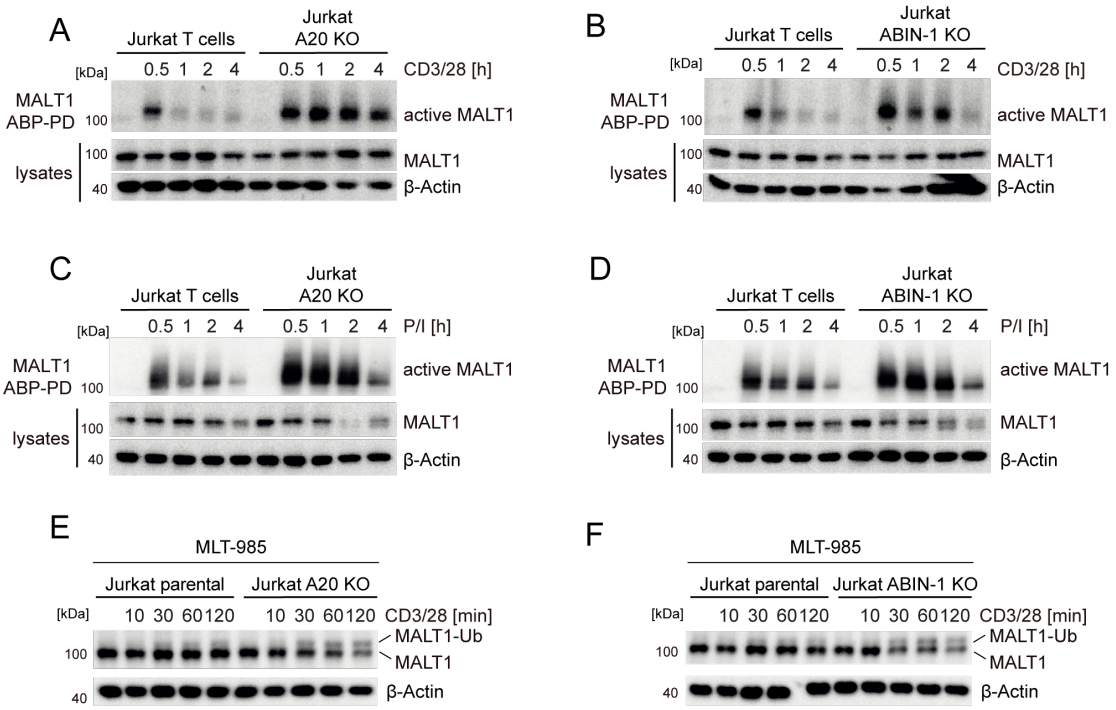

Figure 4-9: Restriction of MALT1 protease activity by ABIN-1 and A20.
A, B MALT1-ABP PD assay and Western blot were used to identify active MALT1 in parental and A20 (A) or ABIN-1 (B) deficient Jurkat T cells upon CD3/CD28 stimulation. **C, D** MALT1-ABP PD assay and Western blot were used to identify active MALT1 in parental and A20 (C) or ABIN-1 (D) KO Jurkat T cells following P/I stimulation. **E, F** Western blot analysis revealed MALT1 monoubiquitination following treatment with the MALT1 protease inhibitor MLT-985. Panel A, B, E, F have been published in Yin et al, Cell Mol Life Sci, 2022, 79:112

4.6 TCR-induced NF-κB signaling and MALT1 protease activity are inhibited by ABIN-1 via A20

To determine if and how A20 and ABIN-1 cooperate to disrupt the CBM complex´s activities, we examined whether ABIN-1 and A20 can recruit to the CBM complex in an independent way. ABIN-1 and A20 are recruited to the BCL10 after 20 min CD3/CD28 or P/I stimulation, and the binding between A20 and BCL10 can still be detected in Jurkat T cells lacking ABIN-1 (**Figure 4-10 A and B**). Absence of ABIN-1 had no effect on the formation of the CBM complex or the recruitment of A20 to the CBM complex. We also observed that when BCL10 IP was performed in the absence of A20 upon CD3/28 or P/I stimulation, ABIN-1 was unable to interact with BCL10, demonstrating that A20 acts as a bridge for the interaction of ABIN-1

to the CBM complex. Absence of A20 had no effect on BCL10-CARD11 interaction, indicating that CBM upstream signaling remained intact **(Figure 4-10 C and D)**.

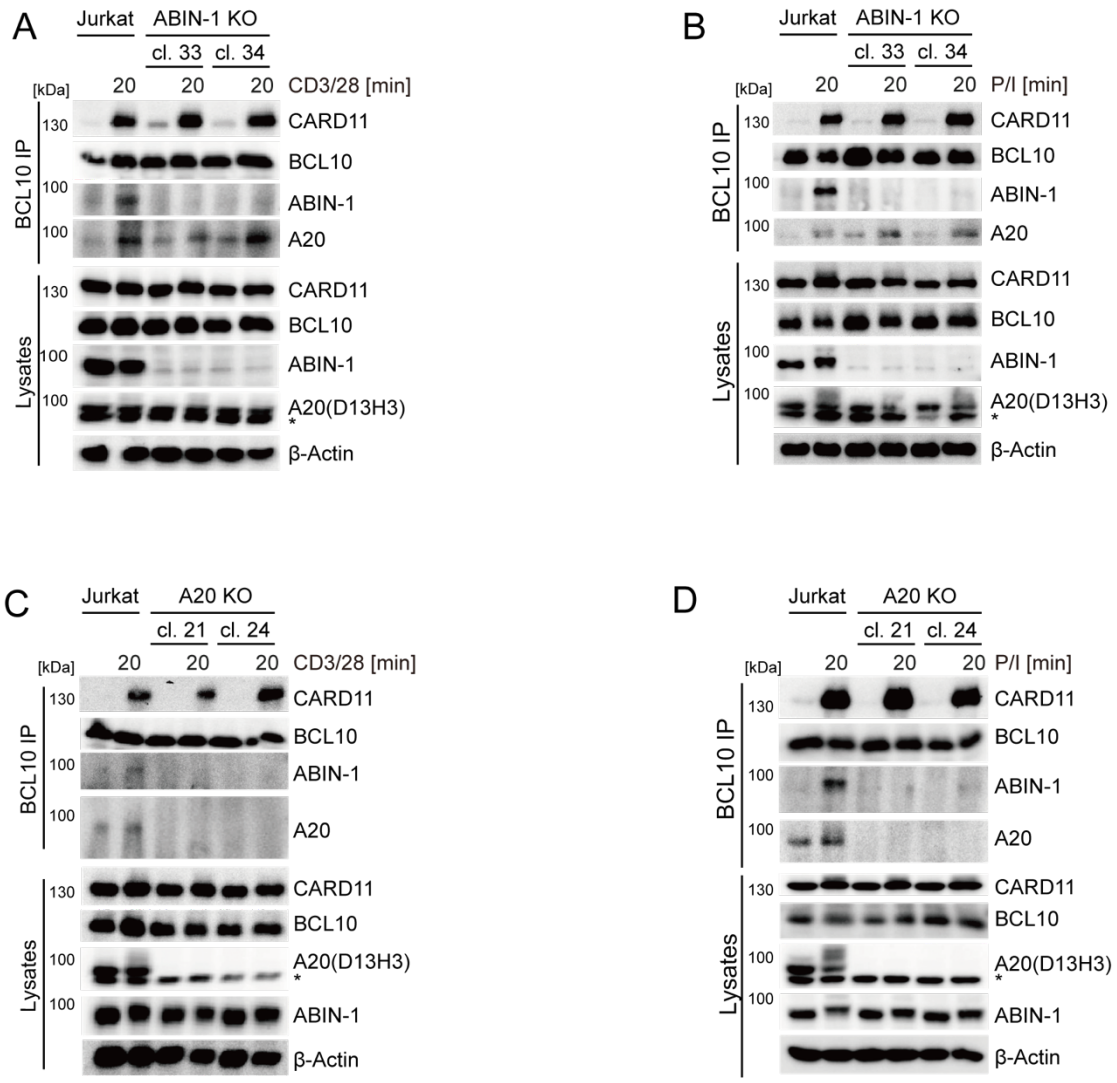

Figure 4-10: ABIN-1 and A20 are recruited to the CBM complex.
A, B Western blot was used to detect the binding of BCL10 to CARD11, ABIN-1 and A20 in and ABIN-1 deficient Jurkat T cells following BCL10 IP and stimulation with CD3/CD28 (A) or P/I (B). **C, D** Western blot was used to detect the binding of BCL10 to CARD11, ABIN-1 and A20 in parental and A20 deficient Jurkat T cells after BCL10 IP and stimulation with CD3/CD28 (C) or P/I (D). Panel A, B, C, D have been published in Yin et al, Cell Mol Life Sci, 2022, 79:112

To demonstrate that the absence of ABIN-1 results in increased NF-κB signaling induced by the CBM complex, we reconstituted ABIN-1 WT construct and overexpressed A20 WT construct in ABIN-1 KO Jurkat T cells to investigate the putative functional interdependence

of ABIN-1 and A20. In ABIN-1-deficient Jurkat T cells, staining for the co-expressed surface marker ΔCD2 showed that all constructs were transduced in a homogeneous manner **(Figure 4-11 A)**. Expression of FS-tagged ABIN-1 and A20 resulted in slightly elevated expression compared to the endogenous levels, showing a mildly overexpressed transduced construct (Figure 4-11 B). We determined the time course of induction of the NF-κB-EGFP reporter gene upon CD3/CD28 stimulation. Reconstitution of ABIN-1 significantly lowered the increase in CD3/CD28 induced NF-κB activation in Jurkat T cells lacking ABIN-1. Additionally, overexpression of A20 markedly decreased NF-κB activation in ABIN-1 KO Jurkat T cells upon CD3/CD28 stimulation, demonstrating that overexpression of A20 sidesteps the requirement for ABIN-1 in repressing NF-κB activation **(Figure 4-11 C)**.

Following that, we examined the impacts of reconstitution or overexpression of ABIN-1 and A20 on MALT1 protease activation in ABIN-1-deficient Jurkat T cells. MALT1-ABP PD assays demonstrated that either rescuing ABIN-1 or overexpressing A20 impairs CD3/28-induced MALT1 protease activity in Jurkat T cells lacking ABIN-1 **(Figure 4-11 D)**. To determine if this increased MALT1 protease activity resulted in greater substrate cleavage, we checked CYLD and HOIL-1 expression and cleavage band in ABIN-1 deficient Jurkat T cells transfected with ABIN-1 or A20, respectively. We quantified the impact of ABIN-1 and A20 on substrate cleavage by determining the ratio of the cleavage product to the corresponding full-length. The expression of ABIN-1 has been found to diminish CYLD and HOIL-1 cleavage following reconstitution. Additionally, overexpression of A20 inhibited CYLD and HOIL-1 cleavage in ABIN-1-deficeint Jurkat T cells **(Figure 4-11 E and F)**. Taken together, overexpression of A20 can inhibit downstream cascades triggered by the CBM complex in the absence of ABIN-1.

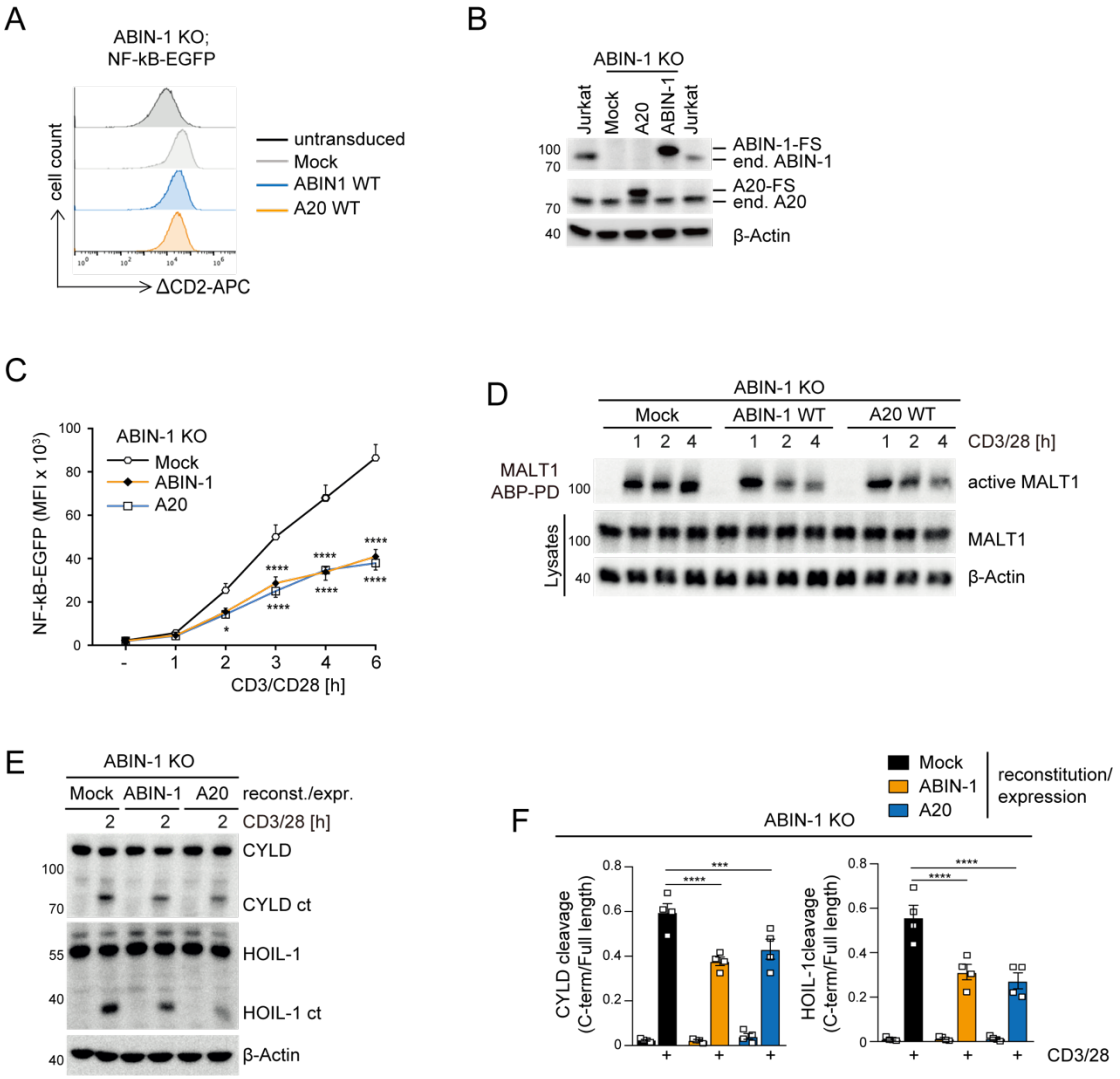

Figure 4-11: A20 counteracts CBM-mediated signaling independent of ABIN-1.

A, Transduction of ABIN-1 or A20 in ABIN-1 KO NF-κB-EGFP reporter Jurkat T cells was tracked by by flow cytometry using the surface-marker hΔCD2. **B,** Western blot analysis of ABIN-1 and A20 expression in parental and ABIN-1-deficient Jurkat T cells following lentiviral transduction. **C,** Flow cytometry analysis of NF-κB-EGFP reporter activation in transduced ABIN-1-deficeint Jurkat T cells upon CD3/CD28 stimulation (1 - 6 h). The median fluorescence intensity (MFI) was calculated for quantification. The data are shown as means ± SEM (n=4) and quantification was performed using a two-way ANOVA with Dunnett's multiple comparisons test in comparison to the Mock group. *$p < 0.05$, ****$p < 0.0001$. **D,** MALT1 activity was determined using the ABP-PD assay and Western blot in ABIN-1 KO Jurkat T cells transduced with ABIN-1 or A20 construct following CD3/CD28 stimulation. **E,** The cleavage of CYLD and HOIL-1 was identified by western blot analysis in ABIN-1 deficient Jurkat T cells transfected with ABIN-1 or A20 upon CD3/CD28 stimulation (2h). **F,** Densitrometric analysis was used to assess the effect of ABIN-1 or A20 reconstitution/expression on MALT1 substrate cleavage. The data indicate the mean ± SEM (n=4), and quantification was performed using a two-way ANOVA with Dunnett's multiple comparisons test in comparison to the Mock group. ns=non-significant, ***$p < 0.001$, ****$p < 0.0001$. Panel A-F have been published in Yin et al, Cell Mol Life Sci, 2022, 79:112

Next, we reconstituted or overexpressed A20 and ABIN-1 WT constructs in A20 KO Jurkat T cells to identify the potential interdependence and effect of ABIN-1 and A20 in this setting. The co-expressed surface marker ΔCD2 demonstrated that all constructs were transduced in A20 KO Jurkat T cells **(Figure 4-12 A)**. The transduced constructs ABIN-1 WT and A20 WT were found to be mildly overexpressed in A20 KO Jurkat T cells **(Figure 4-12 B)**. The time course of NF-κB-EGFP reporter gene activation following CD3/CD28 stimulation demonstrated that reconstitution of A20 WT construct successfully reduced the increase in CD3/28-induced NF-κB activation in A20 KO Jurkat T cells. ABIN-1 overexpression, on the other hand, had no effect on NF-κB activation in A20 KO Jurkat T cells **(Figure 4-12 C)**. This implies that the inhibitory function of ABIN-1 is dependent on A20.

In addition, we checked the impact of reconstitution or overexpression of ABIN-1 and A20 on MALT1 protease activation in ABIN-1-deficient Jurkat T cells. MALT1 ABP- PD assays demonstrated that only A20 rescue inhibited CD3/28-induced MALT1 protease activity, whereas ABIN-1 reconstitution had no effect on MALT1 protease activity in A20-deficient Jurkat T cells **(Figure 4-12 D)**. MALT1 cleavage of the substrates CYLD and HOIL-1 were also evaluated in A20 KO Jurkat T cells after A20 WT construct reconstitution or overexpression of ABIN-1. Only the rescue of A20 can inhibit cleavage of CYLD and HOIL-1, but not overexpression of ABIN-1, by assessing the ratio of the cleavage product to the corresponding full-length protein **(Figure 4-12 E and F)**. Therefore, overexpression of ABIN-1 had no effect on NF-κB activation in Jurkat T cells lacking A20, suggesting that ABIN-1´s negative regulatory role is entirely dependent on the presence of A20.

Taken together, these data indicate that A20 overexpression can attenuate CBM complex-induced downstream processes independent of ABIN-1, whereas ABIN-1 relies only on A20 to counteract NF-κB activation and MALT1 protease activity.

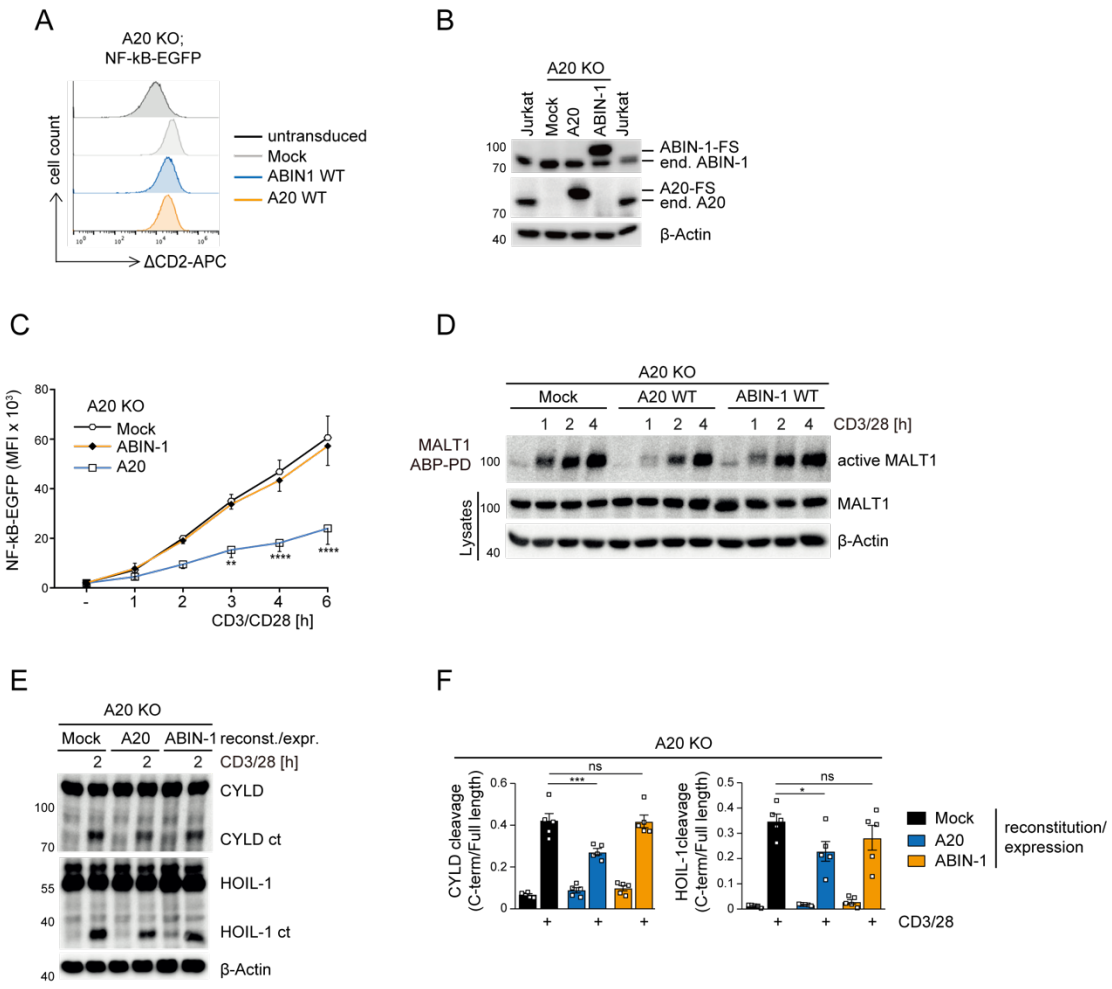

Figure 4-12: Inhibitory function of ABIN-1 is dependent on A20.

A, Transduction of ABIN-1 or A20 in A20 KO NF-κB-EGFP reporter Jurkat T cells was tracked by flow cytometry using the surface-marker hΔCD2. **B,** Western blot analysis of ABIN-1 and A20 expression in parental and A20 KO Jurkat T cells following lentiviral transduction. **C,** Flow cytometry analysis of NF-κB-EGFP reporter activation in transduced A20-deficient Jurkat T cells upon CD3/CD28 stimulation (1 - 6 h). The median fluorescence intensity (MFI) was calculated for quantification. The data are shown as means ± SEM (n=3) and quantification was performed using a two-way ANOVA with Dunnett's multiple comparisons test in comparison to the Mock group. $^{**}p < 0.01$, $^{****}p < 0.0001$. **D,** MALT1 activity was determined using the ABP-PD assay and Western blot in A20 KO Jurkat T cells transduced with ABIN-1 or A20 construct following CD3/CD28 stimulation. **E,** The cleavage of CYLD and HOIL-1 was checked by western blot in A20 deficient Jurkat T cells transfected with ABIN-1 or A20 upon CD3/CD28 stimulation (2h). **F,** Densitrometric analysis was used to assess the effect of ABIN-1 or A20 reconstitution/expression on MALT1 substrate cleavage. The data indicate the mean ± SEM (n=5), and quantification was performed using a two-way ANOVA with Dunnett's multiple comparisons test in comparison to the Mock group. $^{***}p < 0.001$, $^{****}p < 0.0001$. Panel A-F have been published in Yin et al, Cell Mol Life Sci, 2022, 79:112

4.7 The negative effect of ABIN-1 on CBM signaling is dependent on its interaction with A20

To determine whether A20 binding is essential for ABIN-1 to exert its inhibitory effect, we overexpressed different ABIN-1 mutant constructs in Jurkat T cells. Then, we examined the anti-NF-κB activity of ABIN-1 WT, ABIN-1 lacking the A20 binding domain (ABIN-1 ΔAHD1), and ABIN-1 containing the UBAN-defective mutant (ABIN-1 D472N) **(Figure 4-13 A)**[108,160]. As with previous studies, ABIN-1 association with A20 was eliminated when the AHD1 domain was deleted **(Figure 4-13 B)**[160]. Following lentiviral transduction, Jurkat T cells were infected homogeneously, resulting in overexpression of ABIN-1 WT and mutants that were tagged with FS **(Figure 4-13 C and D)**. TCR/CD28-induced NF-κB-EGFP reporter gene induction was inhibited by ABIN-1 WT or D472N overexpression; however, overexpression of ABIN-1 ΔAHD1 did not inhibit NF-κB activation, indicating that association with A20, but not the binding of ubiquitin via the UBAN, is required for the activity of ABIN-1 **(Figure 4-13 E)**.

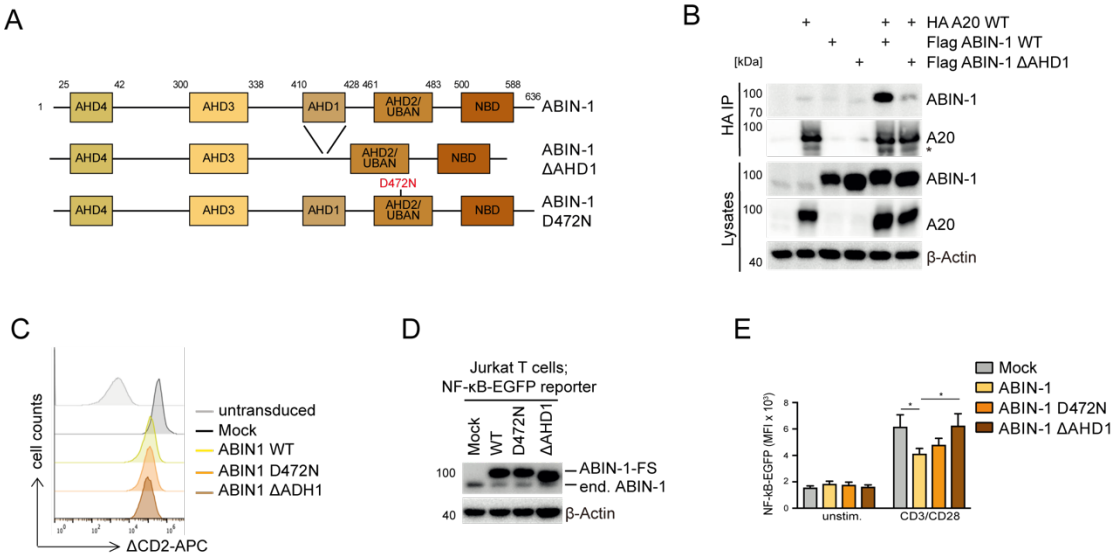

Figure 4-13: ABIN-1 binds A20 via the AHD1 domain and thereby negatively regulates NF-κB-activation.

A, ABIN-1 WT, ΔAHD1 and D472N constructs are depicted schematically. **B,** HA-A20 binding to Flag-ABIN-1 or Flag ABIN-1 ΔAHD1 mt after transfection in HEK 293 cells and HA-IP analyzed by Western blot. **C,** Transduction of ABIN-1 wt and mutants in NF-κB- EGFP reporter Jurkat T cells was tracked by the surface-marker hΔCD2 by flow cytometry. **D,** Western blot analysis of ABIN-1 WT and mutant constructs expressed in Jurkat T cells following transduction. **E,** Flow cytometry analysis of NF-κB-EGFP reporter activation in ABIN-1 WT and mutant constructs transduced Jurkat T cells upon 4h

CD3/CD28 stimulation. The median fluorescence intensity (MFI) was calculated for quantification. The data are present as means ± SEM (n=7), and quantification was performed using a two- way ANOVA with Dunnett's multiple comparisons test, as inducated above. *p < 0.05. Panel A-E have been published in Yin et al, Cell Mol Life Sci, 2022, 79:112

To establish the effect of ABIN-1 mutant constructs on CBM-induced downstream NF-κB signaling, we performed western blot analysis on TCR/CD28-induced IκBα phosphorylation and cleavage of the MALT1 substrates A20 and CYLD. Overexpression of ABIN-1 WT in Jurkat T cells strongly inhibited phosphorylation of IκBα and MALT1-dependent cleavage of A20 and CYLD. **(Figure 4-14 A)**. Comparison between ABIN-1 WT and ABIN-1 AHD1 mutant demonstrated that an intact ABIN-1 AHD1 domain was necessary for regulation of NF-κB signaling and MALT1 protease activity **(Figure 4-14 B)**. Therefore, ABIN-1's antagonistic effect on TCR signaling is dependent on its capacity to interact with A20.

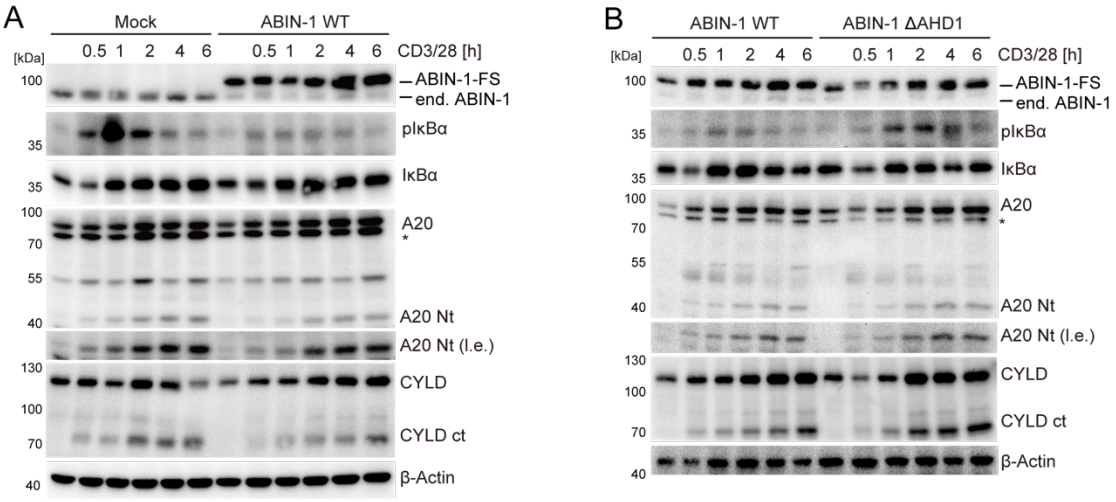

Figure 4-14: ABIN-1´s inhibitory effect on TCR signaling is dependent on its ability to bind to A20. **A,** Western blot analysis was used to compare NF-κB signaling in Jurkat T cells expressing Mock to ABIN-1 WT upon timpoint CD3/CD28 stimulation. **B,** NF-κB signaling in Jurkat T cells expressing ABIN-1 WT and ABIN-1 ΔAHD1 was compared by western blot analysis after stimulation with CD3/CD28. Panel A, B have been published in Yin et al, Cell Mol Life Sci, 2022, 79:112

4.8 Ubiquitin binding to A20 ZnF4 and ZnF7 is required to counteract TCR signaling

Our data show that in A20-deficient Jurkat T cells, ABIN-1 is unable to regulate CBM complex-dependent NF-κB signaling. Thus, we aimed to determine whether the N-terminal OTU domain

of A20, which has the deubiquitinase activity, or the C-terminal ZnF domain, which contains ubiquitin binding activity, are required for ABIN-1 binding and suppressing T cell activation. To do this, we generated A20 mutant constructs with either an OTU domain mutation (C103A:OTU mt) or a ZnF domain mutation at the C-terminus (ZnF4/7 mt: C624/627/779/782A) **(Figure 4-15 A)**[169]. After lentiviral transduction, staining for the co-expressed surface marker ΔCD2 demonstrated that all constructs were transduced in a homogenous manner in A20 KO Jurkat T cells **(Figure 4-15 B)**. A20 WT and mutants were expressed equally and at a level comparable to that found in Jurkat T cells **(Figure 4-15 C)**. A20 WT and OTU mt inhibited NF-κB-EGFP reporter gene induction in response to TCR/CD28 or P/I stimulation, whereas mutation of ZnF4/7 prevented A20 from inhibiting NF-κB activation **(Figure 4-15 D)**. Strep-PD analysis of A20 revealed that ZnF4/7 mutation impairs the capacity of A20 to bind to CARD11 and ABIN-1 in Jurkat T cells activated with P/I **(Figure 4-15 E)**. Thus, A20/ABIN-1 association with the formed CBM complex is dependent on A20's C-terminal ubiquitin binding activity, which is also required to limit NF-κB activation.

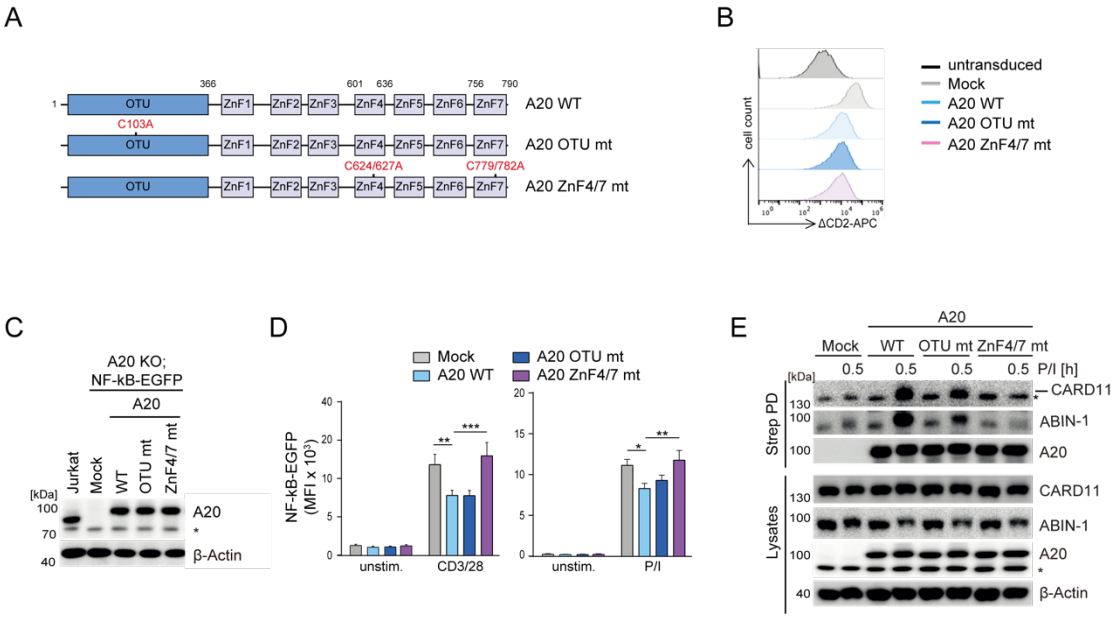

Figure 4-15: A20 ZnF4 and ZnF7 motifs associate with the CBM complex and inhibit NF-κB activation.

A, A20 WT, OTU and ZnF4/7 mutant constructs are depicted schematically. **B,** Transduction of A20 WT and mutants in A20 KO NF-κB-EGFP reporter Jurkat T cells was tracked by flow cytometry using

the surface-marker hΔCD2. **C,** Western blot analysis of A20 WT and mutant constructs following transduction into A20 deficient Jurkat T cells. **D,** Flow cytometry analysis of NF-κB-EGFP reporter activity in A20 deficient Jurkat T cells transduced with A20 WT and mutant constructs upon 4h CD3/CD28 and P/I stimulation. The MFI was calculated to determine the quantification. The data are presented as means ± SEM (n=6), and quantification was performed using two-way ANOVA with Dunnett's multiple comparisons test, as shown above comparisons. *p < 0.05, **p < 0.01, ***p < 0.001. **E,** Western blot was used to check the binding of A20 to CARD11 and ABIN-1 in A20 KO Jurkat T cells expressing A20 WT, A20 OTU mutant, and A20 ZnF4/7 mutant following P/I stimulation using the strep PD assay. Panel A-E have been published in Yin et al, Cell Mol Life Sci, 2022, 79:112

Due to the inefficient recruitment of A20 ZnF4/7 mutant to the CBM complex, we examined the extent to which the mutation of A20 ZnF4/7 impairs A20 cleavage by the MALT1 paracaspase. Interestingly, we discovered that, although A20 WT or A20 OTU mt proteins were cleaved in response to CD3/CD28 or P/I stimulation, the A20 ZnF4/7 mt protein was protected from MALT1-mediated cleavage **(Figure 4-16 A-F)**. By contrast, the reduction of full length CYLD was modestly accelerated in lack of A20 or in the presence of A20 ZnF4/7 mt, indicating that MALT1 protease activation is inhibited by A20 binding to the CBM complex, and A20 ZnF4/7 mt does not result in a general impairment in MALT1 protease activity. We examined ABIN-1 expression in A20 KO Jurkat T cells and found that it was not significantly affected following CD3/CD28 or P/I stimulation. However, reconstitution of A20 resulted in a sustained decline in ABIN-1 levels in response to CD3/CD28 stimulation and a fast decrease of nearly the entire ABIN-1 pool following P/I stimulation **(Figure 4-16 A and B)**. The reduction in ABIN-1 was conditional on the presence of the A20 ZnF4/7 domain, while the OTU domain at the A20 N-terminus had no effect on this reduction. This result suggests that the A20 C-terminal region, which is involved in ubiquitin and ABIN-1 binding, may contribute to the instability of ABIN-1 following T cell activation **(Figure 4-16 C-F)**.

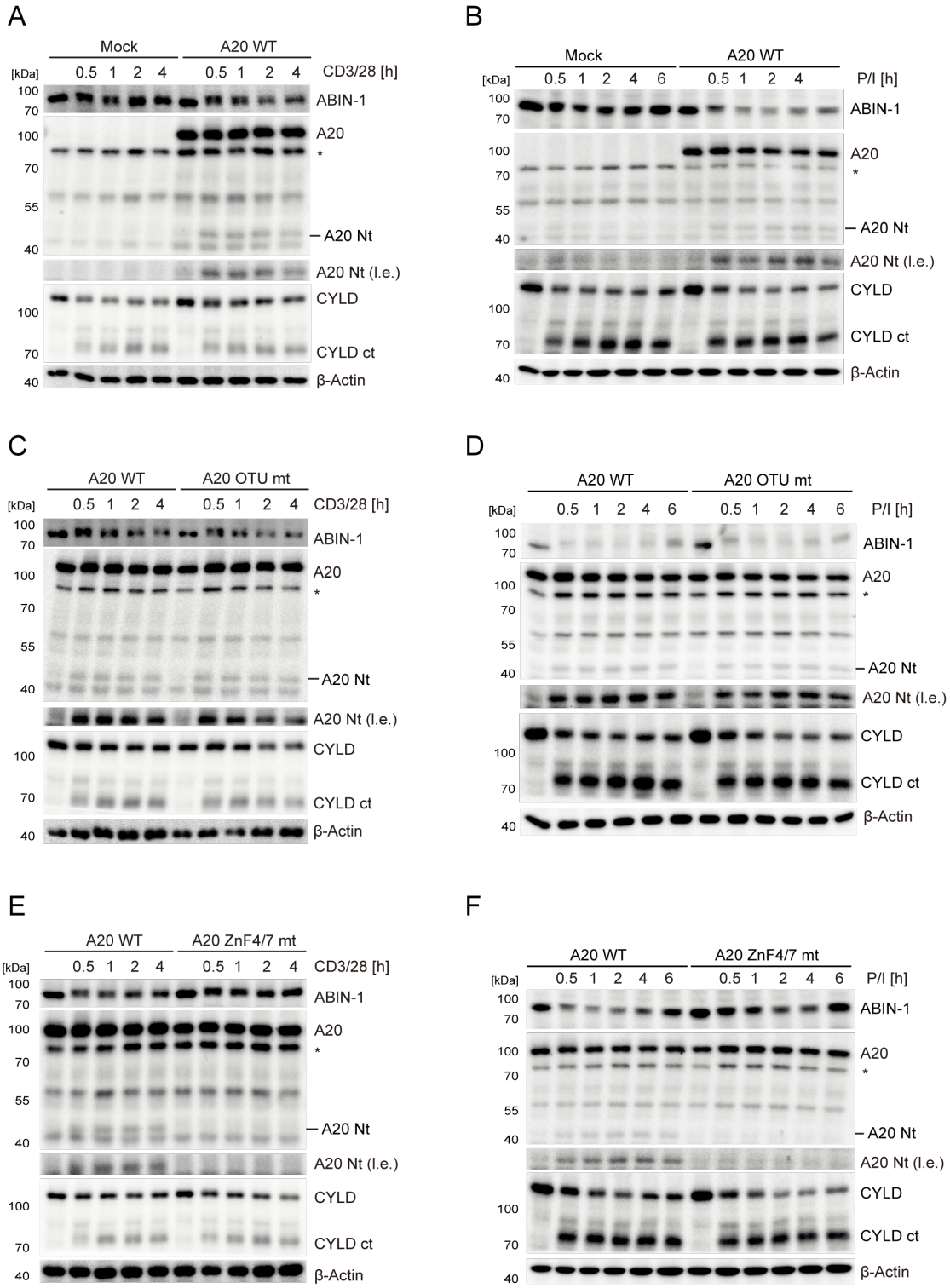

Figure 4-16: A20 ZnF4/7 domain mediate A20 cleavage and ABIN-1 decline.

A-F, Western blot analysis of ABIN-1 stability and A20 cleavage by MALT1 paracaspase in Jurkat T cells expressing A20 WT, OTU mutant, or ZnF4/7 mutant following CD3/CD28 or P/I stimulation. Nt represents N-terminal fragment of A20. l.e. = longer exposure. Panel A-F have been published in Yin et al, Cell Mol Life Sci, 2022, 79:112

4.9 Crosstalk between A20 and ABIN-1 regulates T cell signaling

Given the rapid depletion of ABIN-1 protein levels upon stimulation in Jurkat T cells, we wanted to further investigate the exact post-translational processes that control the protein expression and stability of ABIN-1 and A20. Transcripts of ABIN-1 were not induced by T cell activation or changed in A20 KO Jurkat T cells **(Figure 4-17 A)**. NF-κB-dependent transcriptional activation resulted in the increase of *A20/TNFAIP3* mRNA after CD3/CD28 stimulation as part of a negative feedback loop, which was amplified even more in Jurkat T cells lacking ABIN-1 **(Figure 4-17 A)**. ABIN-1 degradation following CD3/CD28 or P/I stimulation in Jurkat T cells was inhibited by MG132 treatment, suggesting that ABIN-1 is susceptible to proteasomal degradation in response to antigenic stimulation **(Figure 4-17 B and C)**. As previously shown, A20 protein first decreased after 30 min of CD3/CD28 or P/I stimulation, with initial A20 degradation mediated by the proteasome. However, induction of TNFAIP3/A20 transcripts promoted re-synthesis of A20 at 1-6 h post stimulation. Increased A20 expression was impaired by proteasomal inhibition, which also effectively inhibits IκBα degradation and thus NF-κB activation[129] **(Figure 4-17 B and C)**.

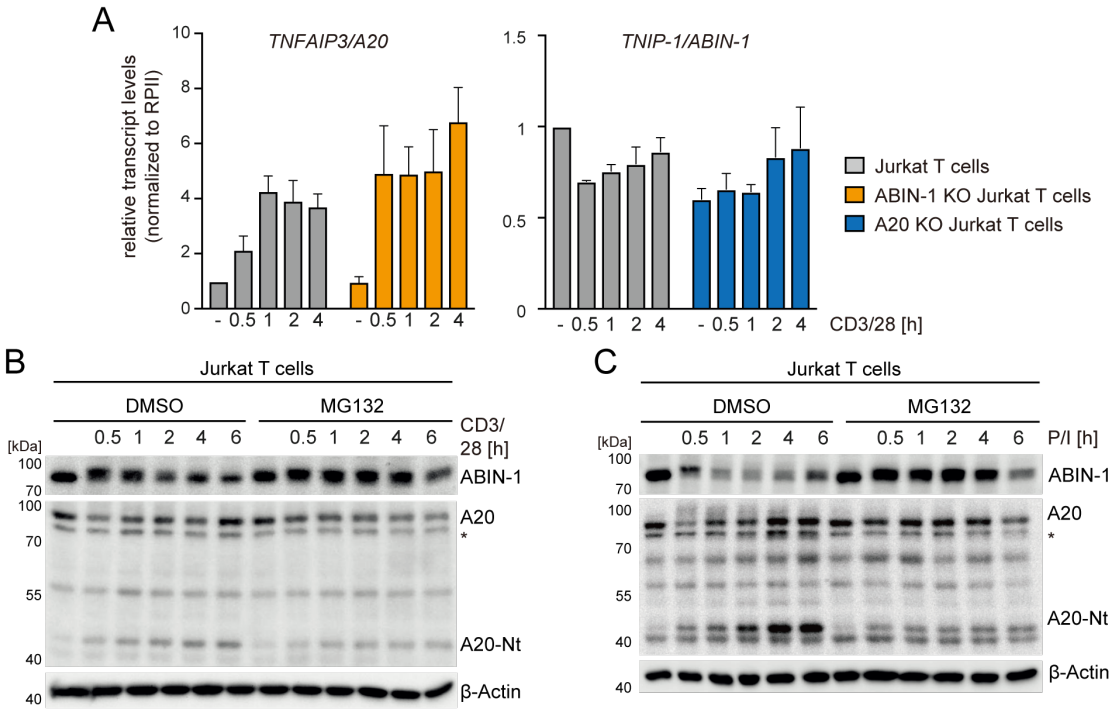

Figure 4-17: Crosstalk between A20 and ABIN-1 controls T cell signaling.

A, Analyses of mRNA expression induction of A20/TNFAIP3 and ABIN-1/TNIP1 in parental and A20 and ABIN-1-deficient Jurkat T cells upon CD3/CD28 stimulation. mRNA levels of RPII were used to normalize transcripts. The data shows mean ± SEM (n=3). **B, C** Western blot analysis of the stability of ABIN-1 and A20 in Jurkat T cells following CD3/CD28 (B) or P/I (C) stimulation with the proteasome inhibitor MG132 (25 μM) pretreatment. Panel A-C have been published in Yin et al, Cell Mol Life Sci, 2022, 79:112

To evaluate the CBM complex´s participation in the regulation of ABIN-1 and A20 degradation, we evaluated the expression of ABIN-1 and A20 in CARD11-deficient Jurkat T cells. The production of ABIN-1 protein in CARD11 defective Jurkat T cells is stable after P/I or CD3/CD28 stimulation. The initial decreased A20 in Jurkat T cells was likewise raised in CARD11 KO Jurkat T cells after 30 min of stimulation **(Figure 4-18 A and B)**. We stimulated parental Jurkat T cells and Jurkat T cells lacking BCL10 with P/I to see if BCL10 deficiency affects ABIN-1 and A20 expression. Strikingly, we discovered that both ABIN-1 and A20 were not degraded in BCL10 KO Jurkat T cells **(Figure 4-18 C)**. Additionally, MALT1 deficient Jurkat T cells also lacked the capacity to degrade ABIN-1 and A20 **(Figure 4-18 D)**. The data indicates that the formation and presentation of a functioning CBM complex is essential to initiate proteasomal degradation of both ABIN-1 and A20.

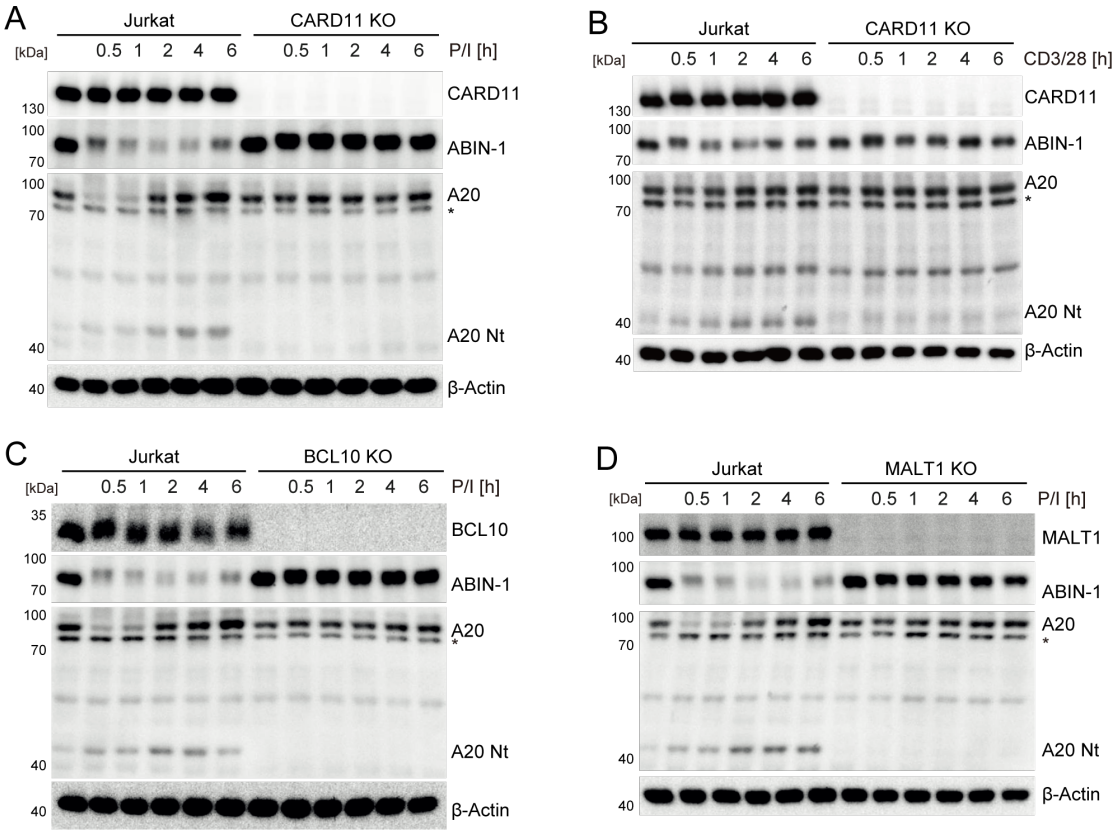

Figure 4-18: CBM complex is required for ABIN-1 and A20 protein degradation.
A, B Western blot were used to check the stability of ABIN-1 and A20 in parental, CARD11-deficient Jurkat T cells following P/I (A) or CD3/CD28 (B) stimulation. **C, D** Western blot analysis of ABIN-1 and A20 stability following P/I stimulation in parental, BCL10-deficient, and MALT1-deficient Jurkat T cells. Panel A, C, D have been published in Yin et al, Cell Mol Life Sci, 2022, 79:112

4.10 TRAF6 and LUBAC are essential for ABIN-1 and A20 degradation

Since the formation of the CBM complex is required for the degradation of ABIN-1 and A20, we aimed to determine whether the E3 ligase TRAF6 and the LUBAC components HOIP and HOIL-1 are also involved in A20 and ABIN-1 protein degradation. TRAF6 and LUBAC can form K63- or M1- linked Ub chains on MALT1 and BCL10, respectively. Eliminating TRAF6 prevented ABIN-1 and A20 degradation, however deletion of the LUBAC subunits HOIP or HOIL-1 only have a minor effect on the stability of ABIN-1 and A20 **(Figure 4-19 A-C)**. By comparing the HOIP, TRAF6 single KO Jurkat T cells to HOIP/TRAF6 double KO Jurkat T cells, we further confirmed that the removal and degradation of A20 and ABIN-1 is mostly dependent on TRAF6 protein **(Figure 4-19 D)**. To investigate if RIP1 was also involved in the stability of ABIN-1 and A20, we pretreated cells with cIAP1 inhibitor. Since cIAP1 is an anti-

apoptotic protein, it directly ubiquitinates RIP1 and increases RIP1 ubiquitination of RIP1 in cancer cells. When cIAP1 ubiquitinates RIP1, the NF-κB signaling pathway is activated. In this scenario, we utilized a cIAP1 inhibitor to ensure that RIP1 remained nonubiquitinated. Depletion of cIAP1 the birinapant had no effect on ABIN-1 and A20 degradation, indicating that cIAPs are not involved in these two protein stabilizing processes **(Figure 4-19 E)**. Thus, proteasomal degradation of ABIN-1 and A20 is mostly dependent on the formation of the CBM complex and the E3 ligase TRAF6, but also on the LUBAC components HOIL-1 and HOIP.

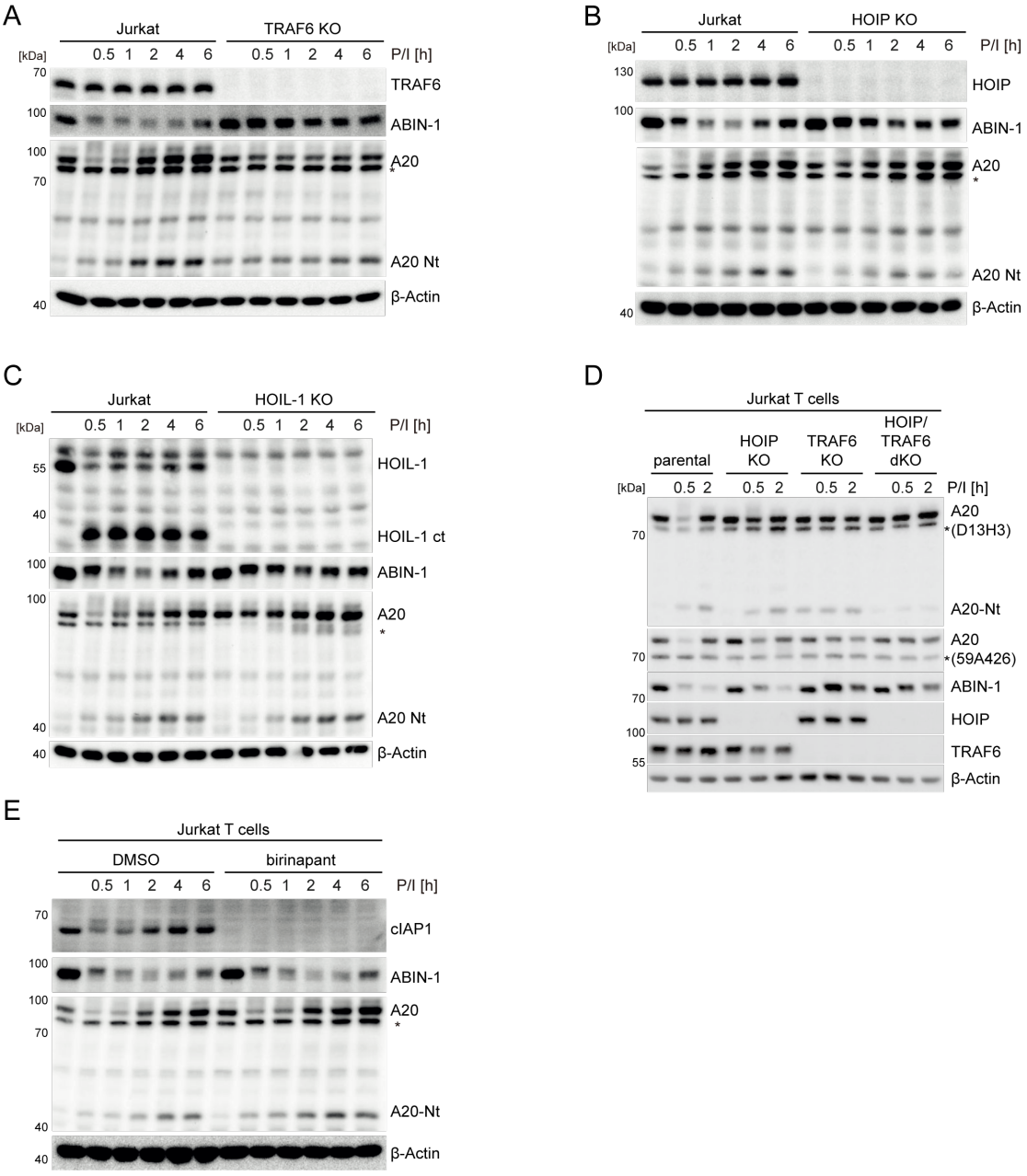

Figure 4-19: TRAF6 and LUBAC are required for the proteasomal degradation of ABIN-1 and A20.

A, Western blot analysis of ABIN-1 and A20 stability in parental Jurkat T cells and TRAF6-deficient Jurkat T cells after P/I stimulation. **B, C, D** Western blot analysis of the stability of ABIN-1 and A20 in parental Jurkat T cells, HOIP-deficient, HOIL-1-deficient or HOIP/ TRAF6-deficient Jurkat T cells following P/I stimulation. **E,** Western blot was used to check the stability of ABIN-1 and A20 in Jurkat T cell treated with the SMAC mimetic birinapant (2.5 μM) after P/I stimulation. Panel A-E have been published in Yin et al, Cell Mol Life Sci, 2022, 79:112

4.11 A20 controls self-destruction and ABIN-1 degradation

To better understand the crosstalk between A20 and ABIN-1 and the effect of A20 KO on ABIN-1 stability, we stimulated parental Jurkat T cells and A20 KO Jurkat T cells with CD3/CD28 or P/I. As previously stated, ABIN-1 was stabilized in A20-deficient Jurkat T cells following stimulation with CD3/CD28 or P/I **(Figure 4-20 A and B)**. Additionally, we decided to analyze A20 in ABIN-1 KO Jurkat T cells. We observed that in the absence of ABIN-1, A20 was highly modified upon TCR activation, and the degradation was at least somewhat impaired **(Figure 4-20 A and B)**. Next, we investigated whether A20 may directly mediate ABIN-1 ubiquitination because intact A20 ZnF4/7 motifs are required for ABIN-1 degradation. Indeed, we discovered the binding of ABIN-1 and A20 was enhanced by prolonged P/I stimulation, with the binding peaking between 30 min and 4 h of P/I stimulation, coinciding with the peak of ABIN-1 degradation **(Figure 4-20 C)**. Additionally, we discovered that A20 co-localized partially with ABIN-1 in the cytoplasm upon overexpression in HEK293 cells, and co-localization was enhanced by P/I stimulation **(Figure 4-20 D)**. Thus, we discovered that the binding between A20 and ABIN-1 is inducible upon TCR stimulation, and that ABIN-1 degradation is also dependent on the expression of A20. Since A20 functions as an E3 ligase, it might target ABIN-1 as a substrate for proteasomal degradation.

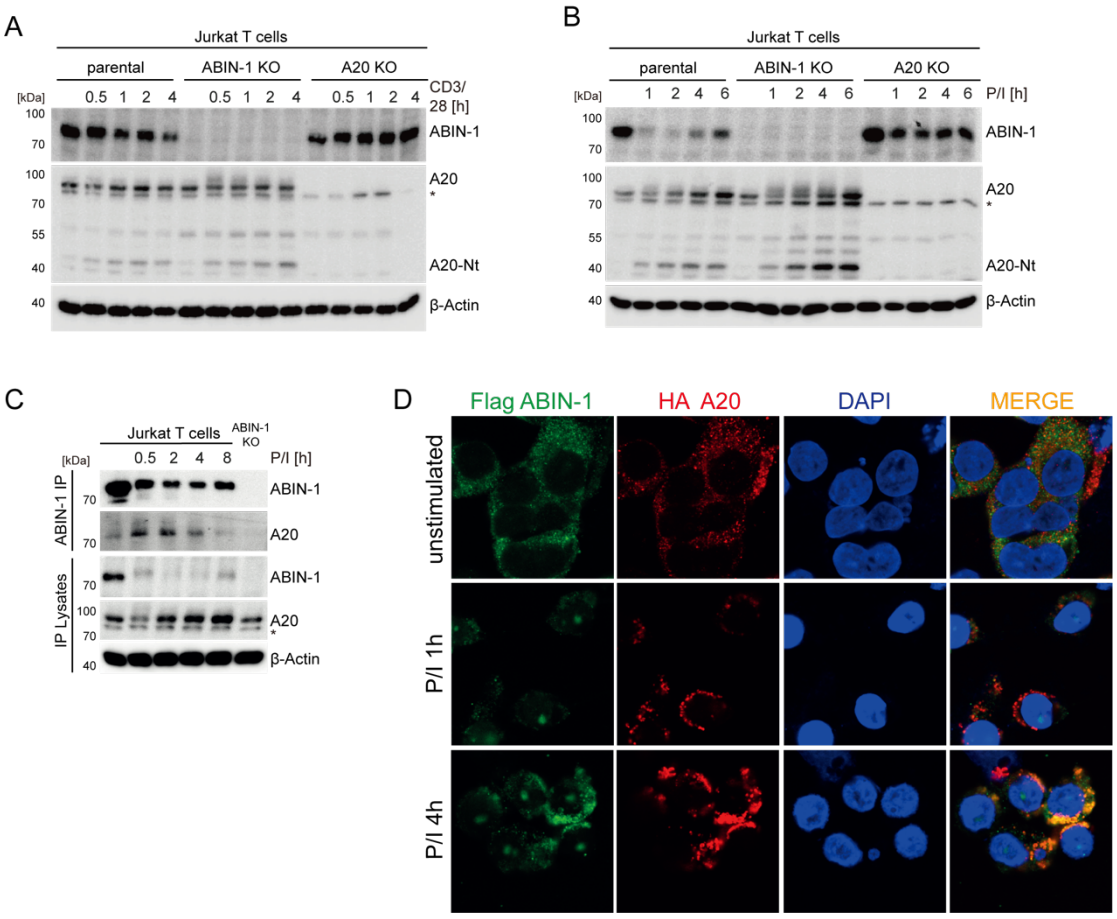

Figure 4-20: TCR stimulation induces ABIN-1 degradation via A20.

A, B Western blot analysis of ABIN-1 and A20 stability in parental Jurkat T cells, ABIN-1-deficient and A20-deficient Jurkat T cells following CD3/CD28 and P/I stimulation. **C,** Western blot analysis of the interaction between A20 and ABIN-1 in Jurkat T cells activated with P/I through ABIN-1 IP. **D,** HEK293 cells grown on 96-well plate were transiently transfected with Flag-tagged ABIN-1 and HA-tagged A20 for 24 h, and then stimulated with P/I for 1 h or 4 h. After counterstained with DAPI, cells were examined by confocal microscope. Panel A, B, C have been published in Yin et al, Cell Mol Life Sci, 2022, 79:112

As previously stated, we found an increase in the A20-ABIN-1 association following TCR stimulation, as well as a significant modification in the molecular weight of A20 is related with ABIN-1, indicating a post-translational modification of A20 **(Figure 4-20 C)**. Besides, ABIN-1 contains a ubiquitin-binding domain and functions as a ubiquitin sensor[89]. Therefore, we examined whether ABIN-1 could promote A20 modification by co-expressing HA-ubiquitin and Flag-A20 in HEK293 cells in the presence or absence of Flag-ABIN-1. As illustrated in **Figure 4-21A**, A20 is ubiquitinated in the absence of ABIN-1, and the amount of ubiquitinated A20 did not change when ABIN-1 was expressed, demonstrating that ABIN-1 had no direct effect on A20 ubiquitination. Because ABIN-1 degradation has been demonstrated to be

dependent on A20, we examined whether ABIN-1 can attach to K48-linked Ub chains. Thus, we co-expressed ABIN-1 and A20 together with HA-K48Ub (K48-only chains) in HEK293 cells. As shown in **Figure 4-21 B**, ABIN-1 has the ability to conjugate the K48-linked Ub chains, and A20 facilitates the binding of K48-linked polyubiquitin chains on ABIN-1. This demonstrated that ABIN-1 is a substrate of A20, allowing it to construct K48-linked Ub chains on ABIN-1 via E3 ligase activity. Since A20's ZnF4 and ZnF7 domains are responsible for E3 ligase activity, and the intact A20 ZnF4/7 domain is required for ABIN-1 degradation, we overexpressed A20 WT, A20 out mt, and A20 ZnF4/7 mt in the presence of ABIN-1 and HA-K48Ub and discovered that the ABIN-1 ubiquitin binding process was dependent on the intact ZnF4/7 domains but not on the A20 OTU domain **(Figure 4-21 C)**. Furthermore, because A20 expression was reduced at early time points after TCR engagement, we investigated if A20 was degraded on its own. First, we overexpressed A20 WT and HA-Ub, HA-K48 Ub and HA-K63 Ub to check which ubiquitin chain A20 would attach to. As shown in **Figure 4-21 D**, A20 could be conjugated with either K48- or K63-linked polyubiquitin chains. By overexpressing A20 WT, A20 OTU mt, and A20 ZnF4/7 mt in the presence of HA-K48Ub, we confirmed that A20 itself was prone to K48-linked polyubiquitination via ZnF4/7, suggesting that ubiquitin binding facilitates A20 auto-ubiquitination and degradation by ubiquitin proteasomal pathway **(Figure 4-21 E)**. Thus, proteasomal degradation mediated by A20 E3 ligase activity protects T cells against the negative regulator A20 and ABIN-1. Furthermore, this proteasome degradation is facilitated by A20´s C-terminal ZnF domain.

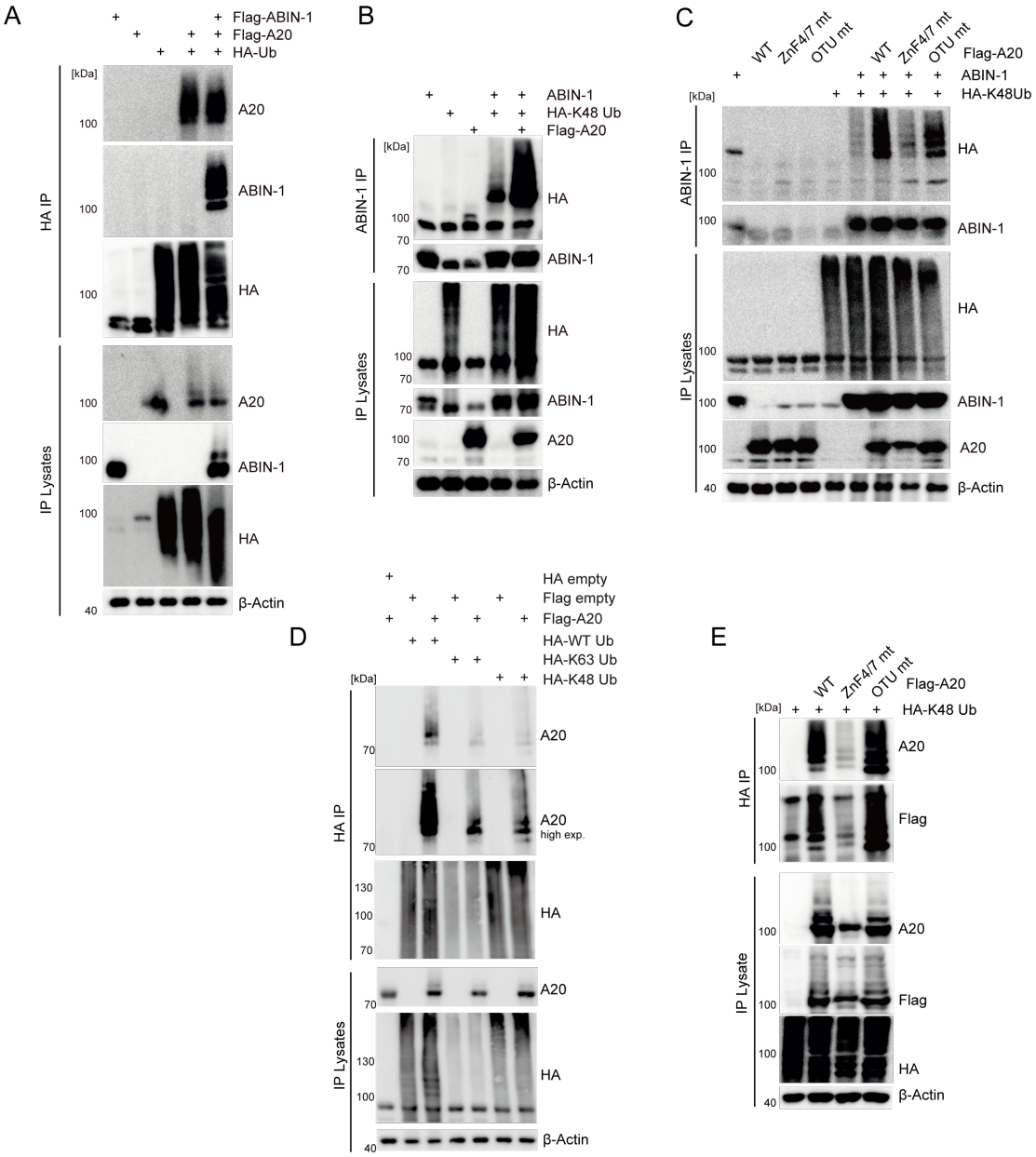

Figure 4-21: A20 and ABIN-1 degradation requires ZnF4/7-mediated K48-linked ubiquitination. **A,** Western blot analysis of the ubiquitination of A20 in HEK293 cells overexpressing Flag-A20 WT, Flag-ABIN-1 WT and HA-K48Ub constructs following HA IP. **B,** Western blot analysis of the ubiquitination of ABIN-1 in HEK293 cells overexpressing Flag-A20 WT, Flag-ABIN-1 WT and HA-K48Ub constructs following ABIN-1 IP. **C,** Western blot analysis of the ubiquitination of ABIN-1 in HEK293 cells overexpressing Flag-A20 WT, A20 ZnF4/7 mt and A20 OTU mt together with ABIN-1 and HA-K48Ub constructs following ABIN-1 IP. **D**, Western blot analysis of the ubiquitination of A20 in HEK293 cells overexpressing Flag-A20 WT, HA-Ub, HA-K48Ub (K48-only) and HA-K63Ub (K63-only) following HA IP. **E,** Western blot analysis of the ubiquitination of A20 in HEK293 cells overexpressing Flag-A20 WT, A20 ZnF4/7 mt and A20 OTU mt following HA IP. Panel A-E have been published in Yin et al, Cell Mol Life Sci, 2022, 79:112

4.12 Influence of ABIN-1 on the cleavage of A20 by MALT1 paracaspase

The proteasomal degradation of A20 protein is associated with the assembly of the CBM complex and the presence of TRAF6 protein in the early phase of activated T cells, and ABIN-1 binding is not required for A20 protein degradation. However, with prolonged T cell activation, A20 can be cleaved by MALT1, which was evident even after A20 re-synthesis, and the cleavage of A20 was enhanced in ABIN-1-deficient Jurkat T cells **(**see **Figure 4-22 A and B)**. This is consistent with our prior findings of enhanced and sustained MALT1 protease activity in ABIN-1 deficient Jurkat T cells compared to the parental cells **(Figure 4-9 B and D)**. MALT1 treatment with the potent allosteric inhibitor MLT-985 or the irreversible inhibitor Z-VRPR-FMK eliminate A20 cleavage **(Figure 4-22 A-C)**. Importantly, in ABIN-1 KO Jurkat T cells, the significant removal of full length A20 was impaired following MALT1 inhibitor treatment, indicating that MALT1 paracaspase activity was enhanced in ABIN-1 KO Jurkat T cells, promoting A20 cleavage and thus causing A20 inactivation following prolonged T cell activation. Thus, during the early phase of CBM complex-induced TCR signaling, A20 target ABIN-1 as a substrate and initiates its proteasomal degradation. ABIN-1 inhibits MALT1 protease activity during prolonged CBM complex signaling in activated T cells, therefore protecting re-synthesized A20 from inactivation by MALT1 cleavage.

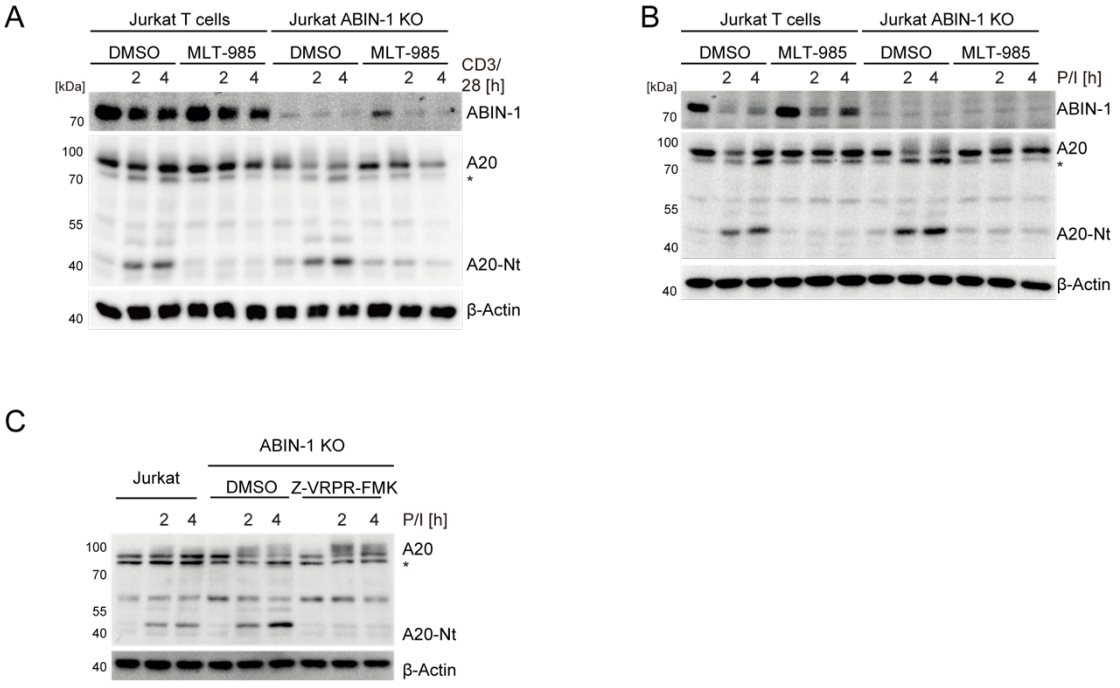

Figure 4-22: ABIN-1 inhibits the inactivation of A20 in activated T cells via reducing MALT1 protease activity.

A, B Western blot analysis of ABIN-1 stability and A20 cleavage in Jurkat T cells stimulated with CD3/CD28 (A) or P/I (B) and treated with the MALT1 inhibitor MLT-985 (1 μM). **C,** Western blot analysis of A20 cleavage in Jurkat T cells treated with MALT1 inhibitor Z-VRPR-FMK (75 μM) after P/I stimulation. Panel A-C have been published in Yin et al, Cell Mol Life Sci, 2022, 79:112

5 Discussion

Following antigen-receptor-induced T cell activation, several signaling pathways are activated, which work together to produce cytokines, differentiate, proliferate, and survive T cells. NF-κB signaling is a critical component of activated T cells. The CBM complex is critical in mediating the connection between proximal TCR signaling and downstream IKK/NF-κB activation[185]. As a component of the CBM complex, MALT1 functions as a scaffold and has proteolytic activity, which plays a critical role in NF-κB signaling pathway. The CBM complex activation is closely regulated by both positive and negative components, which work together to provide immunological protection following infections and to prevent overshooting reactions associated with autoimmunity and inflammation. In activated T cells, positive regulators such as E3 ligase TRAF6 and components of LUBAC complex (HOIL-1, HOIP, and SHARPIN) can recruit to the CBM complex. These E3 ligases activate IKK/NF-κB by accelerating the ubiquitination of BCL10 and MALT1[89,104]. In comparision, the DUBs such as CYLD and A20 operate as negative regulators of CBM complex triggered T cell signaling, limiting the activation of NF-κB during an adaptive immune response[186,187]. In this work, ABIN-1 was discovered as a novel CBM complex regulator in activated Jurkat T cells utilizing immunoprecipitation and quantitative mass spectrometry.

We show here that when T cells are activated, A20 and ABIN-1 are ubiquitinated and attach to the CBM complex, where they collaborate to establish a negative regulatory module for MALT1 protease activity and NF-κB activation. A20, a ubiquitin editing enzyme, has been shown to have a negative regulatory role in activated T cells in previous studies[110,129]. Our findings demonstrate that the expression of A20 and ABIN-1 proteins is accurately controlled by the interdependent post-translational mechanisms, implying the collaboration of these two negative regulators controls the duration and strength of the NF-κB signaling pathway in activated T cells, as supported by gene depletion study in human CD4 T cells. Notably, whereas overexpressed A20 can function independently of ABIN-1, ABIN-1's negative effect is largely dependent on the existence and association of A20. Therefore, A20 plays a dominating role

within the A20/ABIN-1 module, whereas ABIN-1 serves as an auxiliary component that fine-tunes A20 expression, stability, and activity. The absence of A20 or ABIN-1 does not indicate chronic T cell activation without stimulation. A20 deficiency in CD8 T cells results in persistent NF-κB activation and enhanced IL-2 and IFNγ production in response to antigens and increased anti-tumor responses[151]. A20 ablation increased proliferation in CD4 T cells upon TCR stimulation, but also increased cell death susceptibility[173]. In line, in a model of graft versus host disease (GvHD), CD4 and CD8 T cells from A20-deficient donors were less viable but produced more IFNγ, resulting in increased systemic inflammation[152]. These investigations showed that deletion of A20 from T cells boosts effector responses but does not result in spontaneous T cell activation. Thus, A20 and ABIN-1 are required for maintaining a balance between initial and persistent T cell activation following induction. We observed an interdependent interaction in which A20 and ABIN-1 regulate each other's post-translational stability, which can help in the establishment of early signaling thresholds, the regulation of peak signaling, and the balance of sustained signaling following T cell activation. So, in the following discussion, we will outline the three steps of A20 and ABIN-1 involvement in TCR signaling regulation[188].

5.1 In the initial phase of CBM complex recruitment

During the initial phase of T cell activation, the synthesis of the initial CBM complex is triggered and A20 and ABIN-1 are recruited to the CBM complex. Antigen-receptor ligation in T cells has been demonstrated to cause the recruitment of A20 to MALT1, resulting in MALT1-mediated A20 processing[110]. We discovered that ABIN-1, like A20, can be recruited to the CBM complex after P/I or CD3/CD28 stimulation. Because ABIN-1 fails to bind to the CBM complex in A20 KO Jurkat T cells, we assume that A20 functions as an adapter protein, bringing ABIN-1 to the CBM complex. Numerous studies have demonstrated that A20 comprises a C-terminal ZnF4 and ZnF7 domain that acts as a binding surface for M1- and K63- linked ubiquitin chains[32,33]. As a result, we were able to confirm that A20 interacts with the CBM complex via its C-terminal ZnF4 and ZnF7 domains, implying that A20 and ABIN-1 are associated with the CBM complex by polyubiquitin chains bound to BCL10 and MALT1, respectively. A20's ZnF4

and ZnF7 domains are also involved in the interaction between ABIN-1 and A20. In contrast, the loss of ABIN-1 does not affect A20's recruitment to the CBM complex **(Figure 5-1)**. Additionally, we observe that an intact ABIN-1 UBAN is not required to impair TCR signaling, implying that ubiquitin binding of ABIN-1 does not contribute to the A20/ABIN-1 module CBM complex interaction[188].

Because CBM signaling is subjected to both positive and negative regulatory mechanisms, it is able to balance and adjust T cell activation cooperatively. As a result, ABIN-1 and A20 are critical for regulating T cell activation in order to avoid overshooting responses that result in autoimmunity and inflammation. In contrast to the majority of cells, which express modest levels of A20 under baseline circumstances, lymphocytes exhibit high levels of A20 and ABIN-1[159,189]. As a result, steady-state A20 and ABIN-1 concentrations may create an initial threshold that inhibits CBM complex downstream cascades, a process that may guard against unwanted immune activation following weak TCR stimulation in response to self-antigens referred to as tonic signaling. Tonic signaling needs to be restricted because it can produce toxicity and enhance T cell anergy, exhaustion, and activation-induced cell death[190,191].

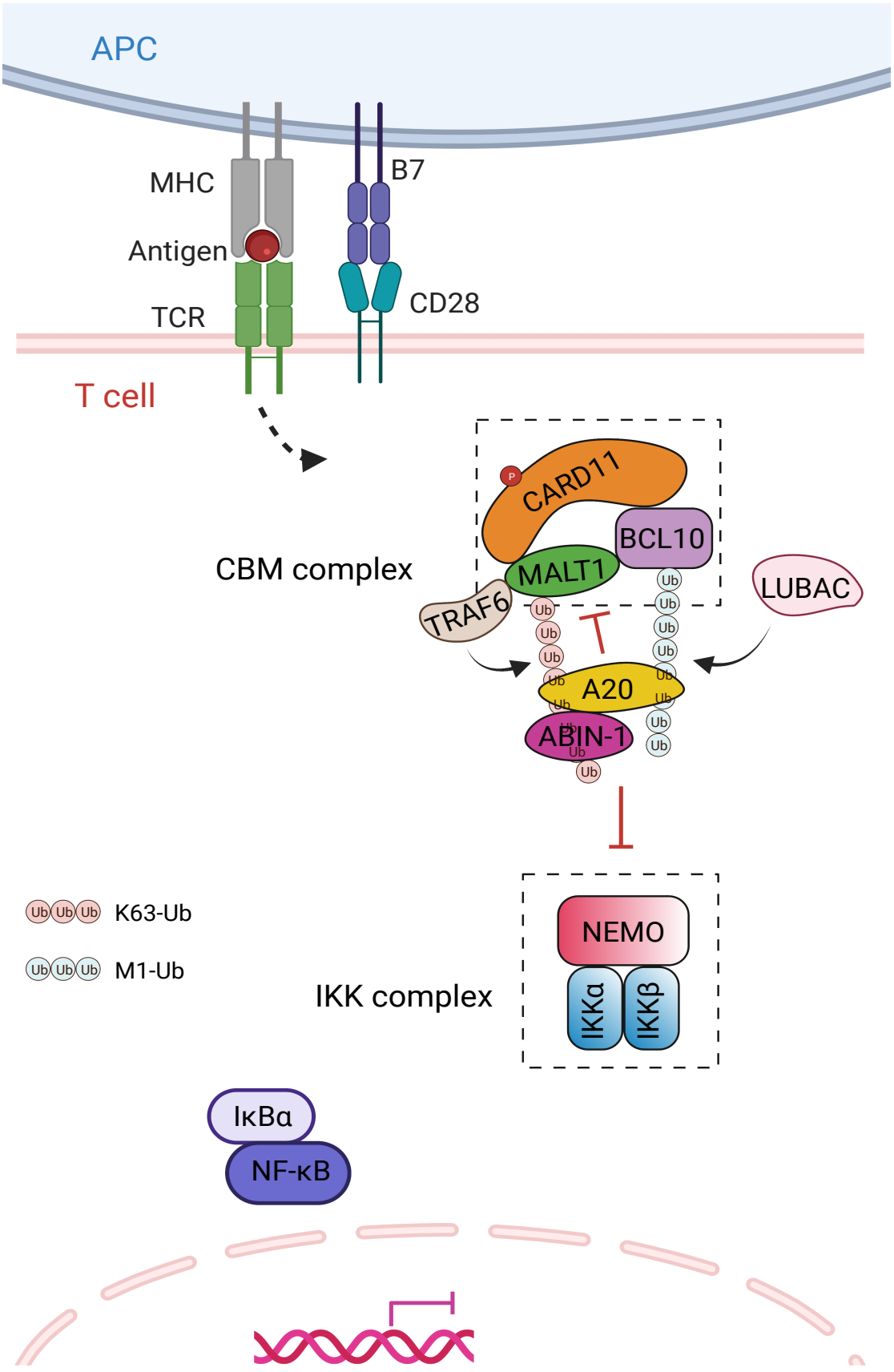

Figure 5-1: The initial phase of CBM complex recruitment.

CARD11 is phosphorylated and recruits BCL10 and MALT1 to form the CBM complex following TCR ligation. TRAF6 and LUBAC, two positive regulators of CBM signaling, add K63- and M1-linked Ub chains to MALT1 and BCL10, respectively. These Ub chains are considered to link the CBM complex to the IKK complex, triggering NF-κB transcriptional activity. TCR activation is balanced by A20 and ABIN-1, which act as negative regulators in CBM signaling. Following initial TCR activation, they can both be recruited to the CBM complex, inhibiting MALT1 protease and NF-κB activation.

5.2 The second phase of peak CBM signaling

During the initial TCR activation, A20 and ABIN-1 operate as negative regulators to limit and balance the immunological response. After around 30min TCR activation, the proteasomal degradation machinery removes the negative regulators ABIN-1 and A20, resulting in increased downstream signaling after CBM complex assembly. The removal of negative factors promotes the activation of IKK/NF-κB, which in turn triggers proteasomal degradation of the NF-κB inhibitor IκBα. Additionally, MALT1 protease activity is increased and A20 as a substrate can be cleaved upon recruitment to the CBM complex by MALT1. As a result, the proteasome can degrade and MALT1 can cleave the negative regulator A20. Thus, the release of the three inhibitory components A20, ABIN-1, and IκBα defines the second phase of persistent CBM complex triggered TCR signaling, allowing for peak activation of canonical NF-κB signaling.

Other studies have revealed that the C-terminus of A20 functions as a ubiquitin ligase. They demonstrated that A20 targets RIPK1 by attaching K48-linked polyubiquitin chains to it, thereby identifying RIP for proteasomal destruction following TNFα activation[140]. In addition, sustained poly(I:C) stimulation has been associated with ABIN-1 degradation[162]. We hypothesized that after TCR activation, A20 identifies ABIN-1 as a substrate and attaches the K48-linked polyubiquitin chains to ABIN-1, resulting in ABIN-1 destruction. Moreover, we found that ABIN-1 is stable in the absence of A20, and that A20 ZnF4 and ZnF7 enhance K48-linked polyubiquitination chains and destruction of ABIN-1 following TCR activation, implying that A20 regulates ABIN-1 in both innate[163] and adaptive immunological responses. Interestingly, after short-term TCR activation, A20 degradation was observed, and we demonstrated that A20 ZnF4/7 promotes K48-linked auto-ubiquitination and A20 self-destruction. Other E3 ligases, such as Itch or RNF11, may be implicated in the ubiquitination

and degradation of ABIN-1 or A20 in an A20-dependent manner, as proposed for RIPK1[158,192]. Since the CBM complex is necessary for TCR signaling, the absence of CARD11, BCL10, or MALT1 causes loss of NF-κB activation. Both ABIN-1 and A20 can be stably expressed in the absence of CARD11, BCL10, or MALT1 Jurkat T cells, showing that the assembly of the CBM complex is essential for the degradation of ABIN-1 and A20. Additionally, the E3 ligase TRAF6, as well as the LUBAC components HOIP and HOIL-1, all have an effect on the destruction of A20 and ABIN-1. TRAF6 and LUBAC components have indirect functions by conjugating K63- or M1-linked polyubiquitin chains to MALT1 and BCL10, respectively[89,182]. These polyubiquitin chains can recruit A20 to the CBM complex upon stimulation via A20 ZnF4 and ZnF7, which are A20´s ubiquitin binding domains, and A20 ZnF4 and ZnF7 are also responsible for ABIN-1 and A20 self-destruction. Furthermore, TCR stimulation induces MALT1 protease activity, and we observed an increase in MALT1 protease activity in ABIN-1 KO or A20 KO Jurkat T cells. However, as previously demonstrated by others, the decline of A20 during the early stages of TCR stimulation is mediated by the proteasome. Because maximal substrate cleavage by MALT1 is not occurring at early time points, the rapid removal of A20 within 30 min of TCR/CD28 stimulation cannot be accounted to the MALT1 protease activity. In general, the peak phase of CBM signaling occurs roughly 30 min after TCR activation. The proteasome degrades the negative regulators A20, ABIN-1, and IκBα, allowing the CBM complex and IKK complex to be connected and active the NF-κB and MALT1 paracaspase[188] **(Figure 5-2)**.

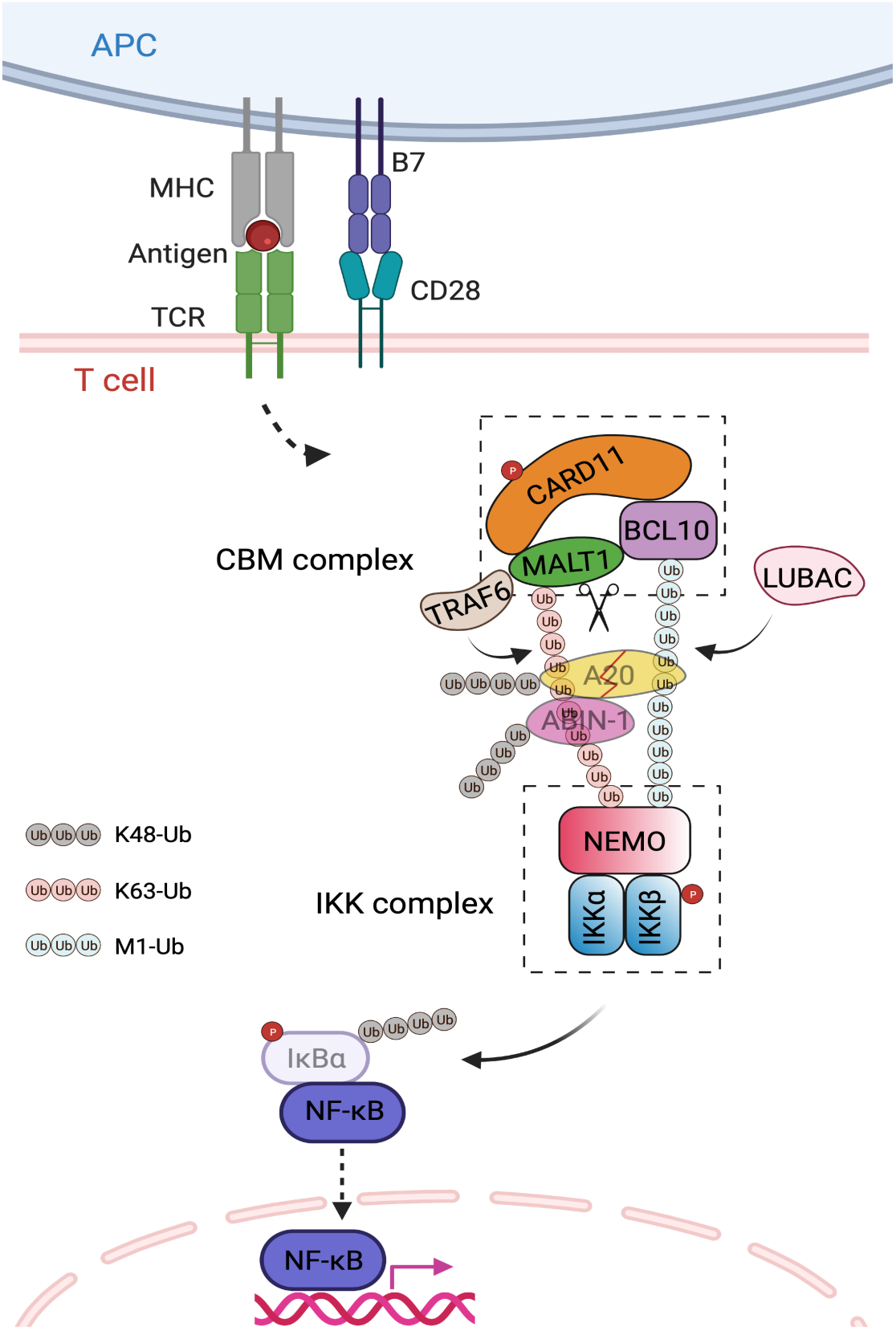

Figure 5-2: The second phase of peak CBM signaling.

The negative regulators ABIN-1, A20, and IκBα can be degraded by the proteasome in the second phase of TCR activation, and A20 can also be cleaved by MALT1, allowing optimal NF-κB activation.

5.3 The third phase of sustained CBM signaling

The third step of sustained CBM complex-triggered T cell activation involves the resynthesis of the negative and inhibitory regulators IκBα and A20 through NF-κB induction. In the absence of ongoing stimulation, the resynthesized molecules inhibit the IKK upstream and downstream cascades. The transcription factor NF-κB is found in the cytoplasm of unstimulated cells, coupled to its inhibitor IκBα. TCR stimulation causes proteasomal degradation of IκBα, allowing NF-κB to translocate into the nucleus and activate transcription of genes that contribute to proliferation, angiogenesis, metastasis, or chronic inflammation. As a result, this transient activity necessitates the rapid induction of negative feedback mechanisms, such as up-regulation of the NF-κB inhibitor IκBα, by NF-κB. Resynthesized IκBα reduces the activity of NF-κB by binding to its nuclear localization sequence[193]. Additionally, various NF-κB activating stimuli were discovered to induce A20 expression via NF-κB sites in the A20 promoter[139] **(Figure 5-3)**.

As previously described, the first degradation of A20 following TCR stimulation is catalyzed by the proteasome, while the subsequent cleavage of A20 is catalyzed by MALT1. MALT1 is required for the maintenance of CBM signaling since it continuously cleaves and inactivates A20, impairing A20's negative regulatory action on the CBM complex. Therefore, MALT1 and A20 are involved in a feedback auto-regulation loop. MALT1 cleaves and inactivates A20 upon prolonged TCR stimulation, hence increasing NF-κB activation. Whereas A20 is re-produced in the nucleus, higher levels of A20 inhibit NF-κB and MALT1 protease activation in conjunction with ABIN-1. A20 and ABIN-1 inhibit MALT1 mono-ubiquitination, which is required for MALT1 protease activation upon TCR/CD28 stimulation. Currently, the exact mechanism how A20 and ABIN-1 suppress MALT1 protease activity are unclear, because it is unknown how MALT1 is mono-ubiquitinated and how ubiquitination controls MALT1 proteolytic activity. The A20/ABIN-1 module may either accelerate the recruitment of a DUB that is responsible for removing mono-ubiquitin or inhibit a mono-ubiquitin ligase from binding to MALT1. Notably, the A20 ZnF4/7 mutant is unable to bind to the CBM complex and is

protected from MALT1 substrate cleavage, indicating the crucial non-catalytic role of the A20 C-terminus in modulating CBM activity. In contrast to A20, ABIN-1 expression cannot be induced in response to T cell activation, but ABIN-1 protein expression is tightly regulated by A20 due to its E3 ligase activity and thus indirectly connected to the transcriptional and post-translational regulations that govern A20 expression. Vice versa, higher ABIN-1 expression helps to counteract MALT1 protease function and NF-κB activation, which in turn increase A20 protein amounts.

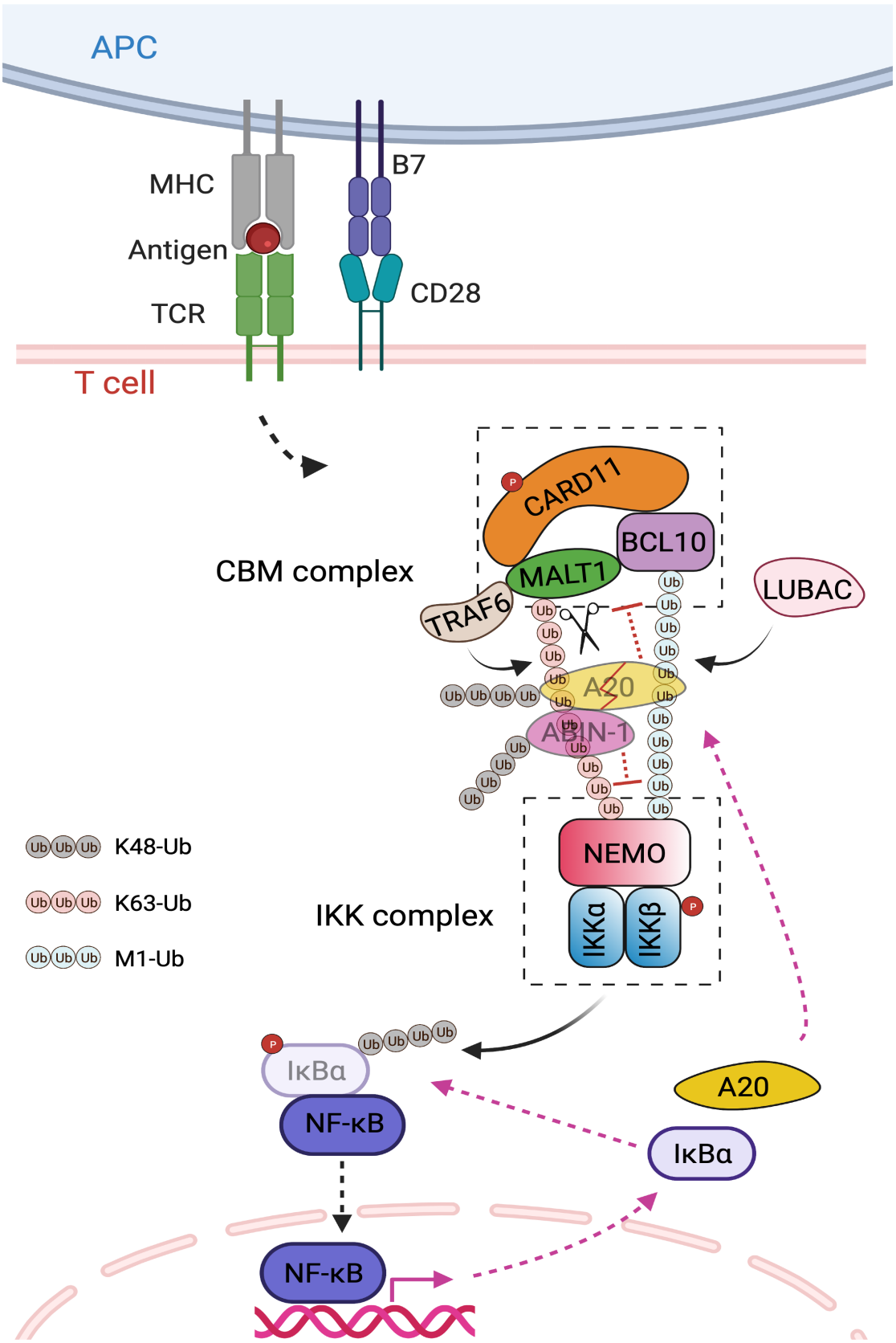

Figure 5-3: The sustained CBM signaling in activated T cells.

The negative regulators A20 and IκBα are re-synthesized in the nucleus during persistent TCR activation. The re-synthesized IκBα can bind to NF-κB in the cytosol and inhibit NF-κB activation, whereas the A20 and ABIN-1 module reduce NF-κB activation and MALT1 protease activation.

We established that the negative effect of A20 on CBM complex triggered NF-κB signaling in T cells is dependent its ZnF4 and ZnF7 domains via polyubiquitin binding. This finding is consistent with recent studies emphasizing the A20 ZnF4 and ZnF7 domains are required for the inhibition of pro-inflammatory and innate immune signals to NF-κB[32,33]. Mechanistically, we show that the A20 is recruited to the CBM complex in activated T cells via polyubiquitin chains mediated by its ZnF4 and ZnF7 domains. Despite the fact that A20 has been shown to cleave the K63-linked polyubiquitin chain on MALT1 in response to T cell activation via its OTU domain, which possesses DUB activity. However, A20 with the OTU mutation has no effect on NF-κB activation in T cells, indicating that A20 blocks NF-κB activation in T cells in a non-catalytic way. Previous research showed that A20 ZnF4/7 mutant is unable to bind to NEMO upon TNFα stimulation[130]. Our data highlights that it is also unable to bind to the CBM complex upon TCR activation in T cells. Thus, the mutation in A20 ZnF4/7 domain may inhibit signal transduction in the TCR signaling pathway both upstream and downstream of the IKK complex. In this study, we identify ABIN-1 as a key component that controls A20's negative effect in T cells.

Both A20 and ABIN-1 can be recruited to the CBM complex, which acts as a gatekeeper for T cell antigenic activation. While A20 has the ability to recruit ABIN-1 to the CBM complex, recruitment between the A20 and the CBM complex is not dependent on ABIN-1. Regardless of the fact that ABIN-1's UBAN domain can interact with K63-linked and linear ubiquitin chains, disruption of the ABIN-1 UBAN domain had no effect on T cell activation, indicating that the A20/ABIN-1 interaction, rather than ABIN-1 ubiquitin binding, is important for antagonizing T cell activation. ABIN-1 UBAN domain , on the other hand, is necessary to reduce innate TLR signaling responses in mouse myeloid and B cells, suggesting that ubiquitin binding is required to regulate innate immunity pathways[194]. However, the ABIN-1 UBAN mutation had no effect on T cell proliferation and activation induced by TCR stimulation. Here, we demonstrate that the inhibitory role of ABIN-1 for T cell signaling activation is A20-dependent. In line, while overexpression of A20 eliminates the need for ABIN-1 to block T cell signaling, ABIN-1's negative effect is entirely dependent on the presence of A20.

Furthermore, A20 and ABIN-1 are degraded by proteasomes, releasing T cells from the negative effects of these proteins following activation. Binding of ubiquitin to A20 ZnF4/7 promotes destructive K48-ubiquitination of itself and ABIN-1. ABIN-1 inhibits A20 cleavage and inactivation by the MALT1 protease, assisting in the reduction of sustained CBM complex signaling in an A20-dependent manner. Thus, ABIN-1 influences A20's negative regulatory activity in T cells. We define and explore how the A20/ABIN-1 module balances and modulates T cell signaling in detail. We show that interconnected post-translational processes closely govern A20/ABIN-1 silencing module expression and activity in T cells. Additionally, it has been demonstrated that A20 and ABIN-1 have distinct roles in the TNF-induced cell death, and block this pathway synergistically, in contrast to what we discovered in TCR signaling, where A20 and ABIN-1 cooperate to inhibit NF-κB activation. Thus, the inhibitory effects of A20 and ABIN-1 on innate and adaptive immune pathways are mediated by different mechanisms, depending on the cellular context and pathways involved[188]. Due to the fact that mutations in ABIN-1 and A20 in humans are highly related with susceptibility to autoimmune chronic inflammatory disease, such as psoriasis vulgaris and systemic lupus erythematosus (SLE) [162,195,196]. Thus, understanding how ABIN-1 and A20 control adaptive immunity is critical to human disease. Here we investigated ABIN-1 is a suppressor of adaptive immune response and the interaction of ABIN-1 with A20 controls adaptive immune response via the NF-κB signaling pathway in T cells.

6 Methods

6.1 Cell culture

6.1.1 Cultivation of Jurkat T cells, HEK293 and HEK293T cells

Jurkat T cells were cultured at 37 °C in Roswell Park Memorial Institute (RPMI)-1640 media supplemented with 10% fetal calf serum (FCS) and 100 units (U)/ml Penicillin/Streptomycin (P/S). Maintain a cell density of 1- 3 x 10^6 cells/ml and split cells every 2–3 days or as required by the cell growth rate. Prior to the experiment, the cells were maintained at a density of around 1 x 10^6 cells/ml. HEK293 and HEK293T cells were cultured at 37 °C with 5% CO_2 in Dulbecco's modified Eagle Medium (DMEM) supplemented with 10% FCS and 100 U/ml P/S. Cells should be passaged at a ratio of 1:10 to 1:20 when they are 80% confluent for general maintenance. To detach cells from the plate, they were gently washed with PBS and then incubated for 5min at 37°C with a 0.5 % trypsin/EDTA solution. To inactivate the reaction, add an adequate volume of DMEM medium to it. Resuspend and dilute cells in fresh flasks or plates with DMEM medium for future experiments.

6.1.2 Isolation and cultivation of primary human CD4 T cells

Human T cells were cultured in RPMI-1640 medium containing 10% FCS (filtered), 100 U/ml penicillin plus 100 µg/ml streptomycin (P/S), 1% GlutaMax (100X), 1% Na-Pyruvate, 1% Non-essential aminoacids, 50mM β-Mercaptoethanol in the presence of IL-2. Peripheral blood mononuclear cells (PBMC) from healthy volunteers were freshly collected for studies with human $CD4^+$ T cells using Ficoll-Pague Plus density gradient sedimentation (GE Healthcare). Positive selection with CD4-specific microbeads was used to isolate $CD4^+$ T cells from PBMC (Miltenyi Biotec).

6.2 Cell stimulation and treatments

6.2.1 Stimulation of Jurkat T cells and primary human CD4 T cells

For P/I stimulation, Jurkat T cells were treated with 200 ng/ml Phorbol 12-myristate 13-acetate (PMA; Merck Millipore) and 300 ng/ml Ionomycin (Calbiochem). For CD3/CD28 antibody

co-ligation, 1µg/ml murine anti-human anti-CD3 antibody (#555336) and 3.3 µg/ml murine anti-human anti-CD28 antibody (#555725) were used in the presence of 1.65 µg/ml anti-mouse IgG1 (#553440) and 1.65µg/ml anti-mouse IgG2a (#5553387) antibodies from BD Pharmigen. Stimulation was carried out in tubes at 37°C. To activate primary T cells, cells were transferred to 96-well plates pre-coated with anti-CD3 (0.5 µg/ml) and stimulated in the presence of soluble anti-CD28 and anti-mouse IgG1/IgG2a, as previously described.

6.2.2 Inhibitor treatment of Jurkat T cells

For proteasome inhibition, 25µM the protease inhibitor MG132 (Calbiochem) were pretreated 1 hour before stimulation. For the inhibition of MALT1 paracaspase activity, cells were pre-incubated with 1µM MLT-985 for 4 hours before stimulation. 75 µM MALT1 inhibitor Z-VRPR-FMK (Enzo Life Sciences) were pretreated 3 hours before stimulation. 2.5 µM cIAP1/2 (BioCat) inhibitor birinapant was pre-treatment 10 min before stimulation. Control cells were incubated with an equal volume of dimethylsulphoxide (DMSO) or water.

6.3 Generation of knockout Jurkat and primary human CD4 T cells

Single guide RNAs (sgRNAs) oligonucleotides against A20 (5′-GAGGCAATTGCCGTCACCTG-3′), ABIN-1 (5′-GAGCTCAGCCAGGGGGTCGA-3′, clone34; or 5′-TTATACCTGTGAGCTCAGCC-3′, clone33), and HOIL-1 (combination of 5′-ATGGACGAGAAGACCAAGAA-3′ and 5′-TGTACCACGATCTGGCACTG-3′) were cloned as previously described into the BbsI–linearized px458 vector (Addgene #48138; a gift from Feng Zhang)[197,198]. Jurkat T cells were electroporated using a Gene Pulser Xcell (BioRad) with the optimum program (220 V, 1000 µF, 0.4 cm cuvettes). Following 24 hours of growth, individual EGFP-positive cells were sorted using a MoFlo sorting system (Beckman Coulter). Serial dilutions were conducted, and cells were plated into 96 well-plates at a density of 2 or 5 cells/well for single cloning, followed by a 1-2-week growth phase. Western blotting was used to check for protein expression changes, and genomic alterations were analyzed by sequencing of genomic DNA. The approach for generating CARD11, BCL10, MALT1, HOIP, and TRAF6 KO cells has previously been reported[105,199,200,201]. $CD4^+$ T cells were stimulated for 3 days with

plate-bound anti-CD3 (2 µg/ml, clone TR66, Enzo Life Sciences) and anti-CD28 (2 µg/ml, CD28.2, BD Biosciences) for experiments with human $CD4^+$ T cells. Genes were depleted utilizing Alt-R CRISPR-Cas9 technology (Integrated DNA Technologies, IDT).

In brief, crRNA and tracrRNA (Integrated DNA Technologies, IDT) were combined in a 1:1 ratio and incubated for 20 min at RT with Cas9 protein (Integrated DNA Technologies, IDT) to create RNP complex. 1 x 10^6 activated human $CD4^+$ T cells were electroporated, and RNP complex was delivered into cells using the Neon transfection system (1600 V, 10 ms pulse width, 3 pulses; Thermo Fisher Scientific). After electroporation, cells were immediately incubated in RPMI-1640 medium supplemented with 10% FCS (filtered), 100 U/ml P/S, 1% GlutaMax (100X), 1% Na-Pyruvate, 1% Non-essential aminoacids, and 50mM Mercaptoethanol in the presence of IL-2 (50 U/ml).

6.4 Lentiviral transduction of Jurkat T cells

The cells were transduced using lentiviruses producing pHAGE-hΔCD2-T2A-A20-Flag-Strep-Strep or pHAGE-hΔCD2-T2A-ABIN-1-Flag-Strep-Strep WT or mutants to achieve sustained protein expression in parental or KO Jurkat T cells. 1.5 x 10^6 HEK293T cells were seeded onto 10 cm^2 dishes and incubated overnight 24 hours before viral infection. To produce lentivirus, 1µg envelope plasmid pMD2.G (Addgene #12259; gift D. Trono), 1.5 µg packaging plasmid psPAX2 (Addgene #12260; gift D. Trono), and 2 µg lentiviral transfer plasmid were transfected into HEK293T cells the next day. After 72 hours, the virus-containing supernatant was collected, sterile filtered, and mixed with 8 µg/ml polybrene in 5 x 10^5 A20 or ABIN-1 defective Jurkat T cells or parental Jurkat T cells. After a 24-hour incubation period with the virus, the cells were replaced with fresh RPMI-1640 medium. Flow cytometry analysis of hΔCD2 can generally be used to quantify the proportion of infected cells after 7 days in culture.

6.5 Transfection of HEK293 cells

For transient expression, Flag-A20, HA-A20, HA-ABIN-1, Flag-ABIN-1, HA-K48-Ub (K48-only), and HA-WT-Ub constructs were cloned into a pEF4 expression vector, and HEK293 cells were transfected using standard calcium phosphate transfection procedures. To summarize,

2.5 x 10^6 cells were plated in a 10 cm^2 dish the day before transfection. For transfection, 50 µl $CaCl_2$ (2.5 M) was mixed with 450 µl H_2O before adding the plasmid. A total of 2.5 µg of plasmid DNA was utilized per construct; if fewer constructs were provided, empty vectors were employed. This combined solution was then vortexed into 500 µl 2 x HEPES-buffered saline (HBS). After 20 min incubation at RT, the mixture was dropped into one cell culture dish dropwise. The cells were harvested 48 hours later, and the following assays were carried out.

6.6 Cell Lysis and Precipitations

For Western Blot or Electrophoretic Mobility Shift Assay (EMSA) protein expression analysis, 1-3x10^6 cells were collected (350 g, 5 min, 4°C), washed with ice cold PBS, and resuspended in 100µl high salt buffer. Cells were shaken for 20-30 min at 4°C before being centrifuged at 21,000 g for 30 min at 4°C. 10-20 µl supernatant was collected and kept at -80°C for EMSA analysis. Before Western Blot analysis, the remaining samples were combined with 4 x SDS loading buffer and cooked at 95°C for 5 min.

6.7 Western Blot

Protein was separated on SDS-PAGE gels (90 V, 120 min) and then transferred to PVDF membranes using an electrophoretic semi-dry transfer technique for immunodetection (70 mA per gel for 100 min). To block the membrane, incubate it for 1 hour at RT in 5% milk powder /PBST, then overnight at 4°C in primary antibody diluted 1:1000 in 2.5% BSA/PBST. After washing the membrane with PBST, incubate it for 1 hour at RT with the HRP-conjugated secondary antibody diluted 1:7000 in 1.25% BSA/PBST. The LumiGlo reagent (Cell Signaling Technologies) was used as directed by the manufacturer to detect HRP via enhanced chemiluminescence (ECL).

6.8 Coimmunoprecipitation (Co-IP) and Strep-Tactin (ST) pulldown

3-5 x 10^7 Jurkat T cells were lysed in 800 µl Co-IP buffer (25 mM HEPES pH 7.5, 150 mM NaCl, 0.2% NP-40, 10% glycerol, 1 mM DTT, 10 mM NaF, 8 mM □-glycerophosphate, 300 µM sodium vanadate) supplemented with protease inhibitors cocktail mix (Roche) for protein interaction analyses. Before centrifugation (21,000 g, 20 min, 4°C), lysates were incubated in an overhead rotator for 20 min at 4°C. 30 µl supernatant was collected and boiled for 5 min at 95°C in 4 x SDS loading buffer as a lysate control, and binding experiments were performed on the remaining supernatant. Immunoprecipitations (IPs) were carried out using antibodies against 0.5 µg BCL10 antibody (C-17, #sc9560), 1 µg ABIN-1 antibody (#68-0002-100, Ubiquigent), and 30 µl HA antibody (12CA5, HMGU), and samples were incubated overnight at 4°C in an overhead rotator. After the antibody incubation, 18 µl recombinant Protein G Sepharose 4B (1:1 suspension, life technologies) was added to the lysates, which were then incubated at 4°C for another 1-2 hours. Cell lysates were treated with 30µl Strep-Tactin Sepharose (1:1 suspension, IBA) and cycled overnight at 4°C for Strep-PD. Beads were washed three times with ice cold Co-IP buffer that was free of protease and phosphatase inhibitors. After removing the supernatant, 25 µl of 2xSDS-PAGE loading buffer was added, and the beads were cooked at 95°C for 5 min before being examined by Western blot.

6.9 Ubiquitination Assays

To evaluate ubiquitination of endogenous MALT1, 3-5 x 10^7 Jurkat T cells were lysed in 450µl Co-IP buffer supplemented with protease inhibitor cocktail mix (Roche) and 1% SDS. Lysates were homogenized using a syringe (26 G) and boiled for 10 min before being lysed for 20 min at 4°C in an overhead rotator, followed by three times sequential centrifugation and transfer of supernatant (21,000 g, 20 min, 4°C). A portion of the supernatant was kept for western blotting, while the rest was diluted 10-fold with Co-IP stock solution without SDS or inhibitors and used for immunoprecipitation.

HEK293 cells were transfected with Flag-A20 WT, OTU mt, ZnF4/7 mt, Flag-ABIN-1, and HA-K48-Ub (K48-only) to detect ABIN-1 ubiquitination, then lysed in 450 µl Co-IP buffer containing 1 percent SDS, 10mM N-ethylmaleimide, and 10mM N-ethylmaleimide (NEM;

Thermo Fisher Scientific), 50 μM MG132, and the processes for cell lysis are the same as described above.

For Co-IP, 250μl MALT1 antibody (21A2, HMGU) and 1μg ABIN-1 antibody (#68-0002-100, Ubiquigent) were immunoprecipitated overnight at 4°C, followed by 1-2 hours incubation with 18l rec-protein G Sepharose 4B beads (1:1 suspension, Life Technologies). After incubation, the samples were centrifuged, and the pellet was washed three times with Co-IP buffer devoid of protease and phosphatase inhibitors. After removing the supernatant, 25μl of 2x SDS-PAGE loading buffer was added, and the beads were cooked at 95°C for 5 minutes before being examined by Western blot.

6.10 Expression of cytokine in primary T cells

Primary human T cells were rested in T cell media in the absence of IL-2 for 24 hours before being stimulated with anti-CD3/CD28 as described above for cytokine induction and analysis by flow cytometry and ELISA.

For the detection of intracellular cytokines by flow cytometry, cells were stimulated for 5 hours in the presence of Brefeldin A (5 μg/ml, Sigma #B7651). The cells were then washed with FACS buffer (PBS + 3 percent FCS) and stained with Fixable Viability Dye eFluor 780 (1:1000 in FACS buffer, Invitrogen #65-0865-14) for 30 minutes at 4°C. Following that, cells were fixed in 2 percent PFA for 15 minutes at room temperature, permeabilized in IC buffer (0.1 percent saponin in PBS) for 15 minutes at room temperature, and Fc block (1:50 in IC buffer, eBioscience #14-9161-73) was conducted for 7 minutes at room temperature.

Cytokine staining was done in the dark at 4°C for 30 minutes with IL2-APC (#554567) and TNF-FITC (#554512) antibodies diluted 1:100 in IC buffer (both from BD Biosciences). After that, the cells were washed twice with IC buffer, resuspended in 100μl FACS buffer, and analyzed with an Attune Acoustic Focusing Cytometer.

Cells were stimulated for 24 hours before being tested using a human IL-2 ELISA kit (#88-7025-88, Thermo Fisher Scientific) according to the manufacturer's instructions.

6.11 The gel electrophoresis mobility shift assay (EMSA)

For EMSAs, double-stranded NF-κB or OCT1 binding sequences (H2K: fw: 5'-GATCCAGGGCTGGGGATTCCCCATCTCCACAGG -3', rev: 5'-GATCCCTGTGGAGATGGGGAATCCCCAGCCCTG -3'; OCT: fw: 5'-GATCTGTCGAATGCAAATCACTAGAA -3', rev: 5'-GATCTTCTAGTGATTTGCATTCGACA -3') were tagged with [α-32P] dATP using Klenow Fragment (NEB). To detect DNA binding, incubate whole cell lysates (3-6 µg) in shift-buffer [HEPES pH 7.9 (20 mM), KCl (120 mM), Ficoll (4%), DTT (5 mM), BSA (10 µg) and poly-dI-dC (2 µg, Roche) and radioactive probe (10000-20000 cpm)] for 30 min at RT. The samples were separated on a 5 percent polyacrylamide gel in TBE buffer, vacuum dried, and autoradiography was performed.

6.12 Labeling and Biotin Pull-Down of Active MALT1 (ABP-PD)

The biotin-labeled MALT1 activity based probe (MALT1-ABP) has been described previously [183]. To investigate MALT1 protease activity, 3-5 x 10^7 Jurkat T cells were collected and washed with PBS before being lysed in 600µl Co-IP buffer without protease inhibitors for 30 min at 4°C. Following a 15 min centrifugation at 21 000 g at 4°C, 30µl supernatant was collected as a lysate control, mixed with 4 x SDS loading buffer, and boiled for 5 min at 95°C. To pre-clear the remaining supernatant, add 12 µl High-Capacity Streptavidin Beads (Thermo Fisher) to 550 µl supernatant and incubate at 4°C for 1 hour. Beads were pelleted (200 g, 2 min, 4°C) and mixed with 450µl of supernatant containing the MALT1-ABP probe (0.1 µM final concentration). After 1hour of rotation at RT, add 15 µl High Capacity Strepavidin and incubate at 4°C for 1-2 hour (rotating). Beads were collected and washed 3 times with Co-IP buffer without protease inhibitors. Beads were resuspended in 22 µl 2x SDS loading buffer and boiled at 95°C for 8 min before SDS-PAGE and Western blot analysis.

6.13 RNA extraction and quantitative reverse-transcriptase polymerase chain reaction (qRT-PCR)

Total RNA was extracted using the QIAGEN RNeasy Kit and transcribed into cDNA using the Thermo Fisher Scientific Verso cDNA synthesis Kit according to the manufacturer's instructions. Primer sequences of the *TNIP1*, *TNFAIP3* and *RPII* genes are as follows (forward and reverse, respectively): *ABIN-1/TNIP1*, 5′-GTTCAACCGACTGGCATCCAA-3′ and 5′-AGACGCACCCTCTTTGTTGC-3′; *A20/TNFAIP3*, 5′-CTGAAAACGAACGGTGACGG-3′ and 5′-CGTGTGTCTGTTTCCTTGAGCG-3′; *RPII*, 5′-GTTCGGAGTCCTGAGTCCGGATG-3′ and 5′-CCTGCCTCGGGTCCATCAGC-3′. The LightCycler 480 equipment (Roche) and Takyon qPCR Kit for SYBR Assays (Eurogentec) were used in conjunction with a typical LightCycler procedure for quantitative real-time PCR. As an internal control, RNA polymerase II (RPII) was used.

6.14 Liquid chromatography and tandem mass spectrometry (LC-MS/MS)

6.14.1 Sample Preparation

To identify BCL10-interaction partners, CK1α KO Jurkat T cells reconstituted with CK1α WT or D136N were utilized.

6 x 10^7 cells per sample were either left untreated or stimulated with P/I for 20 min before lysis in 1% NP-40 buffer (150 mM NaCl, 50 mM Tris-HCl (pH 7.5), 10 mM Na-Pyrophosphate, 10 mM Na-Glycerophosphate, 1% NP-40, 20 mM NaF, 1 mM EGTA, 1 mM EDTA, 1 mM DTT, 10% Glycerol and protease inhibitors). For Co-IP, overnight immunoprecipitation at 4°C was performed with 0.5 µg BCL10 antibody (C-17, #sc-5611), followed by 2 hours incubation with 18µl rec-protein G Sepharose 4B beads (1:1 suspension, Life Technologies) at 4°C. Following Co-IP, beads were washed twice in 1% NP-40 buffer and twice in 50 mM Tris-HCl buffer (pH 7.5). After resuspending the beads in 2M urea dissolved in 50 mM Tris-HCl buffer (pH 7.5) and adding trypsin, the on-bead digestion was carried out overnight at 37°C. Prior to LC-MS/MS analysis, the produced peptides were cleaned using in-house prepared SDB-RPS (Empore) stage tips, as previously reported[202].

6.14.2 LC-MS/MS Analysis

Peptides were separated using a binary buffer system of buffer A (0.1% formic acid (FA) in H2O) and buffer B (80% acetonitrile plus 0.1% FA) on a 50 cm reversed-phase column (75 µm inner diameter, packed in-house with a Reprosil-Pur C18-AQ column (1.9 µm, Dr. Maisch HPLC GmbH) over 60 min gradient (5%-30% buffer B over 40 min, 30%-60% for 4 min, 60%-95% for 4 min and 12 min wash time at 95%) using the EASY-nLC 1200 system (Thermo Fisher Scientific). The column temperature was fixed at 60°C and the flow rate was set at 300 nL/min. The Q Exactive HF-X mass spectrometer (Thermo Fisher Scientific) was used in conjunction with the ASY-nLC 1200 system. It was controlled by Top10 data-dependent acquisition (DDA) settings. The full scan was performed between 300-1650 m/z at 60 k resolution, target value was 3×10^6 allowing a maximum injection time of 20 ms. And the 10 most intense ions were sequentially isolated and fragmented with higher-energy collisional dissociation (HCD) (target 1×10^5 ions, maximum injection time 60 ms, isolation window 1.4 m/z, NCE 27%) and detected in the Orbitrap (resolution 1.5 k at 200 m/z). Dynamic exclusion was set to 20 s.

6.14.3 Data analysis

Raw MS data were processed in the MaxQuant environment (versions 1.5.3.15 and 1.6.0.15) with FDR < 0.01 at the protein and peptide levels, using the MaxLFQ algorithm for label-free quantification and the integrated Andromeda search engine. The search included oxidized methionine (M) and acetylation (protein N-term) as variable modifications and carbamidomethyl (C) was used as a fixed modification. Trypsin digestion was permitted a maximum of two miscleavages. Furthermore, peptides with at least seven amino acids were examined for identification, and ‘‘match between runs’’ was enabled with a matching time window of 0.7 min to allow the quantification of MS1 features which were not recognized in each single measurement. A UniProt FASTA database from Homo sapiens (2015) with 21051 entries was used to identify peptides and proteins.

6.14.4 Bioinformatics

All statistical and bioinformatics analyses, as well as visualization, were carried out using PERSEUS (versions 1.5.4.1 and 1.6.1.3) and GraphPad Prism version 7.03. To determine interaction partners, the proteins identified only by site-modification or found in the decoy reverse database and the contaminants were filtered out before data analysis. MaxLFQ intensities were quantified and converted to a log2 scale. Three biological replicates of each pulldown were grouped, and a minimum of three valid values was required in at least one group. Missing values were imputed based on a normal distribution (width = 0.3, down-shift = 1.8). Significance was assessed by two-sample student's t-test (two-sided) including a permutation-based FDR of 5% and an S0 value of 0.1.

6.15 Flow cytometric analysis

To assess the hΔCD2 surface expression in infected cells, cells were stained with anti-CD2-APC antibody (1:400, Invitrogen #17-0029-42) for 20 min at 4°C in the dark. To evaluate the NF-κB reporter gene activity of the EGFP reporter gene, cells were stimulated as stated above, washed, and resuspended in PBS, then analyzed on Attune Acoustic Focusing Cytometer. FlowJo software 10.7.1. was used to analyze the data.

6.16 Statistics summary

GraphPad Prism version 8.0 was used for statistical analysis and data visualization. Statistical information, including the statistical tests used to calculate p-values, can be found in the figure legends.

7 Material

7.1 Instruments and equipment

Resource	Company
Agarose gel chambers	NeoLab, Heidelberg, Germany
Attune Acoustic Focusing Cytometer	Life Technologies, Carlsbad, USA
Autoradiography MP films	GE Healthcare, Freiburg, Germany
Bacterial culture flasks	BD, Heidelberg, Germany
Cell-counting chamber Neubauer	NeoLab, Heidelberg, Germany
Cell culture flasks	BD, Heidelberg, Germany
Cell culture plates	BD, Heidelberg, Germany
Centrifuge Avanti J-26 XP	Beckmann Coulter, Krefeld, Germany
Cell culture centrifuge, 5804	Eppendorf, Hamburg, Germany
Cooling cell culture centrifuge, 5810R	Eppendorf, Hamburg, Germany
Cooling table centrifuge, 5417R	Eppendorf, Hamburg, Germany
Chemiluminescence ECL films	GE Healthcare, Freiburg, Germany
CO_2 incubator	Binder, Tuttlingen, Germany
Developer Optimax	Protec, Dorfwiesen, Germany
Electroporation cuvettes, Gene Pulser	Bio-Rad, München, Germany
Electroporator, Gene Pulser Xcell System	Bio-Rad, München, Germany
EMSA gel chamber, X952.1	Roth, Karlsruhe, Germany
EASY-nLC 1200 system	Thermo Fisher Scientific, Waltham, USA
Film Cassettes	Roth, Karlsruhe, Germany
Freezers	Liebherr, Ochsenhausen, Germany
Geldocumentation System	Intas, Göttingen, Germany
Gel dryer 583	Bio-Rad, München, Germany
Heatblock	Techne, Staffordshire, UK
Incubator	Sartorius, Göttingen, Germany
Incubator Shaker I26	New Brunswick Scientific, Hamburg, Germany
LightCycler 480	Roche, Mannheim, Germany
LightCycler plates 96 well	4titude, Berlin, Germany
Magnetic stirrer	IKA Labortechnik, Staufen, Germany
Microscopes	Leica, Wetzlar, Germany
Microtiter plate (U- or V-shape),96-well	Greiner Bio-One, Frickenhausen, Germany

Microwave	SHARP, Hamburg, Germany
Nanodrop 2000	Thermo Fisher Scientific, Waltham, USA
Petri dishes	Greiner Bio-One, Frickenhausen, Germany
pH-Meter	Sartorius, Göttingen, Germany
Pipettes	Eppendorf, Hamburg, Germany
Plastic filter tips TipOne (RNase free)	StarLab, Hamburg, Germany
Plastic pipettes	Greiner Bio-One, Frickenhausen, Germany
Plastic tips	Eppendorf, Hamburg, Germany
Power supplies	Consort, Turnhout, Belgium
Precision scales	Kern, Balingen, Germany
PVDF membranes	Merck Millipore, Darmstadt, Germany
Q Exactive HF-X mass spectrometer	Thermo Fisher Scientific, Waltham, USA
Rotator	NeoLab, Heidelberg, Germany
Reprosil-Pur C18-AQ column	Dr. Maisch HPLC GmbH, Ammerbuch, Germany
SDS-PAGE chamber	Roth, Karlsruhe, Germany
Semi-dry western blot transfer system	PHASE, Lübeck, Germany
Thermocycler	Eppendorf, Hamburg, Germany
Thermomix comfort	Eppendorf, Hamburg, Germany
Tissue Culture Hoods Safeflow 1.2	Nunc, Wiesbaden, Germany
Tubes	Eppendorf, Hamburg, Germany
ViCell-XR cell viability analyzer	Beckman Coulter, Krefeld, Germany
Vortexer	Scientific Industries, Bohemia, USA
Whatman paper	Roth, Karlsruhe, Germany
Water Bath	Thermo HAAKE, Karlsruhe, Germany

7.2 Chemical

7.2.1 General Chemicals

Resource	**Company**
4 x Roti-Load	Roth, Karlsruhe, Germany
Acrylamide/Bisacrylamide	Roth, Karlsruhe, Germany
Agar	Roth, Karlsruhe, Germany
Agarose	Biozym, Hessisch Oldendorf, Germany
Ammonium persulfate (APS)	Bio-Rad, München, Germany

Ampicillin	Roth, Karlsruhe, Germany
Autoradiography developing solution	Sigma-Aldrich, Taufkirchen, Germany
Autoradiography fixing solution	Sigma-Aldrich, Taufkirchen, Germany
Boric acid	Roth, Karlsruhe, Germany
Bovine serum albumin (BSA)	GE Healthcare, Freiburg, Germany
Brefeldin-A	Signa-Aldrich, Taufkirchen, Germany
Calcium chloride	Roth, Karlsruhe, Germany
Disodium hydrogen phosphate	Roth, Freiburg, Germany
Dimethyl sulfoxide (DMSO)	Sigma-Aldrich, Taufkirchen, Germany
DNA 1kb plus ladder	Invitrogen, Carlsbad, USA
dNTP-Mix	Thermo Fisher Scientific, Waltham, USA
Dithiothreitol (DTT)	Sigma-Aldrich, Taufkirchen, Germany
DNA 1kb plus ladder	Invitrogen, Carlsbad, USA
Ethylenediaminetetraacetic acid (EDTA)	Roth, Freiburg, Germany
Ethanol (p. a.)	Merck, Darmstadt, Germany
Ethidiumbromide	Roth, Freiburg, Germany
Glycerol	Roth, Freiburg, Germany
Glycine	Roth, Freiburg, Germany
HEPES	Roth, Freiburg, Germany
Isopropyl alcohol (p.a.)	Merck, Darmstadt, Germany
LB	Roth, Freiburg, Germany
Lumi-Glo ECL reagent	NEB, Frankfurt, Germany
Magnesium chloride	Roth, Freiburg, Germany
Methanol (p.a.)	Merck, Darmstadt, Germany
Nonidet P40 substitute (NP-40)	Sigma-Aldrich, Taufkirchen, Germany
PageRuler Prestained Protein Ladder	Thermo Fisher Scientific, Waltham, USA
Paraformaldehyde (PFA)	Sigma-Aldrich, Taufkirchen, Germany
Polybrene	Sigma-Aldrich, Taufkirchen, Germany
Poly dl-dC	Roche, Mannheim, Germany
Potassium chloride	Roth, Freiburg, Germany
Potassium hydrogen phosphate	Roth, Freiburg, Germany
Protease inhibitor cocktail (Roche complete)	Roche, Mannheim, Germany
Protein-G-Sepharose	Invitrogen, Carlsbad, USA
Protein loading buffer (Rotiload)	Roth, Freiburg, Germany
Saponine	Roth, Freiburg, Germany

Sodium acetate	Roth, Freiburg, Germany
Sodium azide	Roth, Freiburg, Germany
Sodium chloride	Roth, Freiburg, Germany
Sodium dodecyl sulfate (SDS)	Roth, Freiburg, Germany
Sodium fluoride	Sigma-Aldrich, Taufkirchen, Germany
Sodium vanadate	Roth, Freiburg, Germany
Strep-Tactin Sepharose	IBA, Göttingen, Germany
Sulfuric acid	Merck, Darmstadt, Germany
Tetramethylethylenediamine (TEMED)	Roth, Freiburg, Germany
Tris(hydroxymethyl)-aminomethan (Tris)	Roth, Freiburg, Germany
Trypan blue	Invitrogen, Carlsbad, USA
Tween 20	Roth, Freiburg, Germany
X-tremeGENE HP Transfection Reagent	Roche, Mannheim, Germany
^{32}P-α-dATP	Perkin Elmer, Wiesbaden, Germany
^{32}P-γ-dATP	Hartmann, Braunschweig, Germany
β-Glycerophosphate	Sigma-Aldrich, Taufkirchen, Germany
β-Mercaptoethanol	Roth, Freiburg, Germany

7.2.2 Cell culture chemicals

Resource	**Company**
DMEM	Life Technologies, Carlsbad, USA
Fetal calf serum (FCS)	Life Technologies, Carlsbad, USA
L-glutamine	Life Technologies, Carlsbad, USA
Non-essential amino acids (NEAA)	Life Technologies, Carlsbad, USA
Optimem	Life Technologies, Carlsbad, USA
Penicillin/Streptomycin (P/S)	Life Technologies, Carlsbad, USA
RPMI 1640	Life Technologies, Carlsbad, USA
Sodium pyruvate	Life Technologies, Carlsbad, USA
Trypsin/EDTA	Life Technologies, Carlsbad, USA
Phorbol 12-myristate 13-acetate (PMA)	Merck Millipore, Darmstadt, Germany
Ionomycin	Calbiochem, Schwalbach, Germany
Tumor necrosis factor alpha (TNFα)	Biomol, Hamburg, Germany

7.2.3 Inhibitors

Resource	Company
MG132	Calbiochem, San Diego, USA
MLT-985	HMGU, Munich, Germany
Z-VRPR-FMK	Enzo Life Sciences, Farmingdale, USA
Birinapant	BioCat, Heidelberg, Germany

7.3 Enzymes

Resource	Company
Dream Taq DNA polymerase	Thermo Scientific, Waltham, USA
Herculase II DNA Polymerase	Agilent Technologies, Waldbronn, Germany
Proteinase K	NEB, Frankfurt, Germany
Restriction enzymes	NEB, Frankfurt, Germany
Restriction buffers	NEB, Frankfurt, Germany
T4 DNA ligase	NEB, Frankfurt, Germany

7.4 Kits

Resource	Company
Gel Extraction Kit	Qiagen, Hilden, Germany
Gel Extraction Kit	Macherey & Nagel, Düren, Germany
KAPA SYBR FAST qPCR Mastermix	Peqlab, Erlangen, Germany
LightCycler 480 SYBR Green I Mastermix	Roche, Mannheim, Germany
QIAshredder	Qiagen, Hilden, Germany
NucleoSpin PCR & Gel Purification Kit	Macherey & Nagel, Düren, Germany
Plasmid Maxi Kit	Qiagen, Hilden, Germany
Plasmid Mini Kit	Qiagen, Hilden, Germany
RNeasy RNA isolation Kit	Qiagen, Hilden, Germany
Superscript First Strand Synthesis Kit	Invitrogen, Carlsbad, USA
Superscript II Reverse Transcriptase	Invitrogen, Carlsbad, USA
Verso cDNA Synthesis Kit	Thermo Fisher Scientific, Waltham, USA

7.5 Cell lines

Resource	Information
HEK293	Human embryonic kidney cell line

HEK293T	Human embryonic kidney cell line; transformed with SV40 large T antigen
Jurkat T cells	Human T cell line
BCL10 KO Jurkat T cells	Generated by S.Widmann, AG Krappmann
CARD11 KO Jurkat T cells	Generated by S.Woods, AG Krappmann
MALT1 KO Jurkat T cells	Generated by T.Gehring, AG Krappmann
CK1α KO Jurkat T cells	Generated by T.Gehring, AG Krappmann
TRAF6 KO Jurkat T cells	Generated by T.Seeholzer, AG Krappmann
HOIP KO Jurkat T cells	Generated by A. Stangl, AG Krappmann
HOIL-1 KO Jurkat T cells	Target exon1 and exon11 by CRISPR/Cas9
A20 KO Jurkat T cells	Target exon3 by CRISPR/Cas9
ABIN-1 KO Jurkat T cells	Target exon3 by CRISPR/Cas9

7.6 Vectors and oligonucleotides

7.6.1 Vectors

Name	**Information**
pHAGE-PGK-L1-hΔCD2-T2A-Flag-Strep-Strep (mock)	Lentiviral vector. Obtained from Dr. Marc Schmidt-Supprian.
pMD2.G	Lentiviral envelope plasmid (addgene #12259; gifted by D.Trono)
psPAX2	Lentiviral packaging plasmid (addgene #12260; gifted by D.Trono)
pEF-3XFLAG empty	pEF4HIS-C is the basis vector (Invitrogen). Three repeated FLAG sequences replaced His sequence
pEF-HA empty	pEF4HIS-C is the basis vector (Invitrogen). HA sequence replaced His sequence
pX458	Cas9 from S.pyogenes with 2A-EGFP, and cloning backbone for sgRNA (addgene #48138; gifted by F.Zhang)
pEF-HA-A20	A20 cDNA was transferred into pEF-HA plasmid
pEF-HA-ABIN-1	ABIN-1 cDNA was transferred into pEF-HA plasmid (

pEF-HA-WT-Ub	Ubiquitin cDNA was transferred into pEF-HA plasmid
pEF-HA-K63-Ub	Ubiquitin cDNA was transferred into pEF-HA plasmid, K63 only, other lysines mutated to arginines
pEF-HA-K48-Ub	Ubiquitin cDNA was transferred into pEF-HA plasmid, K48 only, other lysines mutated to arginines
pEF-3XFLAG A20	A20 cDNA was transferred into pEF-3XFLAG plasmid
pEF-3XFLAG A20 OTU mt	Point mutation (C103A) was introduced by PCR-based mutagenesis. A20 cDNA was transferred into pEF-3XFLAG plasmid
pEF-3XFLAG A20 ZnF4/7 mt	Point mutation (C624/627/779/782A) was introduced by PCR-based mutagenesis. A20 cDNA was transferred into pEF-3XFLAG plasmid
pEF-3XFLAG ABIN-1	ABIN-1 cDNA was transferred into pEF-3XFLAG plasmid
pEF-3XFLAG ABIN-1 ΔAHD1	ABIN-1 ΔAHD1 cDNA was transferred into pEF-3XFLAG plasmid
pHAGE-A20-FSS	A20 cDNA was transferred into pHAGE-FSS
pHAGE-A20 OTU mt-FSS	Point mutation (C103A) was introduced by PCR-based mutagenesis. A20 cDNA was transferred into pHAGE-FSS
pHAGE-A20 ZnF4/7 mt-FSS	Point mutation (C624/627/779/782A) was introduced by PCR-based mutagenesis. A20 cDNA was transferred into pHAGE-FSS
pHAGE-ABIN-1-FSS	ABIN-1 cDNA was transferred into pHAGE-FSS
pHAGE-ABIN-1 D472N-FSS	Point mutation (D472N) was introduced by PCR-based mutagenesis. ABIN-1 cDNA was transferred into pHAGE-FSS
pHAGE-ABIN-1ΔAHD1-FSS	Deletion (AHD1) was introduced by PCR-based mutagenesis. ABIN-1 cDNA was transferred into pHAGE-FSS

7.6.2 SgRNA sequence for KO cell line generation

Name	Sequence (5´-3´)

ABIN-1 ex3 sgRNA cl.34	GAGCTCAGCCAGGGGGTCGA
ABIN-1 ex3 sgRNA cl.33	TTATACCTGTGAGCTCAGCC
A20 ex3 cl.21&cl.24	GAGGCAATTGCCGTCACCTG
HOIL-1 ex1&ex11 cl.5-17	ATGGACGAGAAGACCAAGAA TGTACCACGATCTGGCACTG

7.6.3 EMSA oligonucleotides

Target	**Sequence (5´-3´)**
NF-κB (H2K) forward	GATCCAGGGCTGGGGATTCCCCATCT CCACAGG
NF-κB (H2K) reverse	GATCCCTGTGGAGATGGGGAATCCCC AGCCCTG
OCT1 forward	GATCTGTCGAATGCAAATCACTAGAA
OCT1 reverse	GATCTTCTAGTGATTTGCATTCGACA

7.6.4 Primer for RT-PCT

Target	**Sequence (5´-3´)**
ABIN-1/TNIP1 forward	GTTCAACCGACTGGCATCCAA
ABIN-1/TNIP1 reverse	AGACGCACCCTCTTTGTTGC
A20/TNFAIP3 forward	CTGAAAACGAACGGTGACGG
A20/TNFAIP3 reverse	CGTGTGTCTGTTTCCTTGAGCG
RPII forward	GTTCGGAGTCCTGAGTCCGGATG
RPII reverse	CCTGCCTCGGGTCCATCAGC

7.7 Antibodies

Name	**Company**
Mouse anti-human anti-CD3	BD Pharmigen, Frankfurt am Main, Germany
Mouse anti-human anti-CD28	BD Pharmigen, Frankfurt am Main, Germany
Rat anti-mouse IgG1	BD Pharmigen, Frankfurt am Main, Germany

Rat anti-mouse IgG2	BD Pharmigen, Frankfurt am Main, Germany
anti-CD2-APC (RPA-2.10)	eBioscience, Frankfurt am Main, Germany
anti-APC-APC (#554567)	BD Pharmigen, Frankfurt am Main, Germany
anti-TNF-FITC (#554512)	BD Pharmigen, Frankfurt am Main, Germany
anti-β-Actin	Santa Cruz Biotechnology, Heidelberg, Germany
anti-ABIN-1	Cell Signaling Technology, Frankfurt am Main, Germany
anti-A20 (D13H3)	Cell Signaling Technology, Frankfurt am Main, Germany
anti-A20 (59A426)	Santa Cruz Biotechnology, Heidelberg, Germany
anti-BCL10 (H-197)	Santa Cruz Biotechnology, Heidelberg, Germany
anti-CARD11 (1D12)	NEB, Frankfurt am Main, Germany
anti-CYLD (E-10)	Santa Cruz Biotechnology, Heidelberg, Germany
anti-cIAP1	R&D System, Minneapolis, USA
anti-HA (3F1)	Core facility monoclonal antibodies, HMGU (R.Feederle)
anti-HOIL1 (E-2)	Santa Cruz Biotechnology, Heidelberg, Germany
anti-HOIP	R&D System, Minneapolis, USA
anti-IκBα (L35A5)	NEB, Frankfurt am Main, Germany
anti-MALT1 (human, B12)	Santa Cruz Biotechnology, Heidelberg, Germany
anti-phospho-IκBα (5A5)	NEB, Frankfurt am Main, Germany
Anti-Ubiquitin (P4D1)	Santa Cruz Biotechnology, Heidelberg, Germany
HRP-conjugated anti-rabbit	JacksonlmmunoResearch, Newmarket, UK
HRP-conjugated anti-mouse	JacksonlmmunoResearch, Newmarket, UK
HRP-conjugated anti-goat	JacksonlmmunoResearch, Newmarket, UK
ABIN-1 (used for IP)	Ubiquigent, Dundee, UK

MALT1 (used for IP)	HMGU, Munich, Germany
BCL10 (C-17) (used for IP)	Santa Cruz Biotechnology, Heidelberg, Germany

7.8 Buffers and Solutions

Name	Components
Annealing buffer	Tris-HCl pH 8.0 (50mM), NaCl (70mM)
Blocking buffer	Milk in PBS-T (5%(w/v))
Blotting buffer	Tris pH 8.3 (48 mM), Glycine (39 mM), Methanol (20 % (v/v)), SDS (0.03 % (w/v))
Co-IP buffer	HEPES pH 7.5 (25 mM), NaCl (150 mM), Glycerol (1 mM), NP- 40 (0.2 % (v/v)), DTT (1 mM), NaF (10 mM), β- Glycerophosphate (8 mM), NaVanadate (300 µM), Protease inhibitor mix
FACS buffer	PBS (1x), FCS (2 % (w/v)), NaN3 (0.01 % (v/v))
High salt buffer	HEPES pH 7.9 (20 mM), NaCl (350 mM), Glycerol (20 % (v/v)), MgCl2 (1 mM), EDTA (0.5 mM), EGTA (0.1 mM), NP-40 (1 %), DTT (1 mM), NaF (10 mM), β-Glycerophosphate (8 mM), NaVanadate (300 µM), Protease inhibitor mix
IC buffer	PBS (1x), Saponine (0.5 % (w/v)), NaN3 (0.01 % (v/v))
PBS (1X)	NaCl (137 mM), Na_2HPO_4 (10 mM), KCl (2.7 mM), KH_2PO_4 (1.7 mM)
PBS	PBS, Tween-20 (0.1 % (v/v))
Poly dl-dC	Poly dl-dC (2mg/ml), Tris pH 8.0 (10mM), NaCl (100mM)

Polyacrylamide gel	TBE buffer (1x), Acrylamide/Bisacrylamide (5 %), APS (0.75 % (v/v)), TEMED (0.075 % (v/v))
SDS electrophoresis buffer (1x)	Tris pH 8.8 (25 mM), Glycine (192 mM), SDS (0.1 % (w/v))
Separation gel	Tris/HCl pH=8.8 (375 mM), Acrylamide/Bisacrylamide (7.5-11 %), SDS (0.1 %), APS (0.075 %), TEMED (0.05 %)
Shift buffer (2x)	HEPES pH 7.9 (20 mM), KCl (120 mM), Ficoll (4 % (w/v))
Stacking gel	Tris/HCl pH 6.8 (125 mM), Acrylamide/Bisacrylamide (5 %), SDS (0.1 %), APS (0.1 %), TEMED (0.1 %)
Stripping buffer	Glycine (0.2 M), SDS (0.1 %), Tween-20 (1 % (v/v)), pH 2.2
TBE buffer	Tris (50 mM), Boric acid (50 mM), EDTA (1 mM), pH 8.3
1% NP-40 buffer	NaCl (150mM), Tris-HCl pH 7.5 (50mM), Na-Pyrophosphate (10mM), Na-Glycerophosphate (10mM), 1% NP-40, NaF (20mM), EGTA (1mM), EDTA (1mM), DTT (1mM), 10% Glycerol and protease inhibitors

8 Abbreviations

°C	°Celsius
A/Ala	alanine
aa	amino acid
ABC	activated B cell-like (DLBCL)
ABP	activity based probe
AgR	antigen-receptor
APC	antigen presenting cell
APC	allophycocyanin
APS	ammonium persulfate
ATP	adenosine triphosphate
BCL10	B cell chronic lymphocytic leukemia/lymphoma 10
BCR	B cell receptor
bp	base pair
BSA	bovine serum albumin
BTK	Bruton tyrosine kinase
Cys	cysteine
Ca2+	calcium
CARD	Caspase-recruitment domain
CARMA1	CARD-containing MAGUK 1 (also known as CARD11)
Cas9	CRISPR-associated protein-9
CBM	CARMA1-BCL10-MALT1
CC	Coiled-coil
CD	Cluster of differentiation
cDNA	Complementary DNA
CK1α	Casein kinase 1 alpha
Co-IP	Co-immunoprecipitation
cpm	Counts per minute
CRISPR	Clustered Regularly Interspaced Short Palindromic Repeats
C-terminus	Carboxyl-terminus
CYLD	cylindromatosis
DAG	diacylglycerol
dATP	desoxyadenosine triphosphate
DD	death domain
DLBCL	diffuse large B cell lymphoma

DMEM	Dulbecco´s Modified Eagle Medium
DNA	deoxyribonucleic acid
dNTP	deoxyribonucleotide triphosphate
ds	double-stranded
DTT	dithiothreitol
DUB	deubiquitinase
E/Glu	glutamate
ECL	enhanced chemiluminescence
EDTA	ethylenediaminetetraacetic acid
EGFP	enhanced green fluorescent protein
EGTA	Ethyleneglycol-bis(2-aminoethylether)-N, N, N′, N′-tetraacetic acid
EMSA	electrophoretic mobility shift assay
ERK	extracellular signal-regulated kinase
ES	embryonal stem cell
FACS	fluorescence-activated cell sorting
FCS	fetal calf serum
FITC	fluorescein isothiocyanate
FS	Flag-StrepII
g	gravity
GCB	germinal center B cell-like
GUK	guanylate kinase
h	human
h	hour
HEK	human embryonic kidney
HEPES	2-[4-(2-Hydroxyethyl)-1-piperazino]-ethansulfonic acid
HOIL1	Heme-oxidized IRP2 ubiquitin ligase 1
HRP	Horseradish peroxidase
I	Ionomycin
Ig	immunoglobulin
IKK	IκB kinase
IL	interleukin
IP	immunoprecipitation
IP3	inositol 1,4,5-trisphosphate
ITAM	immunoreceptor tyrosine-based activation motif
ITCH	E3 ubiquitin-protein ligase Itchy homolog
IκB	Inhibitor of κB

JNK	c-Jun N-terminal kinase
K/Lys	lysine
kb	kilo base
kDa	kilo Dalton
KH2PO4	potassium hydrogen phosphate
KO	knockout
LB	Luria-Bertani
LPS	lipopolysaccharide
LUBAC	linear ubiquitin chain assembly complex
MAGUK	membrane associated guanylate kinase
MALT1	mucosa associated lymphoid tissue lymphoma translocation protein 1
MAPK	mitogen activated protein kinase
MFI	median fluorescence intensity
mg	milligram
MgCl2	magnesium chloride
MHC	major histocompatibility complex
min	minute
ml	milliliter
mRNA	Messenger RNA
Na2HPO4	disodium hydrogen phosphate
NaCl	sodium chloride
NaF	sodium fluoride
NaN3	sodium azide
NEAA	non-essential amino acids
NEDD	neural precursor cell expressed developmentally down-regulated protein
NEMO	NF-κB essential modulator
NF-κB	nuclear factor kappa B
ng	nanogram
nm	nanometer
NP-40	nonidet P40 substitude
nt	nucleotide
N-terminus	amino-terminus
P/S	penicillin/streptomycin
PAMP	pathogen-associated molecular pattern

PBS	phosphate buffered saline
PBS-T	PBS-Tween 20
PCR	polymerase chain reaction
PDK1	phosphoinositide-dependent kinase 1
PDZ	PSD-95/DLG/ZO1 homology
PFA	paraformaldehyde
PH	pleckstrin homology
PI3K	phosphoinositide 3 kinase
PKC	protein kinase C
PLC1	phospholipase C1
R	arginine
RHD	Rel homology domain
RNA	ribonucleic acid
RPII	RNA polymerase II
rpm	rounds per minute
RT	room temperature
RT-PCR	Real-time PCR
S	serine
s	second
SDS	Sodium dodecyl sulfate
SDS-PAGE	SDS polyacrylamide gel electrophoresis
Ser/Thr-rich	serine/threonine-rich
siRNA	small interfering RNA
ST-PD	Strep-Tactin pulldown
TAC	tris ammonium cloride
TAK	transforming growth factor beta activated kinase
TBE	Tris borate EDTA
TCR	T cell receptor
TE	Tris EDTA
TEMED	Tetramethylethylenediamine
TH	T helper cells
TLR	Toll like receptor
Tm	melting temperature
TNF	Tumour necrosis factor
TRAF	Tumor-necrosis factor associated receptor-associated factor
Tris	Tris(hydroxymethyl)-aminomethan

U	Unit
UTR	untranslated region
V	Volt
WB	Western Blot
WT	wildtype
ZAP-70	zeta-chain-associated protein 70 kDa
µg	microgram
µl	microliter

9 Appendix

9.1 Table 1: LC-MS/MS screen for BCL10 interaction partners

Ranked by mean enrichment of BCL10 IP. Top 100 hits with a noticeable mean enrichment. Selected proteins presented in **Figure 4-1** are highlighted in blue.

Rank	Gene names	# of peptides	log2 fold change PI vs US	log2 fold change PI CK1WT vs CK1DN
1	CARD11	82	6.39137395	7.61112340
2	TRAF2	6	5.70459684	5.05264346
3	ZNF600	3	3.68933042	3.86228879
4	RBCK1	3	3.67695745	3.71618080
5	TNIP1	3	3.58179220	5.06139437
6	AIP	4	3.54535039	1.50263977
7	HTRA2	2	2.87473933	3.85512861
8	SHARPIN	2	2.60787900	2.81565158
9	CSNK1A1	1	2.48907789	1.97348658
10	DIABLO	1	2.37333997	2.93808810
11	NSF	2	2.34519005	3.41488457
12	MRPL3	2	2.34267616	0.33397102
13	PAFAH1B1	1	2.26792908	0.03537877
14	IKBKE	2	2.07473056	2.55464681
15	AZIN2	1	2.01926931	0.37536494
16	MARK1	5	1.92922592	0.43171755
17	RIF1	5	1.92826017	0.23847516
18	YME1L1	1	1.91048686	-0.29342206
19	Ubiquitin	6	1.89280256	1.43294144
20	ASAP3	3	1.82152430	1.54243851
21	HINT2	1	1.72819964	-0.27427864
22	CLTB	2	1.63046137	0.37087059
23	PRDX3	4	1.61672274	-0.39853795

24	IGLV10-54	1	1.59071795	1.07162348
25	PRC1	2	1.58829816	0.52318255
26	VMA21	3	1.58119392	2.12878927
27	PAFAH1B3	6	1.55602392	0.31957181
28	MRPS31	3	1.50668844	-0.32962481
29	ZBTB21	3	1.50215785	0.08966128
30	PPFIA1;PPFIA2	3	1.48852158	-0.63463338
31	MED4	4	1.48696454	0.85776711
32	RNF2	3	1.48390834	-0.14879417
33	PRKD2;PRKD3	2	1.47544161	0.60925738
34	CYB5B	2	1.46451378	-0.09503682
35	HIST1H1E	13	1.46211243	1.13288816
36	TUBB2B;TUBB2A	14	1.45124181	3.38096174
37	NDUFAF2	1	1.44420560	0.71311251
38	NDUFA13	1	1.43501027	1.03347905
39	UNK	7	1.42987315	-0.01786931
40	VPS35	1	1.41438230	-0.45270729
41	FBXW11	1	1.40079244	0.89879354
42	SORD	2	1.39861933	0.79863040
43	IRF2BP2	1	1.38330460	0.06107521
44	DCTN2	4	1.38152377	0.28049533
45	C2orf49	2	1.37601217	-0.86775780
46	FLYWCH2	2	1.34780629	0.67830594
47	NAA10	1	1.34137599	0.37403361
48	PPIH	2	1.33695602	-0.19284884
49	WIBG	2	1.32680639	-0.30516879
50	TIPRL	1	1.27962557	-0.32634672
51	ESD	2	1.25238228	0.77827390
52	TCF12;TCF4	2	1.23920377	0.61150996
53	C11orf57	2	1.23605982	-0.40324656
54	COX5B	2	1.23237483	2.19919459
55	CD247	2	1.20643616	-0.12724241
56	SCFD1	2	1.17754873	0.38040352

57	PFKFB4	19	1.17571004	0.81786982
58	LTV1	2	1.16077995	0.53887685
59	VAV1	1	1.15125593	-0.63485972
60	MNAT1	2	1.13364220	-0.22217941
61	SZRD1	1	1.12337812	-0.52711105
62	SH3BGRL	2	1.12038994	0.27972221
63	ESRRA	1	1.11795044	2.38627815
64	STRBP	4	1.09644953	0.97081375
65	DCD	5	1.05756378	0.19571241
66	IKBKB	3	1.05594699	0.44758161
67	TAF6L	2	1.05152766	0.47520129
68	GOSR2	1	1.04943339	-0.32618523
69	TIMM23	1	1.03490448	2.36760585
70	BOD1L1	40	1.03370349	0.42164803
71	LMO7	6	1.03270404	1.75400670
72	ERLIN1	2	1.02663231	0.43969091
73	SNX24	1	1.01841482	0.79522705
74	POLR1B	2	1.01211230	0.07622464
75	ACO2	1	0.99569384	-0.66843287
76	UBQLN4;UBQLN1	1	0.98738098	0.89664459
77	RB1CC1	1	0.98668226	0.94707171
78	LARP4	3	0.98595810	-0.00343577
79	VIM	37	0.97598330	0.68633334
80	SP110	1	0.97279549	0.13253911
81	UBASH3B	2	0.97053782	0.07762782
82	MCM4	3	0.96649933	-0.71331406
83	COTL1	7	0.96219381	0.88348770
84	FBF1	33	0.96111488	0.67202950
85	S100A7	3	0.94877179	0.12215678
86	TNRC6C	1	0.94599660	0.02967517
87	PPA1	7	0.92550151	0.34230550
88	ASCC2	2	0.91859245	0.99468549
89	SAE1	1	0.91237005	-0.70936394

90	MRPS33	3	0.90232404	0.54085159
91	CSNK2A2	1	0.89151192	0.58045578
92	CDT1	2	0.89026197	0.49947675
93	EMG1	2	0.87490781	-0.37935829
94	PDE4DIP	2	0.87433370	-0.31756783
95	HMGB3	1	0.85562261	2.71775945
96	YARS	3	0.85404523	0.11315346
97	OSBPL7	1	0.84246381	0.10969035
98	MAP2K2;MAP2K1	1	0.83572006	0.08499336
99	MORC3	2	0.83170319	0.81904920
100	KAT8	7	0.82634544	0.36116664

9.2 Publication during Ph.D. study

1. **Yin, H.**, Karayel, O., Chao, Y.Y., Seeholzer, T., Hamp, I., Plettenburg, O., Gehring, T., Zielinski, C., Mann, M. and Krappmann, D., A20 and ABIN-1 cooperate in balancing CBM complex-triggered NF-κB signaling in activated T cells. ***Cellular and Molecular Life Sciences***, 79.2 (2022): 1-19.

Part of the content of this dissertation is taken from this paper

2. Kutzner, K., Woods, S., Karayel, O., Gehring, T., **Yin, H.**, Flatley, A., Graß, C., Wimberger, N., Tofaute, M.J., Seeholzer, T. and Feederle, R., 2022. Phosphorylation of serine-893 in CARD11 suppresses the formation and activity of the CARD11-BCL10-MALT1 complex in T and B cells. ***Science Signaling***, *15*(723), p.eabk3083.

10 Acknowledgement

Looking back on my four years of Ph.D. study, which have been the most beautiful four years of my life, I truly appreciate everything that has happened and would want to express my sincere appreciation to everyone who has provided me with invaluable help during this period.

First and foremost, I would like to thank my supervisor Prof. Dr. Daniel Krappmann for giving me an opportunity to study and work in this laboratory, as well as providing excellent guidance and support throughout the whole Ph.D. life. He spent a lot of energy and time supervising me, giving me the professional advice that has broaden my sight and made me understand the true meaning of science. I learnt a lot from him, not just academic knowledge but also valuable experience as an entry-level researcher. I consider myself fortunate to have a professional and experienced supervisor who is enthusiastic about research.

Then, I'd want to thank the Thesis Committee members Prof. Dr. Philipp Jost and Prof. Dr. Marc Schmidt-Supprian for attending the progress report meeting and providing me with helpful suggestions and encouragement. And I'd like to express my gratitude to TUM PhD Program co-coordinator Mrs. Bettina Kratzer and Mrs. Raphaela Blum. I've never seen a more dedicated secretary than them. Without their support, I will be unable to complete all the coursework in the PhD program. I am appreciative for their assistance.

I'd want to express my gratitude to Dr. Thomas Seeholzer for reviewing the thesis and doing experiments while my paper is in revision. I'd want to show my thankfulness to Dr. Andreas Gewies for his help when I initially started my study; I remember being confused when I first stepped into the lab. I'd like to thank Dr. Thomas O'Neil and Mrs. Kerstin Kutzner for donating blood for my experiment. I'd also want to thank all present and former members of our laboratory for teaching basic experiments and for their invaluable friendship and support, which make studying here a pleasurable experience.

At the end, I would also like to thank my family for their support all the way from the very beginning of my study. And I'd like to thank Jian. I am extremely grateful to have him in my life; we have shared so many happy experiences over the last ten years. Because of him, I have tasted the sweetness and beauty of love, and no matter what challenges I face, I always feel that there is still strength to sustain me and give me hope. Meeting and marrying you is the nicest thing that has ever happened to me. There is only you in my heart, now and forevermore.

Everyone I've mentioned has helped me in improving, growing, and being a better person. They also sparked my curiosity in science and love. My four years as a Ph.D. student in Munich, Germany, were some of the greatest wonderful of my life, which has left me with many priceless memories that I will cherish for the rest of my life.

Figures in this dissertation were created with BioRender.com

11 Citation

1. Janeway, C. A. & Medzhitov, R. Innate Immune Recognition. *Annual Review of Immunology* **20**, 197–216 (2002).
2. Mogensen, T. H. Pathogen Recognition and Inflammatory Signaling in Innate Immune Defenses. *Clinical Microbiology Reviews* **22**, 240–273 (2009).
3. Bonilla, F. A. & Oettgen, H. C. Adaptive immunity. *Journal of Allergy and Clinical Immunology* **125**, S33–S40 (2010).
4. Cooper, M. D. & Alder, M. N. The Evolution of Adaptive Immune Systems. *Cell* **124**, 815–822 (2006).
5. Iwasaki, A. & Medzhitov, R. Regulation of Adaptive Immunity by the Innate Immune System. *Science* **327**, 291–295 (2010).
6. Tan, T.-T. & Coussens, L. M. Humoral immunity, inflammation and cancer. *Current Opinion in Immunology* **19**, 209–216 (2007).
7. Li, Q. & Verma, I. M. NF-κB regulation in the immune system. *Nat Rev Immunol* **2**, 725–734 (2002).
8. Hayden, M. S., West, A. P. & Ghosh, S. NF-κB and the immune response. *Oncogene* **25**, 6758–6780 (2006).
9. Oeckinghaus, A. & Ghosh, S. The NF-κB Family of Transcription Factors and Its Regulation. *Cold Spring Harbor Perspectives in Biology* **1**, a000034–a000034 (2009).
10. Zinatizadeh, M. R. *et al.* The Nuclear Factor Kappa B (NF-kB) signaling in cancer development and immune diseases. *Genes & Diseases* **8**, 287–297 (2021).
11. Takeshige, K. [IkappaB-zeta: an inducible regulator of nuclear factor-kappaB]. *Fukuoka Igaku Zasshi* **98**, 11–18 (2007).
12. Carmody, R. J., Ruan, Q., Palmer, S., Hilliard, B. & Chen, Y. H. Negative regulation of tolllike receptor signalling by NF-κB p50 ubiquitination blockade. *Science* 675–678 (2007).
13. Sun, S.-C. The non-canonical NF-κB pathway in immunity and inflammation. *Nat Rev Immunol* **17**, 545–558 (2017).
14. Hayden, M. S. & Ghosh, S. Shared Principles in NF-κB Signaling. *Cell* **132**, 344–362 (2008).
15. Baldi, L., Brown, K., Franzoso, G. & Siebenlist, U. Critical role for lysines 21 and 22 in signal-induced, ubiquitin-mediated proteolysis of I kappa B-alpha. *J Biol Chem* **271**, 376–379 (1996).
16. Alkalay, I. *et al.* Stimulation-dependent I kappa B alpha phosphorylation marks the NF-kappa B inhibitor for degradation via the ubiquitin-proteasome pathway. *Proc Natl Acad Sci U S A* **92**, 10599–10603 (1995).
17. Winston, J. T. *et al.* The SCFβ-TRCP–ubiquitin ligase complex associates specifically with phosphorylated destruction motifs in IκBα and β-catenin and stimulates IκBα ubiquitination in vitro. *Genes Dev* **13**, 270–283 (1999).
18. Verstrepen, L. *et al.* TLR-4, IL-1R and TNF-R signaling to NF-κB: variations on a common theme. *Cell. Mol. Life Sci.* **65**, 2964–2978 (2008).
19. Mercurio, F. *et al.* IKK-1 and IKK-2: cytokine-activated IkappaB kinases essential for NF-kappaB activation. *Science* **278**, 860–866 (1997).

20. Ruland, J. Return to homeostasis: downregulation of NF-κB responses. *Nat Immunol* **12**, 709–714 (2011).
21. Ghosh, S. & Hayden, M. S. New regulators of NF-κB in inflammation. *Nat Rev Immunol* **8**, 837–848 (2008).
22. Xiao, G., Harhaj, E. W. & Sun, S. C. NF-kappaB-inducing kinase regulates the processing of NF-kappaB2 p100. *Mol Cell* **7**, 401–409 (2001).
23. Wharry, C. E. Constitutive non-canonical NF-κB signaling in pancreatic cancer. *Dissertations available from ProQuest* 1–104 (2009).
24. Abramson, J. & Anderson, G. Thymic Epithelial Cells. *Annual Review of Immunology* **35**, 85–118 (2017).
25. Damgaard, R. B. The ubiquitin system: from cell signalling to disease biology and new therapeutic opportunities. *Cell Death Differ* **28**, 423–426 (2021).
26. Callis, J. The Ubiquitination Machinery of the Ubiquitin System. in *The arabidopsis book* (2014). doi:10.1199/tab.0174.
27. Chaugule, V. K. & Walden, H. Specificity and disease in the ubiquitin system. *Biochemical Society Transactions* **44**, 212–227 (2016).
28. Dikic, I., Wakatsuki, S. & Walters, K. J. Ubiquitin-binding domains — from structures to functions. *Nat Rev Mol Cell Biol* **10**, 659–671 (2009).
29. Ikeda, F. & Dikic, I. Atypical ubiquitin chains: New molecular signals. 'Protein Modifications: Beyond the Usual Suspects' Review Series. *EMBO reports* **9**, 536–42 (2008).
30. Ea, C.-K., Deng, L., Xia, Z.-P., Pineda, G. & Chen, Z. J. Activation of IKK by TNFα Requires Site-Specific Ubiquitination of RIP1 and Polyubiquitin Binding by NEMO. *Molecular Cell* **22**, 245–257 (2006).
31. Wagner, S. *et al.* Ubiquitin binding mediates the NF-κB inhibitory potential of ABIN proteins. *Oncogene* **27**, 3739–3745 (2008).
32. Tokunaga, F. *et al.* Specific recognition of linear polyubiquitin by A20 zinc finger 7 is involved in NF-κB regulation. *EMBO J* **31**, 3856–3870 (2012).
33. Bosanac, I. *et al.* Ubiquitin Binding to A20 ZnF4 Is Required for Modulation of NF-κB Signaling. *Molecular Cell* **40**, 548–557 (2010).
34. Inflammatory cardiac valvulitis in TAX1BP1-deficient mice through selective NF-κB activation. *The EMBO Journal* **27**, 629–641 (2008).
35. Wertz, I. E. & Dixit, V. M. Signaling to NF-κB: Regulation by Ubiquitination. *Cold Spring Harb Perspect Biol* **2**, a003350 (2010).
36. Makris, C. *et al.* Female Mice Heterozygous for IKKγ/NEMO Deficiencies Develop a Dermatopathy Similar to the Human X-Linked Disorder Incontinentia Pigmenti. *Molecular Cell* **5**, 969–979 (2000).
37. Smith-Garvin, J. E., Koretzky, G. A. & Jordan, M. S. T Cell Activation. *Annual Review of Immunology* **27**, 591–619 (2009).
38. Malmström, V., Trollmo, C. & Klareskog, L. Modulating co-stimulation: a rational strategy in the treatment of rheumatoid arthritis? *Arthritis Res Ther* **7**, S15–S20 (2005).
39. Dustin, M. L. The immunological synapse. *Cancer Immunol Res* **2**, 1023–1033 (2014).
40. Hwang, J.-R., Byeon, Y., Kim, D. & Park, S.-G. Recent insights of T cell receptor-mediated signaling pathways for T cell activation and development. *Exp Mol Med* **52**, 750–761 (2020).

41. Love, P. E. & Hayes, S. M. ITAM-mediated Signaling by the T-Cell Antigen Receptor. *Cold Spring Harbor Perspectives in Biology* **2**, a002485–a002485 (2010).
42. Wang, H. *et al.* ZAP-70: An Essential Kinase in T-cell Signaling. *Cold Spring Harb Perspect Biol* **2**, a002279 (2010).
43. Wange, R. L. & Samelson, L. E. Complex Complexes: Signaling at the TCR. *Immunity* **5**, 197–205 (1996).
44. Chan, A. C., Desai, D. M. & Weiss, A. The role of protein tyrosine kinases and protein tyrosine phosphatases in T cell antigen receptor signal transduction. *Annu Rev Immunol* **12**, 555–592 (1994).
45. Brownlie, R. J. & Zamoyska, R. T cell receptor signalling networks: branched, diversified and bounded. *Nat Rev Immunol* **13**, 257–269 (2013).
46. Wada, T. & Penninger, J. M. Mitogen-activated protein kinases in apoptosis regulation. *Oncogene* **23**, 2838–2849 (2004).
47. Macian, F. NFAT proteins: key regulators of T-cell development and function. *Nat Rev Immunol* **5**, 472–484 (2005).
48. Hoey, T., Sun, Y.-L., Williamson, K. & Xu, X. Isolation of two new members of the NF-AT gene family and functional characterization of the NF-AT proteins. *Immunity* **2**, 461–472 (1995).
49. Isakov, N. & Altman, A. PKC-theta-mediated signal delivery from the TCR/CD28 surface receptors. *Frontiers in Immunology* **3**, 273 (2012).
50. Garçon, F. *et al.* CD28 provides T-cell costimulation and enhances PI3K activity at the immune synapse independently of its capacity to interact with the p85/p110 heterodimer. *Blood* **111**, 1464–1471 (2008).
51. Frauwirth, K. A. *et al.* The CD28 signaling pathway regulates glucose metabolism. *Immunity* **16**, 769–777 (2002).
52. Ragueneau, M. Binding of phosphatidyl- inositoi-3-0H kinase to CD28 is required for T-cell signalling. **369**, 3 (1994).
53. Pagán, A. J., Pepper, M., Chu, H. H., Green, J. M. & Jenkins, M. K. CD28 Promotes CD4+ T Cell Clonal Expansion during Infection Independently of Its YMNM and PYAP Motifs. *The Journal of Immunology* **189**, 2909–2917 (2012).
54. Park, S.-G. *et al.* Phosphoinositide-dependent kinase 1 integrates T cell receptor and CD28 co-receptor signaling to effect NF-κB induction and T cell activation. *Nat Immunol* **10**, 158–166 (2009).
55. Narayan, P., Holt, B., Tosti, R. & Kane, L. P. CARMA1 Is Required for Akt-Mediated NF-κB Activation in T Cells. *Mol Cell Biol* **26**, 2327–2336 (2006).
56. Matsumoto, R. *et al.* Phosphorylation of CARMA1 plays a critical role in T Cell receptor-mediated NF-kappaB activation. *Immunity* **23**, 575–585 (2005).
57. Rueda, D. & Thome, M. Phosphorylation of CARMA1: The Link(er) to NF-κB Activation. *Immunity* **23**, 551–553 (2005).
58. Pomerantz, J. L., Denny, E. M. & Baltimore, D. CARD11 mediates factor-specific activation of NF-kappaB by the T cell receptor complex. *EMBO J* **21**, 5184–5194 (2002).
59. Wang, D. *et al.* A requirement for CARMA1 in TCR-induced NF-kappa B activation. *Nat Immunol* **3**, 830–835 (2002).

60. Bertin, J. *et al.* CARD11 and CARD14 Are Novel Caspase Recruitment Domain (CARD)/Membrane-associated Guanylate Kinase (MAGUK) Family Members that Interact with BCL10 and Activate NF-κB *. *Journal of Biological Chemistry* **276**, 11877–11882 (2001).
61. Gaide, O. *et al.* Carma1, a CARD-containing binding partner of Bcl10, induces Bcl10 phosphorylation and NF-κB activation11The GenBank accession numbers for the human Carma1, Carma2 and Carma3 are AF100338, AF100339 and AF100340, respectively. *FEBS Letters* **496**, 121–127 (2001).
62. Wang, L. *et al.* Card10 is a novel caspase recruitment domain/membrane-associated guanylate kinase family member that interacts with BCL10 and activates NF-kappa B. *J Biol Chem* **276**, 21405–21409 (2001).
63. Blonska, M. & Lin, X. NF-κB signaling pathways regulated by CARMA family of scaffold proteins. *Cell Res* **21**, 55–70 (2011).
64. Hara, H. *et al.* The MAGUK Family Protein CARD11 Is Essential for Lymphocyte Activation. *Immunity* **18**, 763–775 (2003).
65. Egawa, T. *et al.* Requirement for CARMA1 in antigen receptor-induced NF-kappa B activation and lymphocyte proliferation. *Curr Biol* **13**, 1252–1258 (2003).
66. Newton, K. & Dixit, V. M. Mice lacking the CARD of CARMA1 exhibit defective B lymphocyte development and impaired proliferation of their B and T lymphocytes. *Curr Biol* **13**, 1247–1251 (2003).
67. Sommer, K. *et al.* Phosphorylation of the CARMA1 Linker Controls NF-κB Activation. *Immunity* **23**, 561–574 (2005).
68. Shinohara, H. *et al.* PKCβ regulates BCR-mediated IKK activation by facilitating the interaction between TAK1 and CARMA1. *J Exp Med* **202**, 1423–1431 (2005).
69. Schlauderer, F. *et al.* Molecular architecture and regulation of BCL10-MALT1 filaments. *Nat Commun* **9**, 4041 (2018).
70. Thome, M. & Tschopp, J. TCR-induced NF-κB activation: a crucial role for Carma1, Bcl10 and MALT1. *Trends in Immunology* **24**, 419–424 (2003).
71. Uren, A. G. *et al.* Identification of Paracaspases and Metacaspases: Two Ancient Families of Caspase-like Proteins, One of which Plays a Key Role in MALT Lymphoma. *Molecular Cell* **6**, 961–967 (2000).
72. Monks, C. R., Kupfer, H., Tamir, I., Barlow, A. & Kupfer, A. Selective modulation of protein kinase C-theta during T-cell activation. *Nature* **385**, 83–86 (1997).
73. Sun, Z. *et al.* PKC-u is required for TCR-induced NF-kB activation in mature but not immature T lymphocytes. **404**, 6 (2000).
74. Matsumoto, R. *et al.* Phosphorylation of CARMA1 Plays a Critical Role in T Cell Receptor-Mediated NF-κB Activation. *Immunity* **23**, 575–585 (2005).
75. Dufner, A. & Schamel, W. W. B cell antigen receptor-induced activation of an IRAK4-dependent signaling pathway revealed by a MALT1-IRAK4 double knockout mouse model. *Cell Commun Signal* **9**, 1–9 (2011).
76. Scharschmidt, E., Wegener, E., Heissmeyer, V., Rao, A. & Krappmann, D. Degradation of Bcl10 Induced by T-Cell Activation Negatively Regulates NF-κB Signaling. *Molecular and cellular biology* **24**, 3860–73 (2004).
77. Gehring, T., Seeholzer, T. & Krappmann, D. BCL10 – Bridging CARDs to Immune Activation. *Frontiers in Immunology* **9**, 1539 (2018).

78. Gaide, O. *et al.* Carma1, a CARD-containing binding partner of Bcl10, induces Bcl10 phosphorylation and NF-kappaB activation. *FEBS Lett* **496**, 121–127 (2001).
79. David, L. *et al.* Assembly mechanism of the CARMA1–BCL10–MALT1–TRAF6 signalosome. *Proceedings of the National Academy of Sciences* **115**, 1499–1504 (2018).
80. Ruland, J. *et al.* Bcl10 is a positive regulator of antigen receptor-induced activation of NF-kappaB and neural tube closure. *Cell* **104**, 33–42 (2001).
81. Xue, L. *et al.* Defective development and function of Bcl10-deficient follicular, marginal zone and B1 B cells. *Nat Immunol* **4**, 857–865 (2003).
82. Hu, S. *et al.* cIAP2 is a ubiquitin protein ligase for BCL10 and is dysregulated in mucosa-associated lymphoid tissue lymphomas. *J Clin Invest* **116**, 174–181 (2006).
83. Pedersen, S. M., Chan, W., Jattani, R. P., Mackie, deMauri S. & Pomerantz, J. L. Negative Regulation of CARD11 Signaling and Lymphoma Cell Survival by the E3 Ubiquitin Ligase RNF181. *Mol Cell Biol* **36**, 794–808 (2015).
84. Hu, S., Alcivar, A., Qu, L., Tang, J. & Yang, X. CIAP2 inhibits anigen receptor signaling by targeting Bcl10 for degredation. *Cell Cycle* **5**, 1438–1442 (2006).
85. Paul, S., Kashyap, A. K., Jia, W., He, Y.-W. & Schaefer, B. C. Selective autophagy of the adaptor protein Bcl10 modulates T cell receptor activation of NF-κB. *Immunity* **36**, 947–958 (2012).
86. Scharschmidt, E., Wegener, E., Heissmeyer, V., Rao, A. & Krappmann, D. Degradation of Bcl10 induced by T-cell activation negatively regulates NF-kappa B signaling. *Mol Cell Biol* **24**, 3860–3873 (2004).
87. Wu, C.-J. & Ashwell, J. D. NEMO recognition of ubiquitinated Bcl10 is required for T cell receptor-mediated NF-κB activation. *Proc. Natl. Acad. Sci. U.S.A.* **105**, 3023–3028 (2008).
88. Zhou, H. *et al.* Bcl10 activates the NF-kappaB pathway through ubiquitination of NEMO. *Nature* **427**, 167–171 (2004).
89. Yang, Y.-K. *et al.* Molecular Determinants of Scaffold-induced Linear Ubiquitinylation of B Cell Lymphoma/Leukemia 10 (Bcl10) during T Cell Receptor and Oncogenic Caspase Recruitment Domain-containing Protein 11 (CARD11) Signaling. *J Biol Chem* **291**, 25921–25936 (2016).
90. Satpathy, S. *et al.* Systems-wide analysis of BCR signalosomes and downstream phosphorylation and ubiquitylation. *Mol Syst Biol* **11**, 810 (2015).
91. Lobry, C., Lopez, T., Israël, A. & Weil, R. Negative feedback loop in T cell activation through IkappaB kinase-induced phosphorylation and degradation of Bcl10. *Proc Natl Acad Sci U S A* **104**, 908–913 (2007).
92. Zeng, Hu, et al. "Phosphorylation of Bcl10 negatively regulates T-cell receptor-mediated NF-κB activation." *Mol Cell Biol* **27**, 5235-5245 (2007).
93. Wegener, E. *et al.* Essential role for IkappaB kinase beta in remodeling Carma1-Bcl10-Malt1 complexes upon T cell activation. *Mol Cell* **23**, 13–23 (2006).
94. Rebeaud, F. *et al.* The proteolytic activity of the paracaspase MALT1 is key in T cell activation. *Nat Immunol* **9**, 272–281 (2008).
95. Thome, M. Multifunctional roles for MALT1 in T-cell activation. *Nat Rev Immunol* **8**, 495–500 (2008).
96. Thome, M. CARMA1, BCL-10 and MALT1 in lymphocyte development and activation. *Nat Rev Immunol* **4**, 348–359 (2004).

97. Ruefli-Brasse, A. A., French, D. M. & Dixit, V. M. Regulation of NF-κB-Dependent Lymphocyte Activation and Development by Paracaspase. *Science* **302**, 1581–1584 (2003).
98. Ruefli-Brasse, A. A., French, D. M. & Dixit, V. M. Regulation of NF-κB-Dependent Lymphocyte Activation and Development by Paracaspase. *Science* **302**, 1581–1584 (2003).
99. Demeyer, A., Staal, J. & Beyaert, R. Targeting MALT1 Proteolytic Activity in Immunity, Inflammation and Disease: Good or Bad? *Trends in Molecular Medicine* **22**, (2016).
100. Afonina, I. S., Elton, L., Carpentier, I. & Beyaert, R. MALT1 – a universal soldier: multiple strategies to ensure NF-κB activation and target gene expression. *The FEBS Journal* **282**, 3286–3297 (2015).
101. Lu, H. Y. *et al.* The CBM-opathies—A Rapidly Expanding Spectrum of Human Inborn Errors of Immunity Caused by Mutations in the CARD11-BCL10-MALT1 Complex. *Frontiers in Immunology* **9**, 2078 (2018).
102. Lucas, P. C. *et al.* Bcl10 and MALT1, independent targets of chromosomal translocation in malt lymphoma, cooperate in a novel NF-kappa B signaling pathway. *J Biol Chem* **276**, 19012–19019 (2001).
103. Sun, L., Deng, L., Ea, C.-K., Xia, Z.-P. & Chen, Z. J. The TRAF6 Ubiquitin Ligase and TAK1 Kinase Mediate IKK Activation by BCL10 and MALT1 in T Lymphocytes. *Molecular Cell* **14**, 289–301 (2004).
104. Malt1 ubiquitination triggers NF-κB signaling upon T-cell activation. *The EMBO Journal* **26**, 4634–4645 (2007).
105. Meininger, I. *et al.* Alternative splicing of MALT1 controls signalling and activation of CD4+ T cells. *Nat Commun* **7**, 11292 (2016).
106. Gehring, T. *et al.* MALT1 Phosphorylation Controls Activation of T Lymphocytes and Survival of ABC-DLBCL Tumor Cells. *Cell Rep* **29**, 873-888.e10 (2019).
107. Wiesmann, C. *et al.* Structural Determinants of MALT1 Protease Activity. *Journal of Molecular Biology* **419**, 4–21 (2012).
108. Pelzer, C. *et al.* The protease activity of the paracaspase MALT1 is controlled by monoubiquitination. *Nat Immunol* **14**, 337–345 (2013).
109. Cabalzar, K. *et al.* Monoubiquitination and Activity of the Paracaspase MALT1 Requires Glutamate 549 in the Dimerization Interface. *PloS one* **8**, e72051 (2013).
110. Coornaert, B. *et al.* T cell antigen receptor stimulation induces MALT1 paracaspase–mediated cleavage of the NF-κB inhibitor A20. *Nat Immunol* **9**, 263–271 (2008).
111. Kovalenko, A. *et al.* The tumour suppressor CYLD negatively regulates NF-κB signalling by deubiquitination. *Nature* **424**, 801–805 (2003).
112. Klein, T. *et al.* The paracaspase MALT1 cleaves HOIL1 reducing linear ubiquitination by LUBAC to dampen lymphocyte NF-κB signalling. *Nat Commun* **6**, 8777 (2015).
113. Hailfinger, S. *et al.* Malt1-dependent RelB cleavage promotes canonical NF-κB activation in lymphocytes and lymphoma cell lines. *PNAS* **108**, 14596–14601 (2011).
114. Jeltsch, K. M. *et al.* Cleavage of roquin and regnase-1 by the paracaspase MALT1 releases their cooperatively repressed targets to promote TH17 differentiation. *Nat Immunol* **15**, 1079–1089 (2014).
115. Baens, M. *et al.* MALT1 Auto-Proteolysis Is Essential for NF-κB-Dependent Gene Transcription in Activated Lymphocytes. *PLOS ONE* **9**, e103774 (2014).

116. Ginster, S. *et al.* Two Antagonistic MALT1 Auto-Cleavage Mechanisms Reveal a Role for TRAF6 to Unleash MALT1 Activation. *PLOS ONE* **12**, e0169026 (2017).
117. Mathis, B. J., Lai, Y., Qu, C., Janicki, J. S. & Cui, T. CYLD-Mediated Signaling and Diseases. *Current drug targets* **16**, 284 (2015).
118. T-cell receptor-induced JNK activation requires proteolytic inactivation of CYLD by MALT1. *The EMBO Journal* **30**, 1742–1752 (2011).
119. Elton, L. *et al.* MALT1 cleaves the E3 ubiquitin ligase HOIL-1 in activated T cells, generating a dominant negative inhibitor of LUBAC-induced NF-κB signaling. *The FEBS Journal* **283**, 403–412 (2016).
120. Matsushita, K. *et al.* Zc3h12a is an RNase essential for controlling immune responses by regulating mRNA decay. *Nature* **458**, 1185–1190 (2009).
121. Mino, T. *et al.* Regnase-1 and Roquin Regulate a Common Element in Inflammatory mRNAs by Spatiotemporally Distinct Mechanisms. *Cell* **161**, 1058–1073 (2015).
122. Miao, R. *et al.* Targeted Disruption of MCPIP1/Zc3h12a Results in Fatal Inflammatory Disease. *Immunol Cell Biol* **91**, 368–376 (2013).
123. Zhou, Z. *et al.* MCPIP1 Deficiency in Mice Results in Severe Anemia Related to Autoimmune Mechanisms. *PLoS One* **8**, e82542 (2013).
124. Uehata, T. *et al.* Malt1-Induced Cleavage of Regnase-1 in CD4+ Helper T Cells Regulates Immune Activation. *Cell* **153**, 1036–1049 (2013).
125. Yamasoba, D. *et al.* N4BP1 restricts HIV-1 and its inactivation by MALT1 promotes viral reactivation. *Nature Microbiology* **4**, 1 (2019).
126. Dubois, S. M. *et al.* A catalytic-independent role for the LUBAC in NF-κB activation upon antigen receptor engagement and in lymphoma cells. *Blood* **123**, 2199–2203 (2014).
127. Trompouki, E. *et al.* CYLD is a deubiquitinating enzyme that negatively regulates NF-κB activation by TNFR family members. *Nature* **424**, 793–796 (2003).
128. Sun, S.-C. CYLD: a tumor suppressor deubiquitinase regulating NF-κB activation and diverse biological processes. *Cell Death Differ* **17**, 25–34 (2010).
129. Düwel, M. *et al.* A20 Negatively Regulates T Cell Receptor Signaling to NF-κB by Cleaving Malt1 Ubiquitin Chains. *The Journal of Immunology* **182**, 7718–7728 (2009).
130. Skaug, B. *et al.* Direct, Non-catalytic Mechanism of IKK Inhibition by A20. *Mol Cell* **44**, 559–571 (2011).
131. Martens, A. & Loo, G. van. A20 at the Crossroads of Cell Death, Inflammation, and Autoimmunity. *Cold Spring Harb Perspect Biol* **12**, a036418 (2020).
132. Dixit, V. M. *et al.* Tumor necrosis factor-alpha induction of novel gene products in human endothelial cells including a macrophage-specific chemotaxin. *Journal of Biological Chemistry* **265**, 2973–2978 (1990).
133. Dorronsoro Gonzalez, A. *et al.* Identification of the NF-κB inhibitor A20 as a key regulator for human adipogenesis. *Cell death & disease* **4**, e972 (2013).
134. Krikos, A., Laherty, C. D. & Dixit, V. M. Transcriptional activation of the tumor necrosis factor alpha-inducible zinc finger protein, A20, is mediated by kappa B elements. *Journal of Biological Chemistry* **267**, 17971–17976 (1992).
135. Opipari, A. W., Boguski, M. S. & Dixit, V. M. The A20 cDNA induced by tumor necrosis factor alpha encodes a novel type of zinc finger protein. *Journal of Biological Chemistry* **265**, 14705–14708 (1990).

136. Heyninck, K. & Beyaert, R. A20 inhibits NF-κB activation by dual ubiquitin-editing functions. *Trends in Biochemical Sciences* **30**, 1–4 (2005).
137. Beyaert, R., Heyninck, K. & Van Huffel, S. A20 and A20-binding proteins as cellular inhibitors of nuclear factor-κB-dependent gene expression and apoptosis. *Biochemical Pharmacology* **60**, 1143–1151 (2000).
138. Lee, E. G. *et al.* Failure to regulate TNF-induced NF-kappaB and cell death responses in A20-deficient mice. *Science* **289**, 2350–2354 (2000).
139. Shembade, N. & Harhaj, E. W. Regulation of NF-κB signaling by the A20 deubiquitinase. *Cell Mol Immunol* **9**, 123–130 (2012).
140. Wertz, I. E. *et al.* De-ubiquitination and ubiquitin ligase domains of A20 downregulate NF-kappaB signalling. *Nature* **430**, 694–699 (2004).
141. Lu, T. T. *et al.* Dimerization and Ubiquitin Mediated Recruitment of A20, a Complex Deubiquitinating Enzyme. *Immunity* **38**, 896–905 (2013).
142. Shembade, N., Ma, A. & Harhaj, E. W. Inhibition of NF-κB Signaling by A20 Through Disruption of Ubiquitin Enzyme Complexes. *Science* **327**, 1135–1139 (2010).
143. Heyninck, K. *et al.* The zinc finger protein A20 inhibits TNF-induced NF-kappaB-dependent gene expression by interfering with an RIP- or TRAF2-mediated transactivation signal and directly binds to a novel NF-kappaB-inhibiting protein ABIN. *J. Cell Biol.* **145**, 1471–1482 (1999).
144. Wertz, I. E. & Dixit, V. M. Ubiquitin-mediated regulation of TNFR1 signaling. *Cytokine & Growth Factor Reviews* **19**, 313–324 (2008).
145. O'Donnell, M. A., Legarda-Addison, D., Skountzos, P., Yeh, W. C. & Ting, A. T. Ubiquitination of RIP1 Regulates an NF-κB-Independent Cell-Death Switch in TNF Signaling. *Current Biology* **17**, 418–424 (2007).
146. Gerlach, B. *et al.* Linear ubiquitination prevents inflammation and regulates immune signalling. *Nature* **471**, 591–596 (2011).
147. Kanayama, A. *et al.* TAB2 and TAB3 Activate the NF-κB Pathway through Binding to Polyubiquitin Chains. *Molecular Cell* **15**, 535–548 (2004).
148. Boone, D. L. *et al.* The ubiquitin-modifying enzyme A20 is required for termination of Toll-like receptor responses. *Nat Immunol* **5**, 1052–1060 (2004).
149. Lamothe, B. *et al.* SITE-SPECIFIC LYS-63-LINKED TUMOR NECROSIS FACTOR RECEPTOR-ASSOCIATED FACTOR 6 AUTO-UBIQUITINATION IS A CRITICAL DETERMINANT OF IKK ACTIVATION. *The Journal of biological chemistry* **282**, 4102 (2007).
150. Xia, Z.-P. *et al.* Direct activation of protein kinases by unanchored polyubiquitin chains. *Nature* **461**, 114–119 (2009).
151. Giordano, M. *et al.* The tumor necrosis factor alpha-induced protein 3 (TNFAIP3, A20) imposes a brake on antitumor activity of CD8 T cells. *PNAS* **111**, 11115–11120 (2014).
152. Fischer, J. C. *et al.* A20 deletion in T cells modulates acute graft-versus-host disease in mice. *European Journal of Immunology* **47**, 1982–1988 (2017).
153. Li, L., Soetandyo, N., Wang, Q. & Ye, Y. The zinc finger protein A20 targets TRAF2 to the lysosomes for degradation. *Biochim Biophys Acta* **1793**, 346–353 (2009).
154. Hutti, J. E. *et al.* IκB Kinase β Phosphorylates the K63 Deubiquitinase A20 To Cause Feedback Inhibition of the NF-κB Pathway. *Mol Cell Biol* **27**, 7451–7461 (2007).

155. Wertz, I. E. *et al.* Phosphorylation and linear ubiquitin direct A20 inhibition of inflammation. *Nature* **528**, 370–375 (2015).
156. Shembade, N., Harhaj, N. S., Liebl, D. J. & Harhaj, E. W. Essential role for TAX1BP1 in the termination of TNF-α-, IL-1- and LPS-mediated NF-κB and JNK signaling. *EMBO J* **26**, 3910–3922 (2007).
157. Zilberman-Rudenko, J. *et al.* Recruitment of A20 by the C-terminal domain of NEMO suppresses NF-κB activation and autoinflammatory disease. *PNAS* **113**, 1612–1617 (2016).
158. Shembade, N. *et al.* The E3 ligase Itch negatively regulates inflammatory signaling pathways by controlling the function of the ubiquitin-editing enzyme A20. *Nat Immunol* **9**, 254–262 (2008).
159. Verstrepen, L., Carpentier, I., Verhelst, K. & Beyaert, R. ABINs: A20 binding inhibitors of NF-kappa B and apoptosis signaling. *Biochem Pharmacol* **78**, 105–114 (2009).
160. Nanda, S. K. *et al.* Polyubiquitin binding to ABIN1 is required to prevent autoimmunity. *J. Exp. Med.* **208**, 1215–1228 (2011).
161. Heyninck, K. *et al.* The Zinc Finger Protein A20 Inhibits TNF-induced NF-κB–dependent Gene Expression by Interfering with an RIP- or TRAF2-mediated Transactivation Signal and Directly Binds to a Novel NF-κB–inhibiting Protein ABIN. *J Cell Biol* **145**, 1471–1482 (1999).
162. Su, Z. *et al.* ABIN-1 heterozygosity sensitizes to innate immune response in both RIPK1-dependent and RIPK1-independent manner. *Cell Death Differ* **26**, 1077–1088 (2019).
163. G'Sell, R. T., Gaffney, P. M. & Powell, D. W. ABIN1 a Physiological Inhibitor of NF-κB: A Molecular Switch for Inflammation and Autoimmunity. *Arthritis Rheumatol* **67**, 2292–2302 (2015).
164. Fukushi, M. *et al.* Identification and cloning of a novel cellular protein Naf1, Nef-associated factor 1, that increases cell surface CD4 expression1The accession numbers of Naf1α/β are AJ011895 and AJ011896.1. *FEBS Letters* **442**, 83–88 (1999).
165. Gupta, K., Ott, D., Hope, T. J., Siliciano, R. F. & Boeke, J. D. A Human Nuclear Shuttling Protein That Interacts with Human Immunodeficiency Virus Type 1 Matrix Is Packaged into Virions. *J Virol* **74**, 11811–11824 (2000).
166. G'Sell, R. T., Gaffney, P. M. & Powell, D. W. Review: A20-Binding Inhibitor of NF-κB Activation 1 Is a Physiologic Inhibitor of NF-κB: A Molecular Switch for Inflammation and Autoimmunity. *Arthritis & Rheumatology* **67**, 2292–2302 (2015).
167. Mauro, C. *et al.* ABIN-1 binds to NEMO/IKKgamma and co-operates with A20 in inhibiting NF-kappaB. *J. Biol. Chem.* **281**, 18482–18488 (2006).
168. Yuan, S. *et al.* Emergence of the A20/ABIN-mediated inhibition of NF-κB signaling via modifying the ubiquitinated proteins in a basal chordate. *PNAS* **111**, 6720–6725 (2014).
169. Heyninck, K., Kreike, M. M. & Beyaert, R. Structure–function analysis of the A20-binding inhibitor of NF-κB activation, ABIN-1. *FEBS Letters* **536**, 135–140 (2003).
170. Oshima, S. *et al.* ABIN-1 is a ubiquitin sensor that restricts cell death and sustains embryonic development. *Nature* **457**, 906–909 (2009).
171. Cruz, J. A. *et al.* IL-17 Signaling Triggers Degradation of the Constitutive NF-κB Inhibitor ABIN-1. *IH* **1**, 133–141 (2017).
172. Dziedzic, S. A. *et al.* ABIN-1 regulates RIPK1 activation by linking Met1 ubiquitylation with Lys63 deubiquitylation in TNF-RSC. *Nat Cell Biol* **20**, 58–68 (2018).

173. Onizawa, M. *et al.* The ubiquitin-modifying enzyme A20 restricts ubiquitination of the kinase RIPK3 and protects cells from necroptosis. *Nat Immunol* **16**, 618–627 (2015).
174. Kattah, M. G. *et al.* A20 and ABIN-1 synergistically preserve intestinal epithelial cell survival. *The Journal of experimental medicine* (2018) doi:10.1084/jem.20180198.
175. Brady, M. P., Korte, E. A., Caster, D. J. & Powell, D. W. TNIP1/ABIN1 and lupus nephritis: review. *Lupus Science & Medicine* **7**, e000437 (2020).
176. Nair, R. P. *et al.* Genome-wide scan reveals association of psoriasis with IL-23 and NF-κB pathways. *Nat Genet* **41**, 199–204 (2009).
177. Chen, Y. *et al.* Downregulation of TNIP1 Expression Leads to Increased Proliferation of Human Keratinocytes and Severer Psoriasis-Like Conditions in an Imiquimod-Induced Mouse Model of Dermatitis. *PLOS ONE* **10**, e0127957 (2015).
178. Ai, W., Li, H., Song, N., Li, L. & Chen, H. Optimal Method to Stimulate Cytokine Production and Its Use in Immunotoxicity Assessment. *International journal of environmental research and public health* (2013) doi:10.3390/ijerph10093834.
179. Ubiquitination and translocation of TRAF2 is required for activation of JNK but not of p38 or NF-κB. *The EMBO Journal* **23**, 322–332 (2004).
180. Kutzner, K. *et al.* Phosphorylation of serine-893 in CARD11 suppresses the formation and activity of the CARD11-BCL10-MALT1 complex in T and B cells. *Sci. Signal.* **15**, eabk3083 (2022).
181. Gehring, T. *et al.* MALT1 Phosphorylation Controls Activation of T Lymphocytes and Survival of ABC-DLBCL Tumor Cells. *Cell Reports* **29**, 873-888.e10 (2019).
182. Düwel, M. *et al.* A20 negatively regulates T cell receptor signaling to NF-kappaB by cleaving Malt1 ubiquitin chains. *J. Immunol.* **182**, 7718–7728 (2009).
183. Eitelhuber, A. C. *et al.* Activity-based probes for detection of active MALT1 paracaspase in immune cells and lymphomas. *Chem Biol* **22**, 129–138 (2015).
184. Quancard, J. *et al.* Optimization of the In Vivo Potency of Pyrazolopyrimidine MALT1 Protease Inhibitors by Reducing Metabolism and Increasing Potency in Whole Blood. *Journal of Medicinal Chemistry* **63**, 14594–14608 (2020).
185. Ruland, J. & Hartjes, L. CARD–BCL-10–MALT1 signalling in protective and pathological immunity. *Nat Rev Immunol* **19**, 118–134 (2019).
186. Harhaj, E. W. & Dixit, V. M. Regulation of NF-κB by deubiquitinases. *Immunol Rev* **246**, 107–124 (2012).
187. Catrysse, L., Vereecke, L., Beyaert, R. & Loo, G. van. A20 in inflammation and autoimmunity. *Trends in Immunology* **35**, 22–31 (2014).
188. Yin, H. *et al.* A20 and ABIN-1 cooperate in balancing CBM complex-triggered NF-κB signaling in activated T cells. *Cell. Mol. Life Sci.* **79**, 112 (2022).
189. Verstrepen, L. *et al.* Expression, biological activities and mechanisms of action of A20 (TNFAIP3). *Biochem Pharmacol* **80**, 2009–2020 (2010).
190. Myers, D. R., Zikherman, J. & Roose, J. P. Tonic Signals: Why Do Lymphocytes Bother? *Trends Immunol* **38**, 844–857 (2017).
191. Ajina, A. & Maher, J. Strategies to Address Chimeric Antigen Receptor Tonic SignalingStrategies to Address CAR Tonic Signaling. *Mol Cancer Ther* **17**, 1795–1815 (2018).
192. The ubiquitin-editing enzyme A20 requires RNF11 to downregulate NF-κB signalling. *The EMBO Journal* **28**, 513–522 (2009).

193. Konrath, F., Witt, J., Sauter, T. & Kulms, D. Identification of New IκBα Complexes by an Iterative Experimental and Mathematical Modeling Approach. *PLOS Computational Biology* **10**, e1003528 (2014).
194. Zhou, J. *et al.* A20-binding inhibitor of NF-κB (ABIN1) controls Toll-like receptor-mediated CCAAT/enhancer-binding protein β activation and protects from inflammatory disease. *Proc. Natl. Acad. Sci. U.S.A.* **108**, E998-1006 (2011).
195. Caster, D. J. *et al.* ABIN1 Dysfunction as a Genetic Basis for Lupus Nephritis. *JASN* **24**, 1743–1754 (2013).
196. Musone, S. L. *et al.* Multiple polymorphisms in the TNFAIP3 region are independently associated with systemic lupus erythematosus. *NATURE GENETICS* **40**, 3 (2008).
197. Ran, F. A. *et al.* Genome engineering using the CRISPR-Cas9 system. *Nat Protoc* **8**, 2281–2308 (2013).
198. Cong, L. *et al.* Multiplex Genome Engineering Using CRISPR/Cas Systems. *Science* **339**, 819–823 (2013).
199. Bardet, M. *et al.* MALT1 activation by TRAF6 needs neither BCL10 nor CARD11. *Biochemical and Biophysical Research Communications* **506**, 48–52 (2018).
200. Seeholzer, T. *et al.* BCL10-CARD11 Fusion Mimics an Active CARD11 Seed That Triggers Constitutive BCL10 Oligomerization and Lymphocyte Activation. *Frontiers in Immunology* **9**, 2695 (2018).
201. Stangl, A. *et al.* Regulation of the endosomal SNX27-retromer by OTULIN. *Nat Commun* **10**, 4320 (2019).
202. Kulak, N. A., Pichler, G., Paron, I., Nagaraj, N. & Mann, M. Minimal, encapsulated proteomic-sample processing applied to copy-number estimation in eukaryotic cells. *Nat Methods* **11**, 319–324 (2014).